

Efficacy and Durability of Microbially/Enzyme-Induced Carbonate Precipitation  
(MICP/EICP) for Dust Mitigation of Various Soil Types and Under Different  
Environmental Conditions

by

Farideh Ehsasi

A Dissertation Presented in Partial Fulfillment  
of the Requirements for the Degree  
Doctor of Philosophy

Graduate Supervisory Committee:

Edward Kavazanjian, Jr., Chair  
Leon van Paassen  
Hamed Khodadadi Tirkolaei

ARIZONA STATE UNIVERSITY

December 2023

## ABSTRACT

Microbially- and enzyme-induced carbonate precipitation (EICP and MICP) offer potentially sustainable and cost-effective mitigation methods for fugitive dust by forming an erosion-resistant crust on the soil through precipitation of a natural calcium carbonate ( $\text{CaCO}_3$ ) cement. While there have been isolated studies on the efficacy of the carbonate precipitation process, there are few systematic studies of the influence of the properties of the soil being treated (e.g., gradation, salt content) on the precipitation and the resulting wind erosion resistance. Moreover, the influence of environmental conditions on the durability of the crust formed by the induced carbonate precipitation has not been systematically investigated. In this research program, the efficacy and durability of EICP and MICP for dust mitigation were investigated for a variety of soil types and in different environmental conditions. Soil samples from seven sites with fugitive dust problems were treated with MICP or EICP and subjected to lab or field testing. The results of these tests showed that the effectiveness of biocementation treatment varies depending on the grain size distribution of soil and mineralogical composition. Testing on iron ore tailings materials demonstrated that treating by application of EICP solutions at lower concentrations (i.e., 0.5M and 0.75M of urea and calcium chloride) yielded effective results for poorly graded fine sand-sized tailings but the same solutions were ineffective for the well graded sand-sized tailings that contained large gravel-sized particles. Additionally, the application of MICP and EICP on sediments adjacent to a shrinking lake (the Salton Sea) with different salt contents exhibited enhanced performance in soils with lower salt content. The effect of temperature during deployment and precipitation

cycles are shown to be significant environmental factors by simulating wetting-drying and freeze-thaw cycles in the laboratory. A dust-resistance crust formed through biocementation remained mostly intact after undergoing multiple cycles of wetting-drying. However, the durability of a dust-resistance crust formed through biocementation to multiple cycles of freeze-thaw depended on treatment solution concentration and soil grain size. Additionally, high temperature during field deployment of MICP adversely effected crust formation due to rapid evaporation that inhibited the complete hydrolysis of urea and the precipitation of carbonate.

# TABLE OF CONTENTS

	Page
TABLE OF CONTENTS.....	iii
LIST OF FIGURES .....	x
CHAPTER	
1. INTRODUCTION .....	1
1.1. Background .....	1
1.2. Motivation .....	3
1.3. Scope and Organization .....	4
2. LITERATURE REVIEW .....	7
2.1. Dust Generation and Control Measures .....	7
2.1.1. Major Dust Emission Sources .....	7
2.1.2. Fugitive Dust Generation Mechanisms .....	7
2.1.3. Control Measures of Wind Erosion Generated Dust.....	9
2.2. Overview of the MICP and EICP Processes .....	11
2.3. Application of the MICP and EICP Processes for Dust Mitigation.....	12
3. STABILIZATION OF MINE TAILINGS USING MICROBIALLY INDUCED CARBONATE PRECIPITATION FOR DUST MITIGATION .....	15
3.1. Introduction .....	16

CHAPTER	Page
3.2. Materials and Methods .....	18
3.2.1. Tailings Characterization.....	18
3.2.2. Bacteria Cultivation.....	19
3.2.3. Specimen Preparation and Treatment.....	20
3.2.4. Penetration Test .....	21
3.2.5. Carbonate Content Measurement .....	23
3.3. Results and Discussion.....	23
3.4. Conclusions and Recommendations.....	30
 4. INFLUENCE OF FREEZE-THAW CYCLES ON TAILINGS STABILIZED FOR FUGITIVE DUST MITIGATION USING ENZYME-INDUCED CARBONATE PRECIPITATION.....	32
4.1. Introduction .....	33
4.2. Materials and Methods .....	36
4.2.1 Tailings Characterization.....	36
4.2.2. Specimen Preparation and Treatment.....	37
4.2.3. Freeze-Thaw Process.....	39
4.2.4. PI-SWERL Test.....	39
4.2.5. Penetration Test .....	42

CHAPTER	Page
4.2.6. Calcium Carbonate Content Measurement.....	43
4.3. Results and Discussion.....	44
4.3.1. Penetration Test Results .....	45
4.3.2. PI-SWERL results .....	54
4.3.3. Calcium Carbonate Measurements Results .....	60
4.3.4. Discussion.....	60
4.4. Conclusion.....	62
 5. LABORATORY STUDIES ON ENZYME AND MICROBIALLY INDUCED CARBONATE PRECIPITATION FOR MITIGATION OF FUGITIVE DUST FROM SALINE SOIL .....	          64
5.1. Introduction .....	65
5.2. Materials and Methods .....	69
5.2.1. Sediment Characterization.....	69
5.2.2. Bacteria Cultivation.....	77
5.2.3. Enzyme Preparation.....	78
5.2.4. Specimen Preparation and Treatment.....	79
5.2.6. PI-SWERL Test.....	80
5.2.7. Penetration Test .....	81

CHAPTER	Page
5.2.8. Carbonate Content Measurement .....	82
5.2.9. Salt Effect on Enzyme Activity .....	82
5.3. Results and Discussion.....	83
5.3.1. PI-SWERL Test Results .....	83
5.3.2. Penetration Test Results .....	86
5.3.3. Result of Calcium Carbonate Content Measurement .....	90
5.3.4. Discussion on salt effect .....	91
5.4. Conclusion.....	94
 6. EVALUATION OF THE APPLICATION AND DURABILITY OF MICROBIALLY INDUCED CARBONATE PRECIPITATION FOR FUGITIVE DUST CONTROL OF SILTY SAND .....	       97
6.1. Introduction .....	98
6.2. Materials and Methods .....	100
6.2.1. Soil Characterization .....	100
6.2.2. Bacteria Cultivation.....	102
6.2.3. MICP Treatment in the Field.....	103
6.2.4. PI-SWERL Test.....	106
6.2.5. Surface Strength Test.....	107

CHAPTER	Page
6.2.6. Carbonate Content Measurement .....	107
6.2.7. Isotope Ratio Mass Spectrometry .....	108
6.2.8. Induced Disturbance Testing .....	108
6.3. Results and Discussion.....	109
6.3.1. PI-SWERL Test Results .....	109
6.3.2. Surface Resistance Testing .....	112
6.3.3. Calcium Carbonate Content Measurement.....	113
6.3.4. Isotope Ratio Mass Spectrometry .....	115
6.3.5. Induced Disturbance Measurements.....	116
6.3.6. Discussion.....	117
6.4. Conclusion.....	119
<b>7. SUMMARY, CONCLUSIONS, AND RECOMMENDATIONS FOR FURTHER STUDY .....</b>	<b>121</b>
7.1. Summary .....	121
7.2. Conclusion.....	125
7.2.1. Effect of soil type .....	125
7.2.2. Effect of environmental conditions .....	126
7.3. Recommendations .....	127



CHAPTER

Page

REFERENCES ..... 129

## LIST OF TABLES

Table		Page
3. 1.	Results of Soil Classification of the Tailings.....	18
3. 2.	Summary of Treated Samples of Silty Sand and Resulting Peak Strength .....	24
3. 3.	Summary of Treated Silt Samples and Resulting Peak Strength .....	24
4. 1.	Results of Soil Classification of the Tailings.....	36
4. 2.	Summary of Treated Samples and Treatment Results for SP Soil .....	44
4. 3.	Summary of Treated Samples and Treatment Results for SW and SP-SM Soil .....	45
5. 1.	Grain Size Distribution of Samples.....	71
5. 2.	Carbonate Content of Samples.....	73
5. 3.	Soluble Salt Content of Samples Based on Electric Conductivity Measurements..	76
5. 4.	Summary of Samples with Different Treatments .....	90
5. 5.	Results of Carbonate Content Measurement of Unsalted Soil.....	94
6. 1.	SRL Soil Properties .....	101
6. 2.	Concentrations and Application Rates for Treatment Plots in SRL Site .....	104
6. 3.	Average Pocket Penetration Resistance (kPa) of the Soil Crust .....	113
6. 4.	Average Torvane Shear Resistance (kPa) of the Soil Crust.....	113
6. 5.	Average Total CaCO <sub>3</sub> Content in the Crust of Field Specimens.....	114
6. 6.	Isotopic Signature Ranges of $\delta^{13}C$ for Carbon in Carbonates from SRL Soil Test Specimens and Lab Made EICP and MICP Precipitations.....	115

## LIST OF FIGURES

Figure	Page
2. 1. Schematic Representation of the Main Phases Involved in the Wind-erosion.....	8
2. 2. The Most Adopted Methodologies for Fugitive Dust Mitigation.....	9
3. 1. Penetrometer Test on a Pan Specimen and Treated Sample after Performing Five Penetration Tests .....	22
3. 2. Penetration Test Results of Specimens after a Single Treatment.....	25
3. 3. Penetration Tests Results Before and after Wash-Dry Cycles of Specimens.....	27
3. 4. The Precipitated Carbonate Content Profiles.....	29
4. 1. Grain Size Distribution of Two Types of the Tailings .....	37
4. 2. Specimens Prepared by SP and SW Soils in Polystyrene Foam Containers .....	39
4. 3. The PI-SWERL Device and the Rotating Blade in the Chamber.. .....	40
4. 4. Test Cycle of PI-SWERL for Running Over the Specimens .....	41
4. 5. Penetration Test Results for Untreated Specimens of SP and SW Specimens.....	46
4. 6. Average Peak Strength of SP Specimens vs. Number of Freeze-Thaw Cycles .....	48
4. 7. Penetration Test Results of the SP Specimens Treated with Concentrations of 0.5M (a), 0.75M (b), 1M (c), and 0.5M with 30% Saturation (d) .....	49
4. 8. Average Peak Strength of SW Specimens vs. Number of Freeze-Thaw Cycles.....	51
4. 9. Penetration Test Results of the SW Specimens Treated with Concentrations of 0.5M (a), 0.75M (b), 1M (c), and 0.5M with 30% saturation (d). .....	52
4. 10. Average Peak Strength of SP-SM Specimens vs. Number of Freeze-Thaw Cycles .....	53

Figure	Page
4. 11. Penetration Test Results of the Specimens from the Smaller Fraction (< 0.425 mm) of SW Soil (Designated as SP-SM) Treated with Concentrations of 0.5M (a) and 1M (b) .....	54
4. 12. Total Mass Emission ( $\mu\text{g}$ ) at Velocity of 85 cm/s of SP Specimens vs. Number of Freeze-Thaw Cycles.....	55
4. 13. Total Mass Emission ( $\mu\text{g}$ ) at Velocity of 85 cm/s of SW Specimens vs. Number of Freeze-Thaw Cycles.....	56
4. 14. Total Mass Emission ( $\mu\text{g}$ ) at Velocity of 85 cm/s of SP-SM Specimens vs. Number of Freeze-Thaw Cycles. ....	57
4. 15. The Total Mass Loss per Surface Area ( $\text{mg}/\text{m}^2$ ) vs. Friction Velocity for Specimens of SP Soil .....	58
4. 16. The Total Mass Loss per Surface Area ( $\text{mg}/\text{m}^2$ ) vs. Friction Velocity for Specimens of SP-SM Soil .....	59
5. 1. Sample Locations around the Salton Sea.....	70
5. 2. Grain Size Distribution of Two Salton Sea Samples in Wet and Dry Sieving.....	72
5. 3. SWRC Curve of Two Samples .....	74
5. 4. Mass of Water Retained vs. Time in Two Samples .....	75
5. 5. (A) Specimen Holder. (B) a Pan Specimen Placed and Taped in the Holder before Running PI-SWERL Test, (C) PI-SWERL Device on the Specimen .....	81
5. 6. PM10 Emission from HS Samples: EICP, MICP, Salt, Water-treated, and Untreated Samples vs. Friction Velocity of the PI-SWERL.....	84

Figure	Page
5. 7. Total Mass Loss per Unit Area from HS Samples: EICP, MICP, Salt, Water-treated, and Untreated Samples vs. Friction Velocity of the PI-SWERL.....	84
5. 8. PM10 Emission from LS Samples: Low and High Concentrations of EICP and Water-treated Samples. ....	85
5. 9. Total Dust Mass from LS Samples: Low and High Concentrations of EICP and Water-treated Samples. ....	86
5. 10. Penetration Test Results of HS Samples: Treated with 0.5M EICP and 0.5M MICP .....	87
5. 11. Penetration Test Results of HS Samples: Treated with Salt and Water .....	88
5. 12. Penetration Test Results of HS Samples: Treated with 1.5M EICP and 1.5M MICP .....	88
5. 13. Penetration Test Results of HS Sample: Treated with MICP Three Times. ....	89
5. 14. Penetration Test Results of LS Samples: EICP-Treated Samples (Low and High Concentrations) vs. Water-Treated Sample.....	89
5. 15. Precipitation Ratio Versus Electrical Conductivity of the Treatment Solution at Different Enzyme Concentration (Almajed Et Al, 2018) .....	92
5. 16. Precipitation Ratio Versus Electrical Conductivity of the Treatment Solution at Different Cell Concentration. (Khodadadi Tirkolaei, 2016).....	93
6. 1. Configuration of Test Plots Layout for Field Trial at SRL Test Site.....	100
6. 2. Grain Size Distribution for SRL Soil Samples.....	102
6. 3. Bacteria Cultivation in a Plastic Drum in the Laboratory .....	103

Figure	Page
6. 4. Preparing the Cementation Solution and the MICP Treatment in Progress in SRL Field. ....	106
6. 5. Aerial View of the Field Trial Area Immediately after Treatment of MICP Plot.	106
6. 6. Induced Dust Event Along the MICP Plot with the Truck Dragging a Chain Link Fence at Speed of 10 mph. ....	109
6. 7. PI-SWERL Measured TFV Values for Untreated and Treated Soil Surfaces.....	111
6. 8. PI-SWERL Results from All Plots: Average PM10 Concentration from each Plot vs. Threshold Friction Velocity .....	112
6. 9. Comparison of Dust Pollution from the Induced Disturbance Testing for both Pre- and Post-treated Surface Conditions.....	116

## CHAPTER 1

### 1. INTRODUCTION

#### 1.1. Background

Wind erosion is one of the main reasons for soil degradation caused by the natural process of soil particles detachment from the ground surface followed by transportation and deposition of the detached soil. The detached soil is sometimes referred to as fugitive dust and can be harmful to human health and the environment. Biocementation methods, including microbially and enzyme-induced carbonate precipitation (EICP and MICP), offer a potentially sustainable and cost-effective mitigation method for fugitive dust. Fugitive dust emission from wind erosion is a worldwide environmental concern, particularly in arid and semi-arid areas, due to associated health problems, loss of soil fertility, and reduced visibility resulting in increased traffic accidents (Chen et al., 2014).

Conventional techniques for controlling fugitive dust include establishing vegetation, installing barriers such as fences, covering with materials (gravel, mulch, etc.), frequent watering, and surface application of chemical stabilizers (e.g., salt, petroleum products, polymers, biopolymers) (Countess Environmental, 2006). The choice of method may depend upon the particular area of application, as each method has its limitations or may not be viable in all areas with fugitive dust susceptibility problems. For instance, vegetation is the primary means of erosion control in some regions, but it is not easily established in arid and semi-arid regions. Frequent watering reduces dust in untreated surfaces, but water is not readily available everywhere; moreover, use of potable water is usually not a sustainable solution and may also have limited

effectiveness in hot, arid climates. Applying chemicals may control wind erosion for a sustained period of time, but some chemical stabilizers have adverse environmental impact and considering their efficiency and durability, may not be either cost-effective or sustainable. Therefore, the development of sustainable and cost-effective control methods for fugitive dust is an important problem in geoenvironmental engineering.

Biocementation of surficial soils using carbonate precipitation by employing plant-based enzymes (EICP) (Hamdan & Kavazanjian, 2016) or bacteria (MICP) (Gomez et al., 2015) is a relatively new approach to fugitive dust mitigation. This method is reported to meet the criteria for an effective and sustainable dust control method to some extent and may reduce some of the adverse environmental impacts of traditional dust suppression methods (Raymond et al., 2019).

Enzyme and microbially induced calcium carbonate precipitation (i.e., EICP and MICP, respectively) have become popular research topics in the last two decades for stabilization of granular soils by biocementation. In these processes, the enzyme urease is used to catalyze the hydrolysis of urea that yields  $\text{CaCO}_3$  precipitation when in a calcium-rich aqueous solution. In EICP the urease enzyme is typically extracted from plants, mostly from the urease-rich jack bean (*Canavalia ensiformis*) or sword bean (*Canavalia gladiata*). For MICP the source of enzyme is ureolytic (urease-producing) bacteria. Among all the possible ground improvement applications, one of the most promising applications for EICP and MICP treatment is erosion control (Hamdan & Kavazanjian, 2016; Fattahi et al., 2021). EICP and MICP treatment creates a crust at the soil surface preventing detachment of soil particles by binding them, thus, mitigating the soil from



wind erosion. The application of biocementation for dust mitigation in a variety of soil types and in different climate conditions is the focus of this research.

## 1.2. Motivation

The dust susceptibility of soils is related to two general factors: 1) properties (e.g., grain size, mineralogy, and interparticle attraction) of the soil from which the dust is generated; 2) the external forces and environmental conditions causing the disintegration and detachment of soil particles (e.g., wind velocity, temperature, wet/dry and freeze/thaw cycles). The effectiveness of a particular dust control method is site-specific. Therefore, to properly design a dust control strategy for a particular area, these factors should be considered.

The performance of either EICP or MICP as a dust control method is affected by the effectiveness of the biocementation process, which in turn may depend upon nutrient concentration, temperature, the calcium source, and pH value, the soil type. Furthermore, biocementation processes may decay after implementation. Thus, to properly evaluate the potential of a biocementation technique as a dust mitigation method, durability under relevant environmental conditions needs to be evaluated.

The potential application of microbially- and enzyme-induced carbonate precipitation for fugitive dust mitigation has been previously investigated in several studies (Hamdan & Kavazanjian, 2016; Fattahi et al., 2021, Gomez et al., 2015). However, there is a lack of structured studies on the effect of different soil types on the efficacy of biocementation through MICP and EICP for fugitive dust mitigation. And the

treatment efficacy and durability of these MICP and EICP treated soils for fugitive dust control in certain environmental conditions (e.g., when subject to wet/dry or freeze/thaw cycles) is not well-understood.

This study investigates the efficacy of biocementation as a fugitive dust control method regarding soil type and environmental conditions. With respect to soil properties, the grain size distribution and the salt content of the soil have been the focus of this research. The investigated environmental conditions include excessively dry regions (arid and semi-arid climate), climates where temperature drops below freezing, and a hypersaline environment with salt concentrations greater than that of seawater.

Even though most of the research described herein has taken place in the laboratory, the viability of transferring the technique into the field needs to be considered. A field trial was conducted to demonstrate the application of EICP and MICP at a local Arizona landfill site. The field trial also included a section treated with xanthan gum enhanced EICP and control sections with no treatment and where the soil was treated with magnesium chloride, a standard method in mining industry for fugitive dust control.

### 1.3. Scope and Organization

In this research program, the application of MICP and EICP for fugitive dust control for several soil types was investigated on a laboratory scale. A limited field trial (limited to a single site/soil type) was conducted to relate the laboratory results to field deployment of the ECIP and MICP techniques. The goals of this research are to:

- Determine the potential of biocementation for fugitive dust mitigation and identify its limitations associated with soil characteristics, including grain size distribution and salt content of the soil.
- Investigate the efficacy and durability of EICP and MICP for dust mitigation under extreme environments. These extreme environmental conditions include excessively dry regions, climates where the temperature drops below freezing, and a hypersaline environment with salt concentrations greater than that of seawater.
- Evaluate the efficacy of biocementation via MICP for fugitive dust control in the field and compare it to the results from treatment with EICP, EICP enhanced with xanthan gum, and an industry standard mitigation method (i.e., magnesium chloride).
- Investigate how soil properties such as grain size distribution, moisture content, and salinity may affect the application rate of the biocementation treatment solution.

This dissertation is organized as follows:

- Chapter 2 presents an overview of dust generation and control measures, concentrating on the application of biocementation for wind erosion (fugitive dust) control. Included in this chapter are arguments about the necessity of research on the efficacy of biocementation for fugitive dust mitigation with a focus on soil properties and site-specific climate condition.

- Chapter 3 presents the results of a laboratory study on stabilization of two types of mine tailings using microbially induced carbonate precipitation (MICP) for dust mitigation. Optimization of the treatment strategies for these tailing materials and the durability assessment of the treated samples are discussed in this chapter.
- Chapter 4 evaluates the freeze-thaw response of two types of tailings from Minnesota after biocementation treatment using EICP for dust mitigation at the laboratory scale. The durability of specimens treated with a variety of solution concentrations was evaluated by monitoring their crust stability during freeze-thaw cycles.
- Chapter 5 presents the results of a study on enzyme and microbially induced carbonate precipitation for mitigation of fugitive dust from saline soils from the Salton Sea in California. The efficacy of biocementation through MICP and EICP were studied for soils with different salt contents.
- Chapter 6 includes a demonstration of field application of biocementation for fugitive dust control on interim cover soil at a local (Arizona) landfill (the Salt River Landfill). The field trial included sections treated with MICP, EICP with and without xanthan gum, and control sections with no treatment and treated with magnesium chloride, a common material used for dust mitigation at mining sites. The MICP test section was specifically the focus of this study. The performance of the other test sections will be reported by Woolley (2023).
- Chapter 7 presents the conclusions of this research and provides recommendations for areas of future study.

## CHAPTER 2

### 2. LITERATURE REVIEW

#### 2.1. Dust Generation and Control Measures

##### 2.1.1. Major Dust Emission Sources

Fugitive dust emission can be broken down into three main categories based on their sources:

Category 1: Purely anthropogenic sources (e.g., construction, mining, wind erosion and vehicle traffic on paved and unpaved roads, cultivation of agricultural fields).

Category 2: Purely natural sources (e.g., volcanic ash emissions, wind erosion of unstable soil, mineral particle emissions from wave action/sea spray).

Category 3: Natural sources that may be anthropogenically influenced (e.g., wind erosion and mechanical suspension of soil due to animal movement, wind erosion of burn areas on natural lands, wind erosion of sediment from dried ephemeral water bodies) (Countess Environmental, 2006).

##### 2.1.2. Fugitive Dust Generation Mechanisms

Fugitive dust emissions from all sources can be generated through two major mechanisms:

- 1) Wind generated dust, where the wind shear on the ground surface is the main driving factor of dust emission

2) Mechanically suspended dust, where other driving forces cause the detachment and suspension of the particles (such as dust generated due to the machinery activity in the construction sites)

The focus of this dissertation is the dust generated due to wind erosion. The wind erosion process can be separated into three distinct phases, including 1) detachment of soil particles from the ground surface, 2) transport of particles by creep, saltation, or suspension, and 3) deposition of the detached particles. These phases are schematically depicted in Figure 2.1:

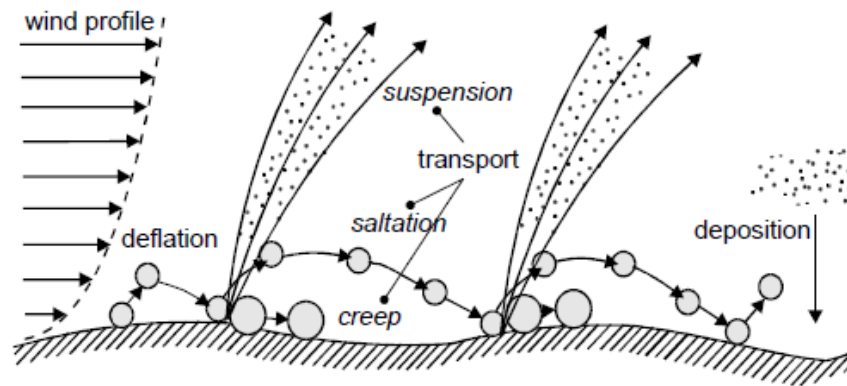


**Figure 2. 1.** Schematic Representation of the Main Phases Involved in the Wind-Erosion Process (D’Odorico & Porporato, 2006).

Factors influencing fugitive dust generation include meteorological conditions (wind shear, precipitation, evaporation, humidity, and temperature), soil characteristics (particle size distribution and particle shape, soil water characteristics, organic matter, and salt content), and land-surface properties (roughness, coverage of vegetation, surface disturbance) (Watson et al., 2000).

### 2.1.3. Control Measures of Wind Erosion Generated Dust

The most adopted methodologies currently used in the US for fugitive dust mitigation can be categorized as detailed in the chart below:

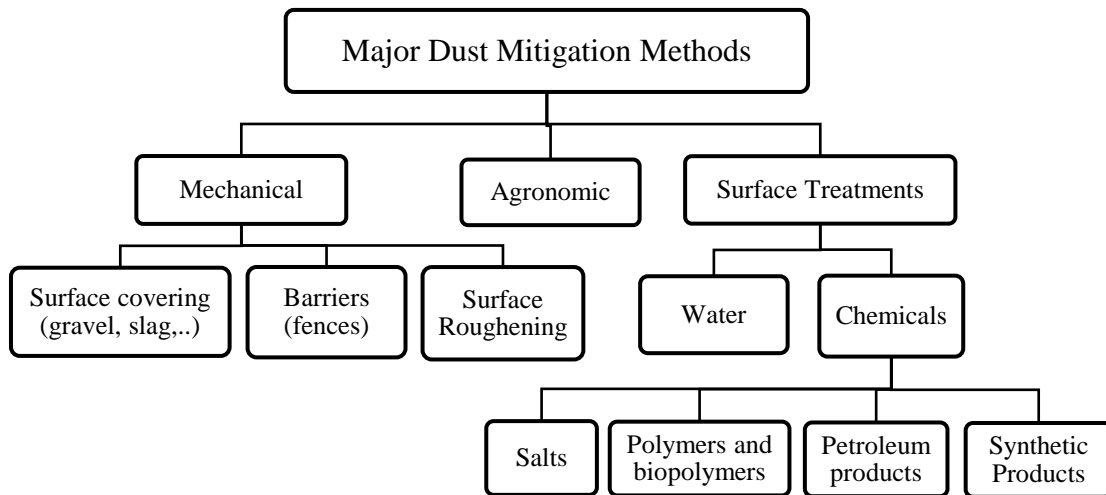


**Figure 2. 2.** The Most Adopted Methodologies for Fugitive Dust Mitigation

Performance of a dust control agents may be quantified using control efficiency (CE).

Control efficiency compares the dust concentration of a treated surface to that of an untreated or uncontrolled surface and is defined in Eq. 2.1 (Niosh, n.d.):

$$CE = 1 - \left(\frac{T}{U}\right) \times 100 \quad (1)$$

where  $CE$  = control efficiency, percent.

$U$  = untreated or uncontrolled dust concentration,  $\text{mg}/\text{m}^3$ ; and

T = treated or controlled dust concentration, mg/m<sup>3</sup>.

Generally, the higher the control efficiency for a dust control agent, the better its performance, i.e., the lower the fugitive dust emissions (Niosh, n.d.). Cost effectiveness of a dust control method can be calculated by dividing the annual cost of treatment by the emission reduction in which the emission reduction is the total of emissions eliminated by control application (Countess Environmental, 2006).

The feasibility of a dust control method, technically and economically, is site specific (Countess Environmental, 2006). Various dust control techniques may be applicable in specific areas and/or under specific conditions, e.g., based on availability of the dust mitigation tools and meteorological condition. For example, vegetation is the primary means of erosion control in some regions, but it is not easily established in arid and semi-arid regions. Frequent watering reduces dust in untreated surfaces, but use of potable water for this purpose may be neither a sustainable solution, as potable water may be a scarce commodity, nor an effective solution. Applying chemicals may control wind erosion for sustained durations, but some chemicals have adverse environmental impact, may not work in a particular meteorological condition and chemical treatment can be very expensive. Therefore, mitigating fugitive dust generation, particularly in arid regions and at mine tailings sites, remains an important problem in geoenvironmental engineering and innovations in dust control methodologies are needed.

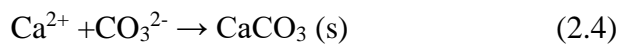
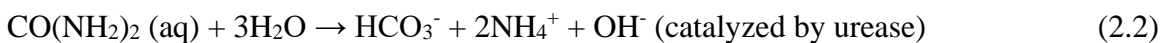


## 2.2. Overview of the MICP and EICP Processes

Biocementation for ground improvement, including soil surface stabilization for fugitive dust mitigation has been a subject of increasing interest in the last two decades.

Biocementation strengthens and stiffens granular soil and protects the soil surface against erosion by forming a crust through binding the soil particles together. A brief overview of MICP and EICP processes is provided in the following section.

Kucharski, et al. (1996) evaluated the use of what they termed the “Calcite In situ Precipitation System (CIPS)” for cementing calcareous and silica sands. Twenty-seven years later, enzyme and microbially induced calcium carbonate precipitation (i.e., EICP and MICP, respectively) have become popular research topics for stabilization of granular soils by biocementation. In the EICP and MICP biocementation processes, urease enzyme catalyzes urea hydrolysis which increases the pH and alkalinity of the reaction solution by the production of dissolved inorganic carbon and ammonium. Sufficient alkalinity production, in the presence of dissolved calcium ( $\text{Ca}^{2+}$ ) cations, will lead to the precipitation of calcium carbonate, as shown by the reactions in Eqs. 2.2 to 2.4):



The ammonium ions either volatilize as ammonia ( $\text{NH}_3$ ) or, if  $\text{CaCl}_2$  is the source of the calcium ions, form ammonium chloride ( $\text{NH}_4\text{Cl}$ ) that may also precipitate from the treatment solution if water is allowed to evaporate (van Paassen, 2009). In EICP the

urease enzyme is typically extracted from plants, mostly from the urease-rich jack bean (*Canavalia ensiformis*) or sword bean (*Canavalia gladiata*) (Lakshminarayanan, 2022). For MICP the source of the urease enzyme is urease-producing (ureolytic) bacteria. There are many ureolytic bacteria. However, the bacterium *Sporosarcina pasteurii* is particularly popular for MICP as it can be cultivated aerobically relatively easily and is a good source of urease.

The precipitation of calcium carbonate crystals can lead to improvement of geotechnical properties such as stiffness and shear strength (DeJong et al., 2006; Whiffin et al., 2007; Van Paassen et al. 2009, 2010; Montoya et al., 2012). Potential applications of EICP and MICP include the improvement of foundation soils, mitigation of earthquake-induced liquefaction, and preventing detachment of soil particles by binding them and creating a crust at the soil surface, thus, mitigating the potential for fugitive dust from wind erosion.

### 2.3. Application of the MICP and EICP Processes for Dust Mitigation

Erosion control is one of the most promising applications for EICP and MICP treatment. Various researchers have already demonstrated in the laboratory and field the effectiveness of using EICP and MICP for creating surface crusts and mitigating fugitive dust for various soil types and treatment protocols (Hamdan and Kavazanjian, 2016; Fattahi et al., 2021; Ghasemi et al., 2022; Bang et al. 2011; Meyer et al. 2011; Gomez et al. 2015; Naeimi and Chu 2017; Wang et al. 2018).

Hamdan and Kavazanjian (2016) evaluated the use of EICP for fugitive dust control in three different soils, including a native Arizona silty sand, a uniform medium-grained silica sand, and fine sand-sized mine tailings from southern Arizona. They showed that EICP holds promise as a method for mitigation of fugitive dust emissions. Fattahi et al., (2021) examined the durability of MICP (biocemented) crust in comparison with a *Microcoleus aginatus* cyanobacterium-created crust (cyanocrust) in poorly graded sand. They suggested that the MICP sand crust has a comparatively stronger bonding and more coherent structure than that of the cyanocrust and is also more durable than the cyanocrust. Ghasemi et al., (2022) implemented MICP on a sandy slope field site and showed that there was a significant enhancement in erosion resistance and surficial soil strength. The post treatment monitoring of the treated area indicated no significant degradation after major storm events.

The aforementioned studies collectively demonstrate the effectiveness of both EICP and MICP techniques for mitigating dust. However, there are several aspects of application of biocementation for dust mitigation which are not fully investigated. Understanding how MICP and EICP can be applied in various natural settings is essential to widespread adoption in practice. The impact of environmental conditions, e.g., temperature and rainfall, on effectiveness of biocementation also needs further investigation. Given most of the studies to date have been conducted on sandy soils, expanding research on biocementation to mitigate fugitive dust to include a wider range of soil types is also advisable. In this context, soil chemistry assumes a significant role, including the consideration of soil salinity as an important factor to be considered in some environments. Moreover, scaling up the MICP and EICP processes from laboratory

or pilot-scale experiments to practical field applications can be challenging. Research to focus on overcoming these obstacles related to wide-scale commercial use of EICP and MICP for fugitive dust control seems warranted.

## CHAPTER 3

### 3. STABILIZATION OF MINE TAILINGS USING MICROBIALLY INDUCED CARBONATE PRECIPITATION FOR DUST MITIGATION

This chapter is an extended version of work previously published in the *Proceedings of the 2022 ASCE GeoCongress: Soil Improvement, Geosynthetics, and Innovative Geomaterials* as Ehsasi, F., van Paassen, L., and Wang, L. (2022). “Stabilization of Mine Tailings Using Microbiological Induced Carbonate Precipitation for Dust Mitigation: Treatment Optimization and Durability Assessment,” pp. 326-334.

[10.1061/9780784484012.034](https://doi.org/10.1061/9780784484012.034)

#### ABSTRACT

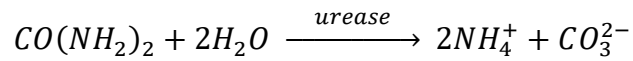
Wind erosion (dust) is a severe problem for the mine tailings industry, as it poses environmental and safety concerns to the public. In this study, microbially induced carbonate precipitation (MICP) based on urea hydrolysis was used to stabilize the surface of different tailings materials in the laboratory. An experimental study was performed on soil-filled pans that were prepared using loosely packed tailings material and treated using percolation of reactive solutions. Penetration testing and calcium carbonate content analysis were used to assess the strength and durability of the cemented crusts and optimize the treatment strategy. The MICP treated pans showed an increase in strength and durability with increasing concentration of the cementation solution and number of treatments.

### 3.1. Introduction

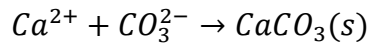
Fugitive dust emissions resulting from wind erosion in mine tailing impoundments can have a detrimental effect on surrounding environment (Wijewickreme et al. 2005; Mendez and Maier 2008). By polluting the air and contaminating the soil and water, dust emission can cause serious health problems. Asthma and lung disease can arise as a consequence of exposure to air pollution. It can also cause safety problems by reducing the visibility along nearby roads (Chen et al., 2014). A lot of mining companies have experienced economic losses due to environmental issues resulting from blowing tailings dust.

Different methods of fugitive dust control have been used to mitigate dust at mine tailings storage facilities. The most commonly used methods are by application of water to wet the soil and by spraying hygroscopic salts (e.g., magnesium chloride or calcium chloride) which can absorb moisture from the atmosphere to keep the soil surface wet and also increase the surface tension of the pore water. Use of these techniques has limitations and sustainability issues. Due to the rapid evaporation of water, particularly in arid and semi-arid areas, water needs to be applied regularly to maintain the wet condition (Countess Environmental, 2006). Also, salt treatment has a short effective life span that requires frequent re-application in dry climates (Countess Environmental, 2006) and rain events will dissolve and wash the salt away. Further, biopolymers have been proposed for dust control: normally long-chain polymers like xanthan gum and guar gum that have high viscosity and are able to bond to the soil particles (Chen et al., 2014).

In this study, the use of Microbially Induced Calcium Carbonate Precipitation (MICP) as a dust suppressant was investigated. In the MICP process bacteria with ureolytic activity catalyze hydrolysis of urea ( $CO(NH_2)_2$ ) in the supplied treatment solution that results in the production of ammonium ( $NH_4^+$ ) and carbonate ( $CO_3^{2-}$ ) ions:



Production of carbonate ions in presence of calcium ions results in precipitation of solid calcium carbonate crystals:



The precipitation of calcium carbonate crystals can lead to improvement of geotechnical properties such as stiffness and shear strength (DeJong et al., 2006; Whiffin et al., 2007; Van Paassen et al. 2009, 2010; Montoya et al., 2012).

The objective of this study was to determine the potential of MICP to create a crust and enhance wind erosion resistance for mine tailings. Various researchers have already demonstrated the effectiveness of using MICP for creating surface crusts and mitigating fugitive dust for various soil types and treatment protocols (Bang et al. 2011; Meyer et al. 2011; Gomez et al. 2015; Maleki et al. 2016; Shanahan and Montoya 2016; Naeimi & Chu 2017; Wang et al. 2018). Compared to alternative dust suppressants like water, hygroscopic salts or biopolymers, a mineral crust (i.e., of a crust created using MICP) offers the potential for a longer time between re-applications, less water use, and enhanced durability to surface water washout and wetting-drying cycles.

In this study, two types of tailings were characterized and treated using MICP with varying strategies. The effect of treatment was evaluated by performing strain-controlled penetration tests and measuring the CaCO<sub>3</sub> content in a vertical profile directly after treatment and drying and after several washing and drying cycles.

### 3.2. Materials and Methods

#### 3.2.1. Tailings Characterization

Two different types of tailings were classified in accordance with the Unified Soil Classification System (USCS) using ASTM D2487-17. Grain size and Atterberg limits test results indicate one specimen was a silty sand (classified SM in the USCS) and the other was a low plasticity silt (classified ML in the USCS) Hydraulic conductivity was determined using falling head tests as described in ASTM 5084 but using the KSAT device (Metergroup, Pullman, Oregon) instead of a flexible wall permeameter. Both materials were also tested for CaCO<sub>3</sub> content. Carbonate content was measured following ASTM D 4373-84, where the carbonate content is based on the volume of carbon dioxide gas generated by the reaction between the hydrochloric acid and the carbonates. Results of the classification tests are shown in Table 3.1.

**Table 3. 1.** Results of Soil Classification of the Tailings

Property	Unit	Sand	Silt
Coarse fraction > 0.075 mm	[%]	88	34
Fine fraction < 0.075 mm	[%]	12	66
Liquid Limit	[%]	n.d.	22.6
Plastic Limit	[%]	n.d.	19.7
Plasticity index	[%]	n.d.	2.9
USCS Classification	[-]	Silty sand (SM)	Low plasticity Silt (ML)
Hydraulic conductivity	[m/s]	$2.7 \times 10^{-5}$	$3.2 \times 10^{-7}$
CaCO <sub>3</sub> content	[%]	0	2



### 3.2.2. Bacteria Cultivation

The bacteria *Sporosarcina pasteurii* were used as the source of the enzyme urease. To cultivate the bacteria, a medium was prepared containing 20 g L<sup>-1</sup> yeast extract, 10 g L<sup>-1</sup> NH<sub>4</sub>Cl, and 24 mg L<sup>-1</sup> NiCl<sub>2</sub>. The pH of the medium was adjusted to 9 by slowly adding 4M NaOH. For the first cultivation, ureolytic bacteria were obtained using a culture from previous studies growing on nutrient agar on a Petri dish plate. The resulting active culture was stored in the refrigerator during the entire duration of the experiments (3 months). For each subsequent cultivation, about 5 mL of the initial active bacterial culture was used as an inoculum and added to 200 mL of prepared medium and were cultivated under aerobic conditions for 24-30 hours at 30°C. After cultivation, the bacteria were transferred to the refrigerator and stored at 4°C in their growth medium before they were used.

Urease activity was measured using the electrical conductivity (EC) method (Whiffin et al. 2007). Measurement of the urease activity was conducted by adding 1 mL of bacterial suspension to 9 mL of urea solution, to obtain a total concentration of 1 M urea. As the urease catalyzes the hydrolysis of the non-ionic urea substrate to ionic products, it generates a proportionate increase in EC under standard conditions. Relative EC change in mS cm<sup>-1</sup> min<sup>-1</sup> was recorded over 10 minutes at 20°C. A change in EC of 1 mS cm<sup>-1</sup> min<sup>-1</sup> corresponds to a urease activity 11 mM urea min<sup>-1</sup> (Whiffin et al. 2007). The urease activity was also measured prior to use for every treatment.

### 3.2.3. Specimen Preparation and Treatment

The specimens were prepared inside circular pans with a volume of 1.48 L, a surface diameter of 22 cm, a bottom diameter of 18 cm, and a depth of 3.5 cm by dry pluviation. The pan was placed on a flat surface, the tailings were placed loosely in the pan, and the pan surface was leveled. All the specimens were prepared in the same way to allow for comparisons between treatments. The MICP treatment solution was prepared as two separate solutions: 1) a cementation solution containing calcium chloride ( $\text{CaCl}_2$ ) and urea ( $\text{CO}(\text{NH}_2)_2$ ) and 2) a suspension containing the ureolytic bacteria.

The treatment solution was applied in different ways to determine the effect of the application method. The concentration of the urea and calcium chloride was varied to investigate the effect of reagent concentration. Some specimens were treated by spraying the MICP solution onto the soil surface immediately after mixing the bacteria suspension and the cementation solution. Other specimens were treated with bacteria and reagents sprayed sequentially onto the soil surface in order to achieve a more efficient use and homogeneous distribution of the bacteria and the resulting precipitation rate and prevent the clogging on top of the surface (Harkes et al. 2008). In addition, some specimens were prepared by multiple applications of MICP onto the soil surface with sequential spraying of bacteria and cementation solution. For all the specimens, the two components of MICP treatment solution (i.e., the bacteria suspension and the cementation solution) were applied at a 50:50 ratio with a total volume of  $3 \text{ L/m}^2$ , which corresponds to 120 mL per pan. To determine the effect of urea concentration on treatment effectiveness, different concentrations of substrate solution were applied on samples from each tailings type. The

molar ratio of urea to calcium chloride was kept at 1.5:1 (urea: calcium), which is the optimal ratio based on a study by Song et al. (2019).

#### 3.2.4. Penetration Test

The detachment of the soil particles from the surface is the first step in wind erosion, thus the amount of fugitive dust generated by wind depends on the surface strength of the soil (Chen et al. 2014). A variety of surface strength measurement methods have been used by researchers for this purpose, including the flat-ended cylindrical punch method and a flat-tipped penetrometer (Rice et al. 1997), the fall cone or cone penetrometer (Campbell and O'Sullivan 1990), and the pocket penetrometer that is a flat end cylindrical penetrometer adopted for the field use (Woolley et al. 2022). Rice et al. (1996) recommended a simple flat-ended cylindrical penetrometer method for estimating the surface soil strength as the preferred method because it applies a load to an area with many grains rather than just a few grains as with a needle penetrometer. Chen et al. (2014) recommended flat-ended cylindrical penetrometer method for the crust evaluation as they found a strong correlation between the weight loss from the wind tunnel test and the penetration test results. In this study, the flat-ended cylindrical probe method was used on treated pan specimens to evaluate the strength of the cemented crust. This test is conducted by pushing a cylindrical flat-ended steel probe, 6 mm in diameter, into the samples. The probe affixed to a load cell (Figure 3.1.a) and pushed into the samples at a constant rate of 1 mm/min, while the normal force exerted on the crust and the vertical deformation were recorded (Woolley et al., 2020).



(a) (b)  
**Figure 3. 1.** a) Penetrometer Test on a Pan Specimen and B) Treated Sample after Performing Five Penetration Tests

The durability of the dust suppressant against rain events is an important issue in tailings management. To evaluate durability of the crust to rainfall, rainfall was simulated by spraying water on the specimens' surface at 25 mm/min for 10 min (a total of 2.5 cm of rain) while the pans were allowed to drain through a perforated bottom. After the laboratory rain event, the pans were allowed to dry in the oven at a temperature of 55°C. Specimens were subjected to up to three wetting and drying cycles. Penetration tests were conducted on the specimens following the treatment with the MICP solution and after each rainfall-drying cycle. At least five penetration tests were performed on each specimen pan and the force and penetration were recorded during the test. Figure 3.1. (b) shows a treated sample after performing five penetration tests on it.

### 3.2.5. Carbonate Content Measurement

Carbonate content was measured following ASTM D 4373-84 using Calcimeter, where the carbonate content is based on the volume of carbon dioxide gas generated by the reaction between the hydrochloric acid and the carbonates. The precipitated calcium carbonate content of the crust of each specimen was measured after treatment and after every wash-dry cycle. CaCO<sub>3</sub> content versus depth profiles were determined to provide insight about changes in the carbonate distribution in treated specimens and following washing. To measure the carbonate content, discrete samples were collected from a given depth interval and mixed thoroughly to obtain a representative sample. Each sample was split into two parts for two separate measurements and to quantify the possible variation. The carbonate content of the untreated sample was subtracted from the total carbonate content values to identify the amount of CaCO<sub>3</sub> generated through treatment.

### 3.3. Results and Discussion

The penetration resistance of the specimens was measured after it was dried in the oven after treatment and after multiple wash and dry cycles. The treatment strategy, urea concentration, and the peak strength for the silty sand and silt samples are presented in Table 3.2 and Table 3.3.

For the samples treated using an application procedure in which bacteria and reagents are sprayed sequentially, the maximum peak strengths show similar values as the results for the samples which are treated with mixed bacteria and reagent solution. For all the specimens, the surface strength increases with increasing concentration of urea

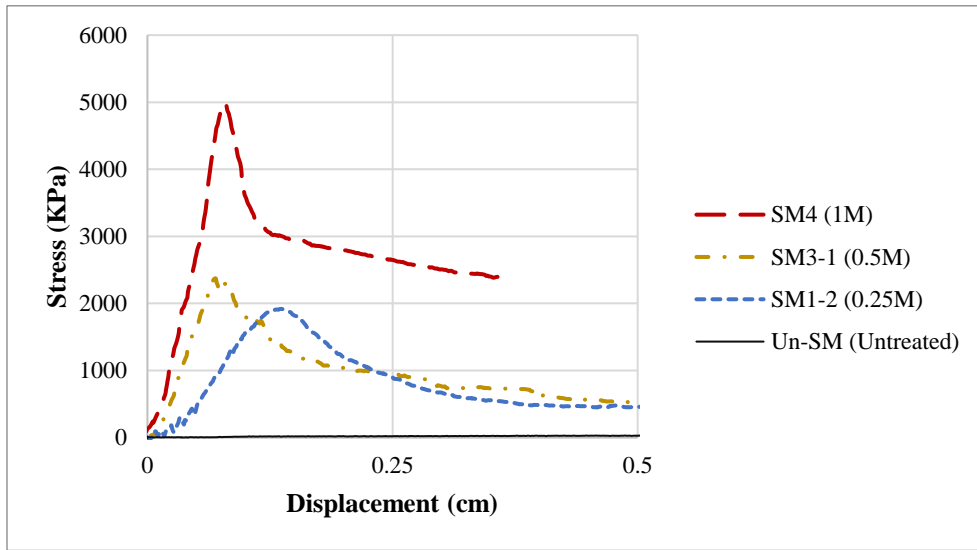
and calcium chloride. Sand specimens have higher strength increase than silt for the same treatment.

**Table 3. 2.** Summary of Treated Samples of Silty Sand and Resulting Peak Strength

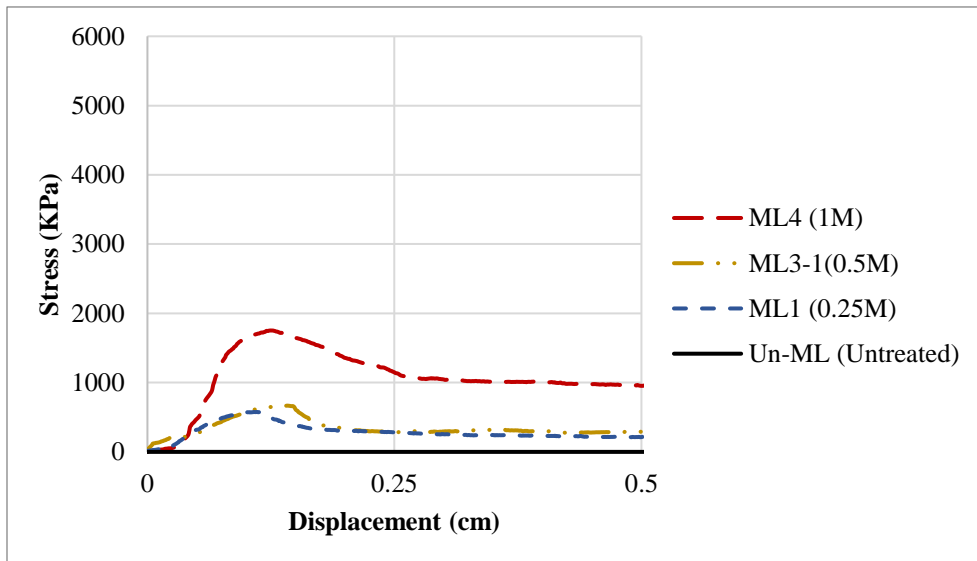
Treatment Strategy	Symbol	Concentration of urea (molar)	Test	Peak strength (KPa)
Untreated	Un-SM	Untreated	No washing	No peak
Mixed solution	SM1	0.25	No washing	1714
Mixed solution	SM2	0.5	No washing	2650
Sequential	SM1-2	0.25	No washing	1900
Sequential	SM3-1	0.5	No washing	2270
Sequential	SM3-2	0.5	No washing	1759
Sequential	SM3-2	0.5	Washed-dried	763
Sequential	SM4	1	No washing	4990
Sequential	SM4	1	2×washed-dried	503
Multiple sequential	SM5	1	No washing	11056
Multiple sequential	SM5	1	Washed-dried	10763
Multiple sequential	SM5	1	2×washed-dried	7965

**Table 3. 3.** Summary of Treated Silt Samples and Resulting Peak Strength

Treatment Strategy	Symbol	Concentration of urea (molar)	Test	Peak strength (KPa)
Untreated	Un-ML	-	No washing	No peak
Mixed solution	ML1	0.25	No washing	593
Mixed solution	ML2	0.5	No washing	741.57
Sequential	ML3-1	0.5	No washing	866
Sequential	ML3-2	0.5	No washing	760
Sequential	ML3-2	0.5	Washed-dried	No peak
Sequential	ML4	1	No washing	1791
Sequential	ML4	1	Washed-dried	1372
Sequential	ML4	1	2×washed-dried	863
Multiple sequential	ML5	1	No washing	4356
Multiple sequential	ML5	1	Washed-dried	3969
Multiple sequential	ML5	1	2×washed-dried	3648



(a)



(b)

**Figure 3. 2.** Penetration Test Results of Specimens after a Single Treatment with Concentrations of 0.25, 0.5, and 1 Molar of Urea in Treatment Solution: a) Sand And b) Silt.

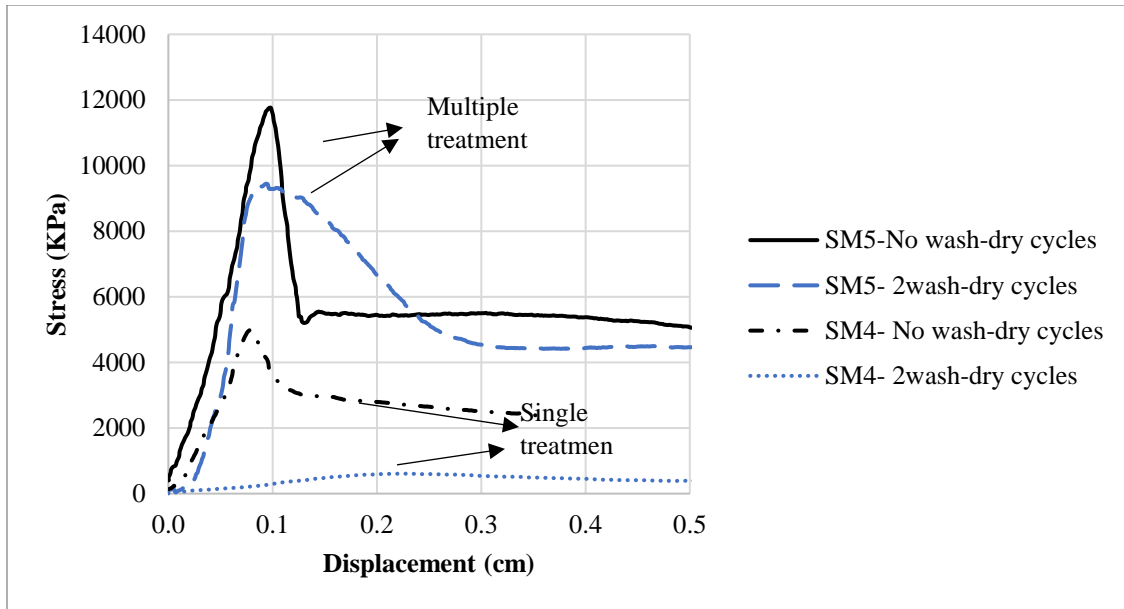
Figure 3.2 shows the result of penetration test of the untreated specimens (UN-SM and UN-ML) and treated specimens after a single treatment with concentrations of 0.25 (SM1-2 and ML-1), 0.5 (SM3-1 and ML3-1), and 1 (SM4 and ML-4) molar of urea. As

the concentration increases from 0.5 M to 1 M, the peak surface strength increases from about 2000 kPa to 5000 kPa in the sand specimens and 800 kPa to 1800 kPa in the silt specimens.

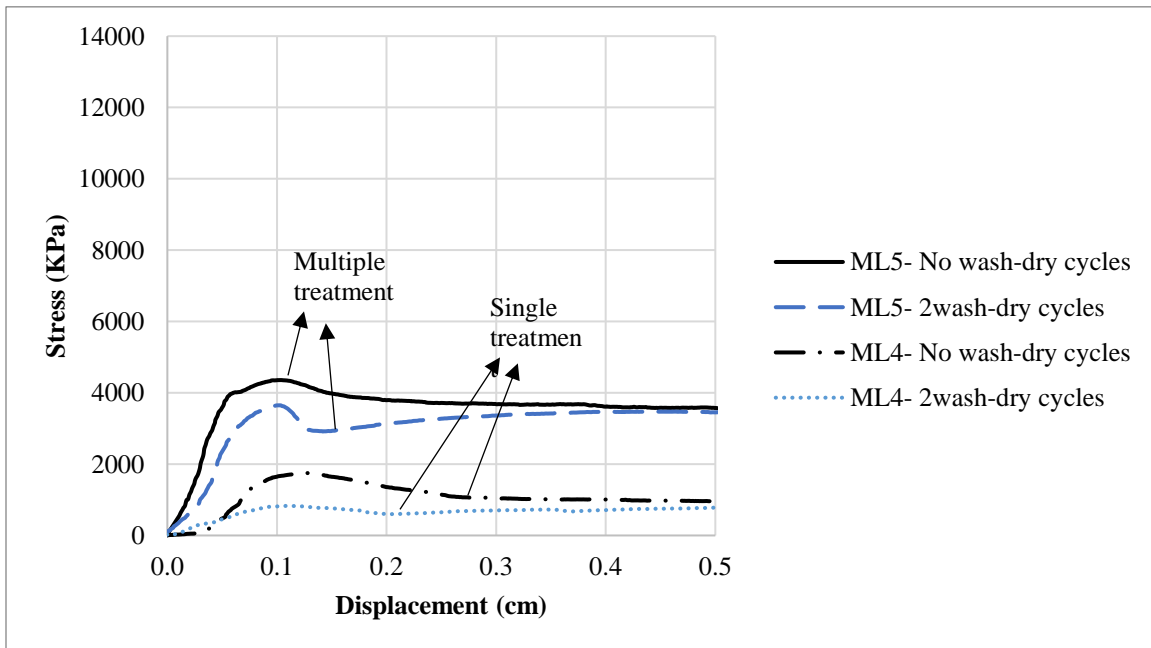
Samples were washed after treatment to check for the durability of the treatment by evaluating the changes in penetration behavior. The washed samples were tested for strength after they were dried again. The silty sand (SM) sample with concentration of 0.5 molar (SM3-2) lost about 50% of the strength after a single wash-dry cycle, whereas the silt (ML) samples showed a significant reduction in stiffness with no clear peak in the strength that indicated weakening of the crust.

To reach a higher level of cementation that results in a stronger and more durable state of the crust, multiple treatments were applied on some samples. These samples were treated three times with a 1 molar concentration of urea and 0.67 molar calcium chloride. There was a significant improvement in surface strength of the specimens subject to multiple treatment cycles compared to the specimens treated a single time with the same concentration. Figure 3.3 shows the penetration results before and after two wash-dry cycles of sand (SM) samples with single and multiple (three times) treatment cycles with a treatment concentration of 1 M of urea. In the sample treated a single time, a significant amount of strength is lost upon two wash-dry cycles. In the sample subject to multiple treatments, the strength showed a significantly lower reduction after several wash-dry cycles. After the second wash and dry cycle, the surface of the soil sample with three cycles of treatment lost only about 25-30% of its peak strength for the sand specimen (SM5) and 10-15% of its peak strength for silt specimen (ML5).





(a)



(b)

**Figure 3. 3.** Penetration Tests Results before and After Wash-Dry Cycles of Specimens with Single and Multiple Treatment (1M Concentration of Urea): a) Sand and b) Silt.

The carbonate content profiles of samples from the crust were measured for each specimen to evaluate the relation between the resulting strength and precipitated  $\text{CaCO}_3$ . Figure 3.4 (a) shows the profiles of carbonate content from top to the bottom for the sand specimens subject to a single treatment (0.5 M) with no washing (SM3-1) versus a similar sample (SM3-2) after one cycle of wash and dry. The unwashed sample showed the highest level of  $\text{CaCO}_3$  at the surface, rapidly decreasing with depth. At 2 cm depth, no  $\text{CaCO}_3$  was found. The average carbonate content did not decrease by washing, but the profile moved downwards from surface to the bottom with washing. Figure 3.4 (b) shows the profiles of carbonate content for the sand (SM) specimens with single treatment versus multiple treatments after they were subjected to three wash and dry cycles. The sand sample still showed the highest calcium carbonate content at the surface after three wash and dry cycles, reaching almost 3% for the sample with three treatment cycles. The silt sample with multiple treatment seemed to show some wash out of  $\text{CaCO}_3$  from the surface to deeper levels after 3 cycles of wash and dry as shown in the figure 3.4 (d).

The results of the tests presented in Figures 3.3 and 3.4 indicate that MICP treatment increases the surface strength of soil samples and that higher concentrations leading to greater strength increases. This pattern of behavior may be mainly attributed to the bonding of  $\text{CaCO}_3$  between the soil particles.

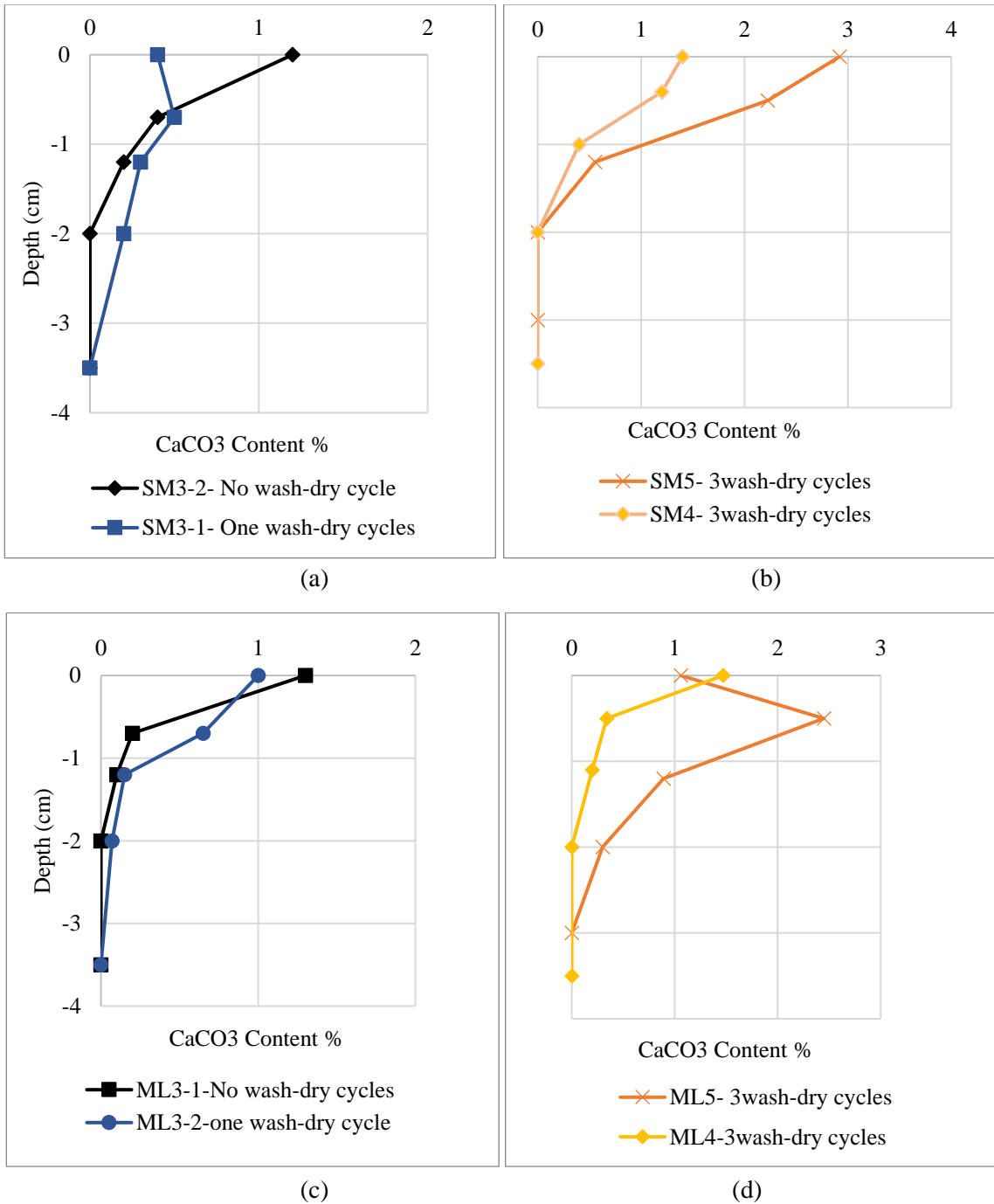


**Figure 3. 4.** The Precipitated Carbonate Content Profiles (a-b) Sand: a) Samples Treated with 0.5 M Concentration of Urea Before and after One Wash-Dry Cycle. b) Samples Treated with Single and Multiple Treatment (1M Concentration of Urea) after Three Wash-Dry Cycles. (c-d) Silt: c) Samples Treated with 0.5 M Concentration of Urea before and after One Wash-Dry Cycle. d) Samples Treated with Single and Multiple Treatment (1M Concentration of Urea) after Three Wash-Dry Cycles.

A significant strength increase was achieved by spraying higher concentrations of urea and calcium chloride and applying multiple flushes which increased the carbonate content to up to about 3% for sand and 2.5% for silt. Besides showing a higher strength and CaCO<sub>3</sub> content, the durability was significantly improved upon 3 cycles of treatment.

### 3.4. Conclusions and Recommendations

In this study the potential of using MICP by urea hydrolysis as a dust suppressant for mine tailings was evaluated using penetration resistance and carbonate content as the metric for performance. An experimental study was performed to optimize the treatment strategy and assess the strength performance and durability of the cemented crusts using penetration testing and calcium carbonate content analysis. The study employed two dust-susceptible tailings specimens, one classified as a silty sand (SM) and one as a low plasticity silt (ML). The main conclusions of this experimental study are:

- For both types of the soils MICP treatment resulted in the formation of a crust layer on the surface.
- Both metrics (carbonate content and strength) increased with an increase of the solution concentration and number of treatment applications.
- Sand specimens have higher increase from their untreated strength than silt for the same treatment.
- Three MICP treatment applications with a 1 M urea and 0.67 M Calcium chloride solution resulted in significantly higher peak strength than any of the other treatment methods.

- In the specimens subjected to multiple treatment cycles, the strength and  $\text{CaCO}_3$  content prevailed even after multiple (three) washing and drying cycles.
- This consistent performance of multiple treatment approach in both silty sand and silt specimens suggests that this approach is the most effective method, as it leads to a substantial increase in strength and maintains the  $\text{CaCO}_3$  and strength after three washing and drying cycles.

## CHAPTER 4

### 4. INFLUENCE OF FREEZE-THAW CYCLES ON TAILINGS STABILIZED FOR FUGITIVE DUST MITIGATION USING ENZYME-INDUCED CARBONATE PRECIPITATION.

#### ABSTRACT

The effectiveness of using enzyme-induced carbonate precipitation (EICP) for fugitive dust mitigation of tailings subject to the freeze-thaw cycles was evaluated in the laboratory. Wind erosion and the resulting fugitive dust emission is an environmental concern associated with many mine tailings impoundments. EICP offers a potentially sustainable and cost-effective mitigation method for fugitive dust generation by forming a wind erosion-resistant crust on the soil through precipitation of calcium carbonate ( $\text{CaCO}_3$ ) that binds the soil particles together. However, seasonal freeze-thaw cycles may disaggregate the tailings, eliminating the beneficial effect of EICP stabilization.

Two types of iron ore mine tailings, a poorly graded fine sand (SP) and a well-graded sand (SW), were tested to evaluate the effect of freeze-thaw cycles on the fugitive dust resistance of EICP-treated specimens. The specimens were prepared and treated by two applications of EICP solutions with concentrations of 0.5, 0.75, and 1 molar of calcium chloride and urea. The fugitive dust resistance on the specimens was assessed experimentally in the laboratory using the Portable In-Situ Wind EROsion Lab (PI-SWERL<sup>TM</sup>) device, performing strain-controlled penetration tests, and measuring the

CaCO<sub>3</sub> content of the treated samples. All the tests were performed on untreated samples and EICP-treated samples after 0, 3, 5, 7, and 10 freeze-thaw cycles.

The results of the laboratory tests indicated that EICP treatment on the poorly graded fine sand resulted in the formation of a dust-resistant crust on the specimens which remained mostly intact even after undergoing 7 cycles freezing and thawing. However, EICP treatment of the specimens prepared from the well-graded sand failed to create a dust-resistant crust in specimens with low treatment solution concentrations (0.5 and 0.75 molars) while a crust formed following treatment but lost its dust resistance after undergoing even 3 cycles of freezing and thawing. However, by increasing the concentration of cementation solution to 1 molar, erosion resistance after treatment was improved and remained elevated after 3 freeze-thaw cycles. Subsequent removal of coarse particles (i.e., particles larger than 0.425 mm) from the well-graded tailings facilitated effective binding of smaller soil particles through carbonate precipitation via EICP, forming a cohesive structure that was durable when subjected to 10 freeze-thaw cycles.

#### 4.1. Introduction

Mine tailings are the relatively finely ground waste that remain after removing the ore and main products of extracted materials from the mine. They often have no economic value and are mixed with water and processing fluid to facilitate discharge into impoundments as a thickened slurry. Embankment dams are built from the coarse tailings to retain the slurry and the tailings after they settle out of the slurry in the impoundment.

These dams are raised during the life of the mine as needed by active discharge of tailings material (Mendez and Maier, 2008). Due to the large surface area of the impoundments and the typically small particle size of the tailings material, tailings are susceptible to wind erosion and wind-blown dust (i.e., fugitive dust) is a significant environmental concern associated with tailings impoundments (Zwissler 2016). When eroded by wind, the fine particles in the tailings can become airborne and spread over a wide area. This can result in a range of negative impacts, including soil and water contamination, health hazards, and habitat destruction (Blight 2008; Bang et al., 2009; Chen et al., 2014).

Proper management and containment of tailings can help minimize the potential for environmental impacts of wind erosion. Some of the techniques to reduce wind erosion and contain dust at tailing impoundments include building barriers, planting vegetation, and covering the tailings with a layer of clean soil or other material to prevent exposure of the tailings to the wind (Watson et al., 2000). To develop a method for controlling wind erosion of tailings, it is essential to understand how the tailings are affected by wind erosion and how to detect when they may be susceptible to fugitive dust generation.

To properly assess the efficiency of a fugitive dust control method, it is necessary to test it in an experimental setting that simulates the same type of disturbance that occurs to the surface soil. In northern climates in North America, when the soil experiences freeze-thaw, the soil structure is disturbed during freezing due to the ice expansion, after thawing, this results in a reduction in shear strength (Zwissler 2016) and that increases dust susceptibility of soil (Zhang et al. 2021).



For soils that experience dust generation due to freezing and thawing, chemical dust suppression has been shown to be ineffective (Vasher 1999; Zwissler 2016). However, bio-based enzyme induced carbonate precipitation (EICP) and microbially induced carbonate precipitation (MICP) technologies offer a potentially sustainable and cost-effective mitigation method for fugitive dust from mine tailings in cold climates by forming a dust-resistant crust on the soil through the precipitation of natural calcium carbonate ( $\text{CaCO}_3$ ) cement if it can be demonstrated that the crust resists the effects of freezing and thawing.

The effect of freeze-thaw on biocemented sand columns created in the laboratory using MICP has been investigated (Gowthaman et al., 2020; Sharma et al., 2021). Gowthaman et al. studied the shear responses of cemented slopes treated by MICP to control the erosion induced by cyclic freeze-thaw. Sharma et al. investigated the effect of freeze-thaw cycles on shear strength and shear modulus on a liquefiable sand. But, to date, no study has looked at using the EICP method for wind erosion control in soils susceptible to freeze-thaw cycles. In this study, the effects of freeze-thaw cycles on the surface strength and wind erosion resistance of mine tailings in which a biocemented crust formed through EICP was investigated. Two types of tailings, a poorly graded fine sand (SP) and a well graded sand (SW), were subject to freeze-thaw cycles. After freeze-thaw cycles, the crust strength and wind resistance of the crust were evaluated by penetration testing, PI-SWERL testing, and calcium content measurements of the cemented crust.

## 4.2. Materials and Methods

### 4.2.1 Tailings Characterization

Two types of tailings (SP and SW) from an iron mine tailings impoundment were classified using ASTM D2487-17. Additionally, to account for the influence of large particles on crust formation (as discussed later in this chapter) a third soil sample, SW-SM, was obtained by separating smaller particles from SW sample. SP-SM is also characterized herein. Hydraulic conductivity was determined following the falling head tests as described in ASTM 5084, using the KSAT device (Metergroup, Pullman, Oregon). Carbonate content was measured following ASTM D 4373-84, where the carbonate content is based on the volume of carbon dioxide gas generated by the reaction between hydrochloric acid and the carbonates in the specimen. The results of the classification tests are shown in Table 4.1. The grain size distributions for the three materials tested herein are presented in Figure 4.1.

**Table 4. 1.** Results of Soil Classification of the Tailings

Soil type	Unit	SP	SW	SP- SM
4.75 mm < Gravel fraction	[%]	0	8.7	0
0.075 mm < Sand fraction < 4.75 mm	[%]	97.4	87.9	88.8
Fine fraction < 0.075 mm	[%]	2.6	3.4	11.2
Cc	[-]	2.17	1	0.9
Cu	[-]	1.21	8	3.33
USCS Classification	[-]	SP	SW	SP - SM
Hydraulic conductivity	[m/s]	$4.83 \times 10^{-5}$	$6.36 \times 10^{-5}$	$2.5 \times 10^{-5}$
Natural CaCO <sub>3</sub> content	[%]	4.15	4.87*	4.87

\*Carbonate content of only particles smaller than 0.425 mm were measured for the samples of this soil.

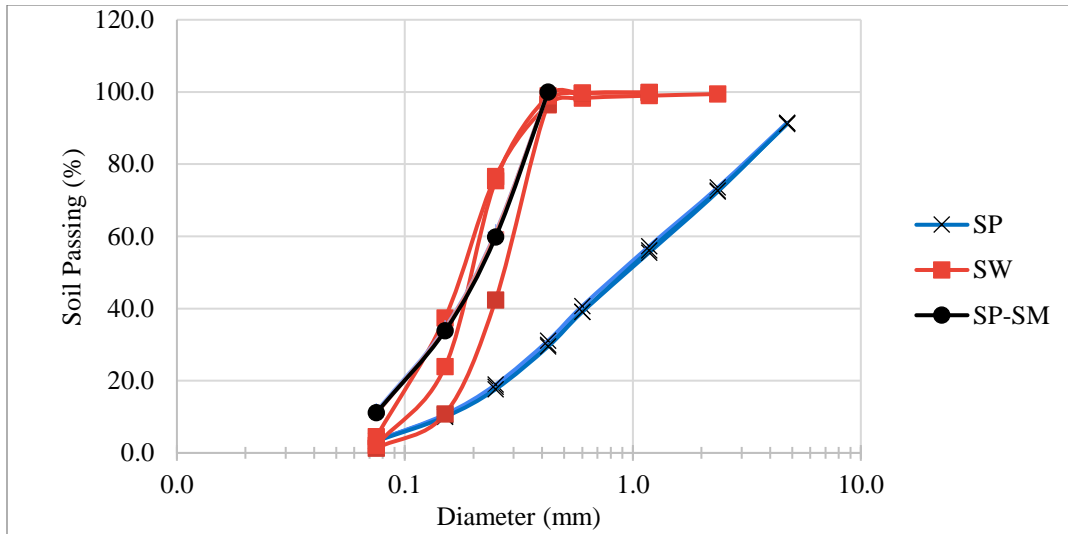


**Figure 4. 1.** Grain Size Distribution of Two Types of the Tailings

#### 4.2.2. Specimen Preparation and Treatment

To prepare the specimens for PI-SWERL and penetration testing, round containers made of polystyrene foam with a volume of 1.7 liters, a diameter of 24 cm, and a depth of 3.8 cm were used. Polystyrene foam was used so that freezing can occur in one dimension (from the surface of the specimen downward). Tailing materials were loosely placed in the polystyrene containers by dry pluviation and the surface was leveled at the top of the container. All the specimens were prepared in the same way to allow for comparisons between test results. The initial moisture content of the samples as they were received varied between 5 to 10 percent by mass. Water was added to the specimens of SP and SW soils to reach a water content of 30 percent, which was assumed to be the representative of maximum surface moisture content of the tailings in cold-weather climates based upon Zwissler (2016). All other specimens were prepared with the initial moisture content of the tailings (i.e., 5 to 10 percent). The varied moisture content of the specimens was

employed to investigate the formation of an EICP crust in different field conditions and the effect of freeze-thaw on moist-treated specimens.

The EICP treatment solution was prepared as two separate solutions: 1) a cementation solution containing calcium chloride ( $\text{CaCl}_2$ ) and urea ( $\text{CO}(\text{NH}_2)_2$ ) and 2) an enzyme solution containing both the urease enzyme extracted from jack beans (25 mL/L of the total final treatment solution) and fat-free milk powder (4g/L of the total final treatment solution).

Specimens were treated by spraying the EICP solution onto the soil surface immediately after mixing the two above-mentioned solutions with a total volume of 3 L/m<sup>2</sup>, which corresponds to 135 mL per specimen. All specimens were subjected to two applications of EICP (at a 24 hr interval) onto the soil surface uniformly at a rate designed to reach the target concentrations of the urea and calcium chloride. Specimens were prepared from SP and SW soils at concentrations of 0.5M, 0.75M, and 1M. Specimens from SP-SM soil were prepared at two treatment concentrations of 0.5M and 1M. The specimens were given enough time to react and form the crust and were then saturated with water followed by free draining from the bottom just before putting them into a freezer at a temperature of -20° C. This process was repeated following thawing the specimen for each cycle of freeze/thaw. However, one specimen from each treatment concentration did not undergo freezing and thawing. All the specimens were dried in the oven after thawing in the last freeze-thaw cycle and before PI-SWRL and penetration testing. Figure 4.2 shows the specimens prepared by SP and SW soils in polystyrene foam containers after they are treated by application of EICP.

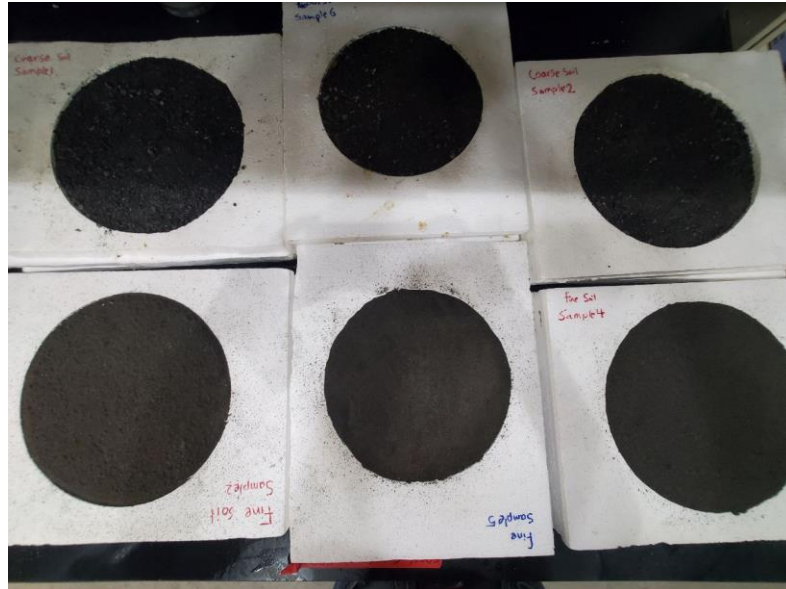


**Figure 4. 2.** Specimens Prepared by SP and SW Soils in Polystyrene Foam Containers after They Are Treated by Application of EICP.

#### 4.2.3. Freeze-Thaw Process

The freeze-thaw tests were conducted in accordance with the methodology recommended in ASTM D 5312-04 (1997). This standard calls for a freezing period of 12 hours at  $-20 \pm 1^\circ\text{C}$  followed by a thawing period of 12 hours at room temperature ( $25 \pm 1^\circ\text{C}$ ) per cycle.

The impact of freeze-thaw cycles on the dust susceptibility of specimens was assessed using the PI-SWERL machine, penetration testing, and carbonate content measurements. The freeze-thaw testing started with 3 cycles of freeze and thaw and continued up to 10 cycles based on the results from the testing of these specimens.

#### 4.2.4. PI-SWERL Test

The PI-SWERL® (portable in-situ wind erosion laboratory), as described by Etyemezian et al. (2007), is a device that measures the emission of particulate matter with an aerodynamic diameter of  $\leq 10\mu\text{m}$  (PM10) from surfaces that are subject to wind erosion.

This device has a rotating blade in cylindrical chamber that creates a wind shear correlated to the rotational velocity of the blade, entraining soil, sand, and dust particles into the chamber. Figure 4.3 shows the PI-SWERL device and the rotating blade in the chamber.

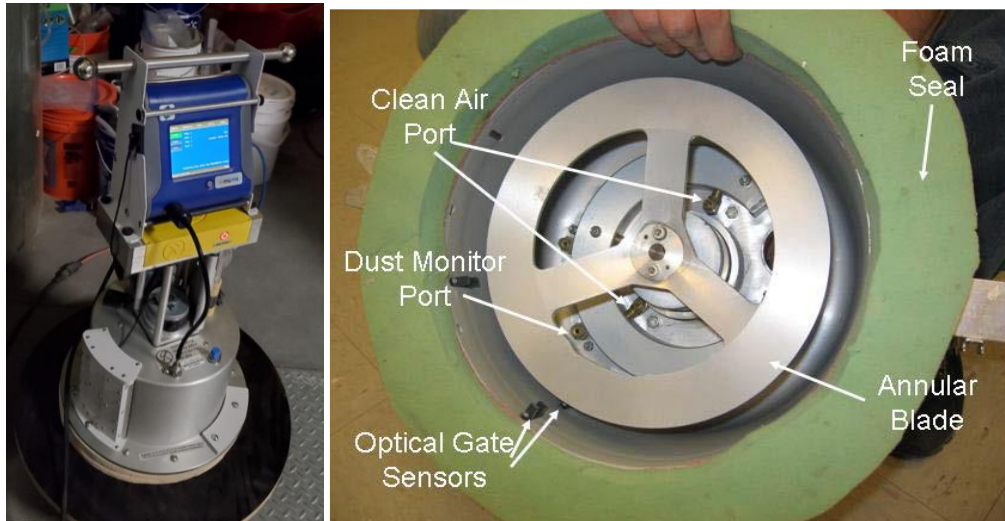


**Figure 4. 3.** The PI-SWERL Device and the Rotating Blade in the Chamber. (Etyemezian et al. 2014).

The DustTrack nephelometer measures concentrations of PM<sub>10</sub> (mg/m<sup>3</sup>) over four orders of magnitude as the rotational speed of the blade progressively increased. Concentrations measured by the DustTrack are converted to total mass of dust (in micrograms) that has been suspended since the beginning of the measurement in subsequent analyses by the software that accompanies the PI-SWERL device. In this study, the dust mass per unit surface area (mg/m<sup>2</sup>) is reported. This value is determined by dividing the total dust mass by the effective surface area of the PI-SWERL (0.035 m<sup>2</sup>) from which PM<sub>10</sub> is

generated. Figure 4.4 presents the test cycle that was run by PI-SWERL over the specimens.

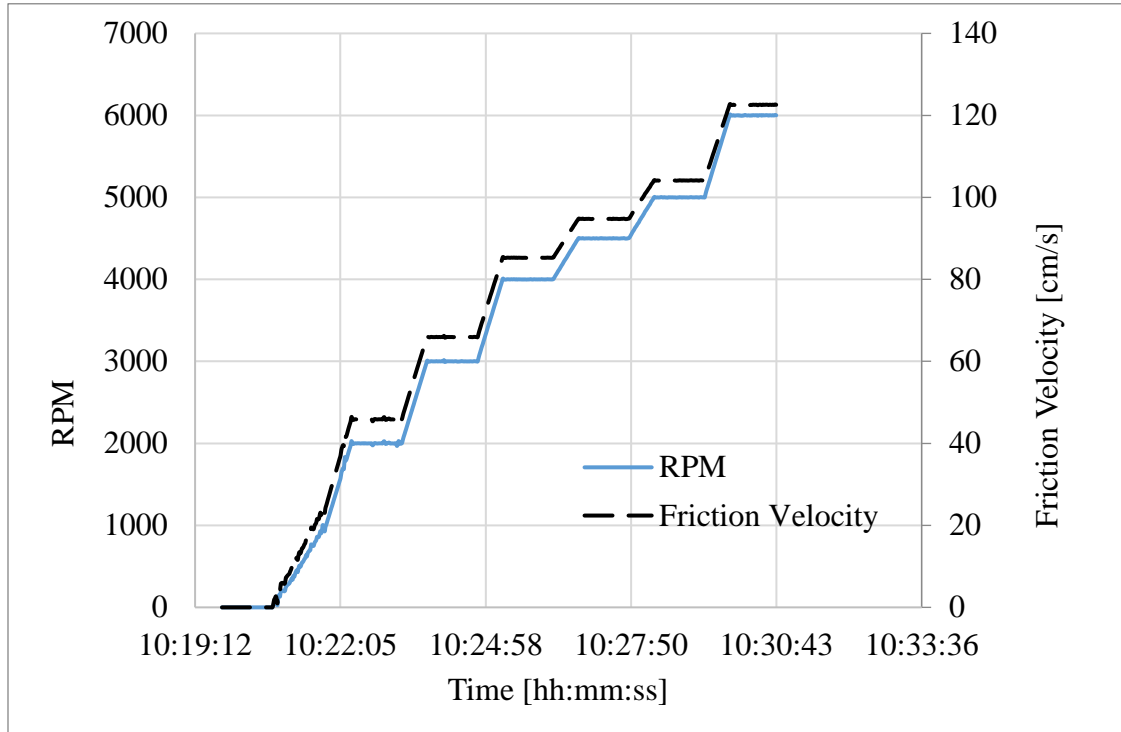


**Figure 4. 4.** Test Cycle of PI-SWERL for Running Over the Specimens

The program was defined to be held at 0 rpm for 60 seconds to clear the system of particles from previous test runs. The rotor speed then was increased to 2000 rpm over a 90 second period and held constant for 60 seconds. The speed increased over 30 seconds and then hold constant for 60 seconds was for rotor speeds of 3000, 4000, 4500, 5000, and 6000 rpm (the limit of the device) before dropping to 0 rpm for 30 seconds at the end of the test run. Each rotor speed relates to a friction velocity ( $u^*$ ) through an empirical expression (Eq. 4.1) provided by Etyemezian et al. (2014).

$$u_* = C_1 \alpha^4 RPM^{C_2/\alpha} \quad (4.1)$$

where  $C_1$  is a constant (=0.000683) and  $C_2$  is a constant (=0.832) and the value of  $\alpha$  depends on the surface roughness. The surface roughness in this study is considered to be 0.93.

Besides the data from DustTrack, four optical gate sensors (OGS) are included as part of the PI-SWERL instrumentation. The OGS sensors measure the number of saltating particles passing the sensor, expressed in Hz. (Vos et al. 2021). The OGS sensors (two sensors at each of two heights above the surface being tested) are designed to assess sand motion induced by the rotating blade inside the PI\_SWERL's chamber. The measurements from the PI-SWERL therefore offer indications of both sand motion and dust concentrations, although the OGS sensors did not provide any useful data probably due to the abrasion of these sensors over time. In this study, the results from DustTrack, i.e., the PM10 measurements, are considered the primary metric for evaluating windblown dust emissions from the tested specimens.

Compared to traditional straight-line wind tunnels, the PI-SWERL® is more accessible to researchers due to its compact size, portability, and ease of use. Furthermore, it is more efficient than observational studies that are influenced by unpredictable weather patterns because it can collect repeated measurements over a shorter period of time (Munkhtsetseg et al. 2016). In this study, the PI-SWERL test was run first on all specimens, prior to penetration testing or carbonate content measurement.

#### 4.2.5. Penetration Test

The properties of the soil surface in the upper few centimeters are important for characterizing the dust susceptibility of a soil. Therefore, in addition to PI-SWERL



testing, surface strength measured through penetration testing was used for characterizing the specimen's susceptibility to dust. The penetration test involved using a 6 mm diameter cylindrical steel probe with a flat end attached to a universal testing machine with rate control and a load cell. This probe was advanced into the samples at a constant rate of 1 mm/min while recording both the normal force and vertical deformation. Penetrometer testing is more accurately described as a bearing capacity test. However, because penetrometers only penetrate the surface and near-surface of the soil, they can be used as an index of surface shear strength. In this study, penetration tests were conducted on all specimens, both with and without freeze-thaw cycles.

#### 4.2.6. Calcium Carbonate Content Measurement

Carbonate content was measured following ASTM D 4373-84, where the carbonate content is based on the volume of carbon dioxide gas generated by the reaction between hydrochloric acid and the carbonates in the specimen. The calcium carbonate content of the crust of all specimens was measured after treatment and after each freeze-thaw cycle. To measure the carbonate content, discrete samples were collected from the surface of the sample (from up to 0.5 cm in depth) and mixed thoroughly to obtain a representative sample. Each sample was split into three parts for three separate measurements to quantify the possible variation of carbonate content. For the SW sample only the small soil grains (smaller than 0.425 mm) were collected from the crust of specimens and used for carbonate content measurements.

### 4.3. Results and Discussion

To confirm the formation of a crust on the treated tailings specimens before any disturbance, and to observe its changes after undergoing various freeze-thaw cycles, all the samples were visually assessed. A distinct crust was formed in the specimens from SP soil except for the specimens which were treated with an initial moisture content of 30%. The summary of the test results for SP soil is presented in Table 4.2. The detailed results of each measurement method will be presented in the following sections.

**Table 4. 2. Summary of Treated Samples and Treatment Results for SP Soil**

Specimens Symbol	Treatment Concentration (Molar)*	Freeze-thaw Cycles	PI-SWERL test- Total mass ( $\mu\text{g}$ ) at 85 cm/s	Penetration test- Average Peak strength (KPa) **	Deformation at peak strength (mm)	Precipitated Calcium carbonate content of crust (%)
SP0	Untreated	-	2160	20	1	0
SP1	0.5M	-	33	1600 $\pm$ 110	2	0.54
SP2	0.5M	3	208	1150 $\pm$ 100	1	0.34
SP3	0.75M	-	38	2150 $\pm$ 190	1.2	0.61
SP4	0.75M	3	21	1350 $\pm$ 16	2	0.81
SP5	0.75M	5	150	1180 $\pm$ 117	1.7	0.69
SP6	0.75M	7	57	1120 $\pm$ 50	2	0.77
SP7	1M	-	12	3200 $\pm$ 20	3	1.10
SP8	1M	7	10	-	-	1.49
		10	45	2900 $\pm$ 135	2.1	
SP9w	0.5M	-	200	385 $\pm$ 14	2	0.14
SP10w	0.5M	3	970	155 $\pm$ 25	1.5	0.22

\*All treated specimens received 2 cycles of treatment

\*\*A minimum number of two penetration tests were run on each specimen

For the SW soil specimens, a well-defined crust was not visible, and the relatively coarse particles (coarse sand and gravel sized) appeared loose and uncemented on the surface.

However, the SP-SM specimens that contained only the fraction smaller than 0.425 mm of SW soil showed a distinct and unbroken crust. The summary of the test results for SW soil and the SP-SM soil is presented in Table 4.3. A detailed discussion of the results of each measurement method is presented in the following sections.

**Table 4. 3.** Summary of Treated Samples and Treatment Results for SW and SP-SM Soil

Specimens Symbol	Treatment Concentration (Molar)*	Freeze-thaw Cycles	PI-SWERL test- Total mass ( $\mu\text{g}$ ) at 85 cm/s	Penetration test- Average Peak strength (KPa)**	Deformation at peak strength (mm)	Precipitated Calcium carbonate content of crust (%)
SW0	Untreated	-	1500	900 $\pm$ 103	2.3	0
SW1	0.5M	-	85	820 $\pm$ 220	2.3	0.29
SW2	0.5M	3	500	650 $\pm$ 10	2.1	0.24
SW3	0.75M	-	220	1200 $\pm$ 150	1.9	0.51
SW4	0.75M	3	1620	500 $\pm$ 10	2.5 $\pm$ 0.2	0.45
SW5	1M	-	20	4280 $\pm$ 300	3.2 $\pm$ 0.7	1.30
SW6	1M	3	16	2680 $\pm$ 100	3.2	0.89
SW9w	0.5M	-	220	680 $\pm$ 14	2.8 $\pm$ 0.4	0
SW10w	0.5M	3	52	630 $\pm$ 50	2.6	0
<b>Subset of SW soil: grain size <math>\leq</math> 0.425 mm</b>						
SP-SM11	0.5M	-	500	2250 $\pm$ 180	2.4	0.37
SP-SM12	0.5M	5	532	1350 $\pm$ 47	2.3	0.45
SP-SM13	1M	-	33	2500 $\pm$ 50	3.2	1.00
SP-SM14	1M	10	130	2300 $\pm$ 55	3.1	0.96

\*All treated specimens received 2 cycles of treatment

\*\*A minimum number of two penetration tests were run on each specimen

#### 4.3.1. Penetration Test Results

The penetration resistance was measured for the untreated and EICP- treated specimens, including those that did not undergo any freeze-thaw and those that underwent freeze-thaw cycles. Specimens from SW soil demonstrated a higher untreated surface strength

compared to those from SP soil. Figure 4.5 displays penetration test results for untreated specimens of both soils. SW soil specimen exhibits a higher surface strength than SP soil specimen. This is probably due at least in part to the higher ratio of the particle-probe diameter in SW soil compared to SP soil.

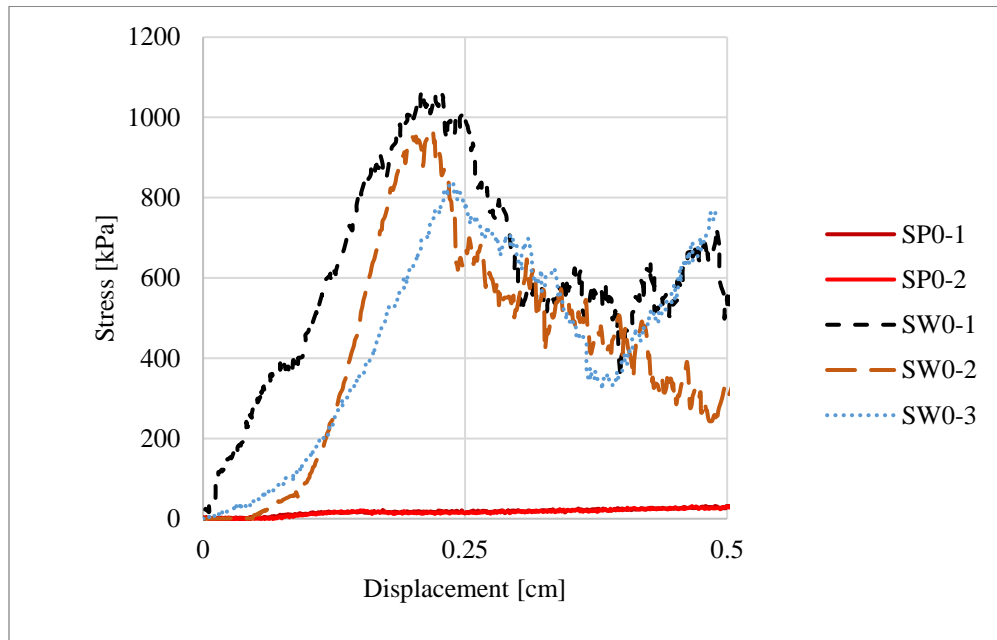


**Figure 4. 5.** Penetration Test Results for Untreated Specimens of SP and SW Specimens.

#### *SP soil*

In SP soil, the EICP-treated specimens consistently exhibit higher surface strength compared to the untreated specimens, with a further increase observed as the concentrations of urea and calcium chloride are raised. When subjected to 3 freeze-thaw cycles, specimens of SP soil exhibited a decrease in penetration resistance. However, as the number of freeze-thaw cycles increased, the additional reduction in strength was less pronounced. For the specimens treated with 0.5M cementation solution, when treated in a

high moisture condition (moisture content of 30%), the specimen (SP9w) showed 70% lower penetration resistance compared to the specimen with a low moisture condition of 5-10% (SP1). This may have been due to the difference between the capillary force in various saturation conditions. In unsaturated condition, capillary enables soil to retain the solution and there is more interaction between dissolved and suspended matter in the liquid (enzymes in the case of EICP) and the surface of the grains. As the saturation degree rises, the treatment solution drains further down that causes insufficient cementation of the grains. Replicated treated specimens, SP10w and SP2, exhibited about 60% and 30% less penetration resistance following three freeze-thaw cycles, respectively. For the samples with higher concentrations of cementation solution (i.e., 1M), the penetration resistance increased and the strength loss due to the freeze-thaw cycles was significantly less than that for the specimens treated with 0.5M of cementation solution. Figure 4.6 presents the plots of average peak strength of SP soil specimens as a function of number of freeze-thaw cycles for different treatment solution concentrations.

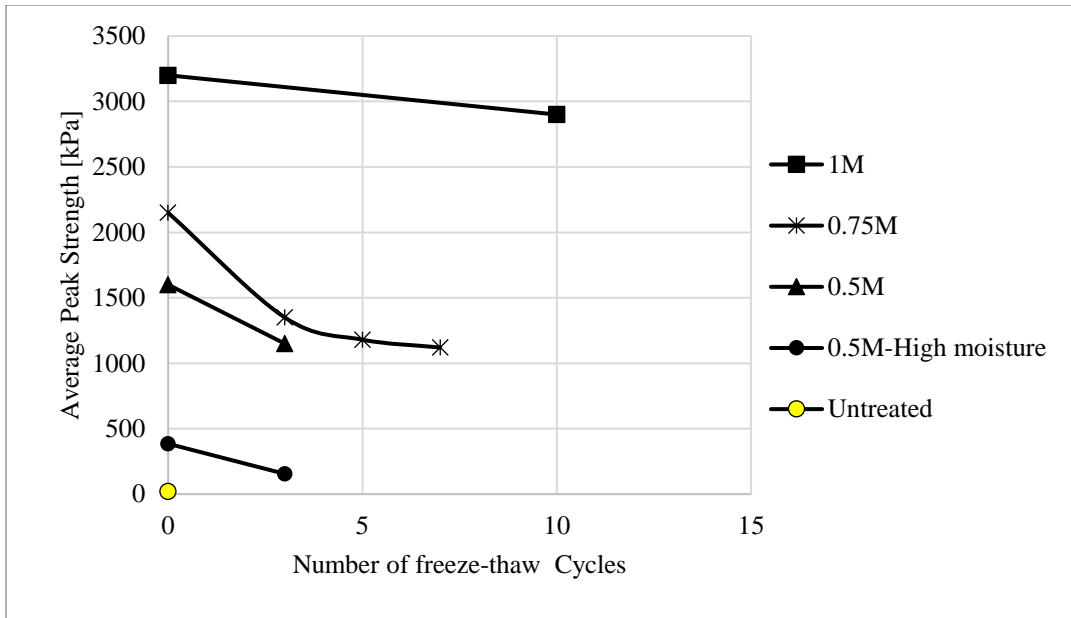


**Figure 4. 6.** Average Peak Strength of SP Specimens vs. Number of Freeze-Thaw Cycles

Figure 4.7 presents the penetration test results for SP specimens treated with different treatment concentrations, before and after freeze-thaw cycles. For each sample designation, the numerical components represent specific information: the first number corresponds to the sample number, the second number signifies the penetration number, the third number denoted by 'M' indicates the treatment concentration, and the fourth number marked with 'FT' represents the number of freeze-thaw cycles if there was any Freeze-thaw cycle, if applicable, for that sample.

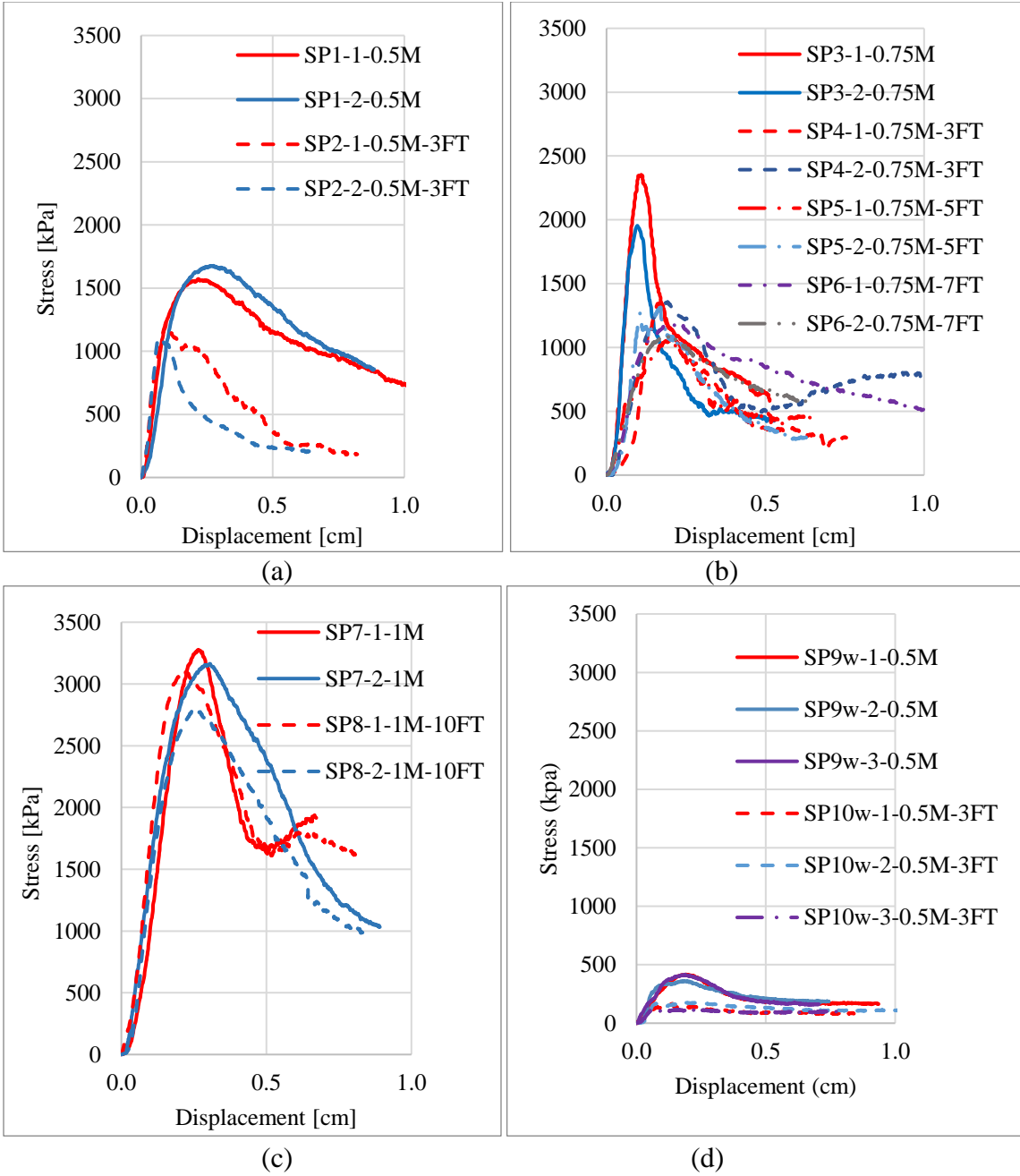


**Figure 4. 7.** Penetration Test Results of the Specimens from SP Soil Treated with Concentrations of 0.5M (a), 0.75M (b), 1M (c), and 0.5M with 30% Saturation (d); with no Freeze-thaw (Solid Lines) and with Freeze-Thaw (Dashed Lines) Cycles.

### *SW soil*

For SW soil, treatment had a less pronounced effect on increasing the strength (i.e., penetration resistance) as compared to SP soil for concentrations of 0.5 and 0.75 M. The effect of treatment on penetration resistance is not clear except when using the high concentration of 1 M. For the specimens treated with 0.5M cementation solution, the surface strength of the specimens with different moisture contents (SW1 and SW9w) was comparable with that of the untreated samples (SW0). It is possible that the penetration resistance obtained for these samples is not reliable, perhaps elevated, due to the presence of the coarse-grained fraction. This hypothesis is in accordance with the observations made by other researchers who have noted that evaluating gravelly soil properties with the Standard Penetration Test (SPT) or Cone Penetration Test (CPT) presents challenges due to significant particle size-to-penetrometer diameter ratios (DeJong et al. 2017; Daniel et al. 2004). Figure 4.8 presents the plots of the average peak strength of SW specimens as a function of the number of freeze-thaw cycles, for different treatment concentrations.



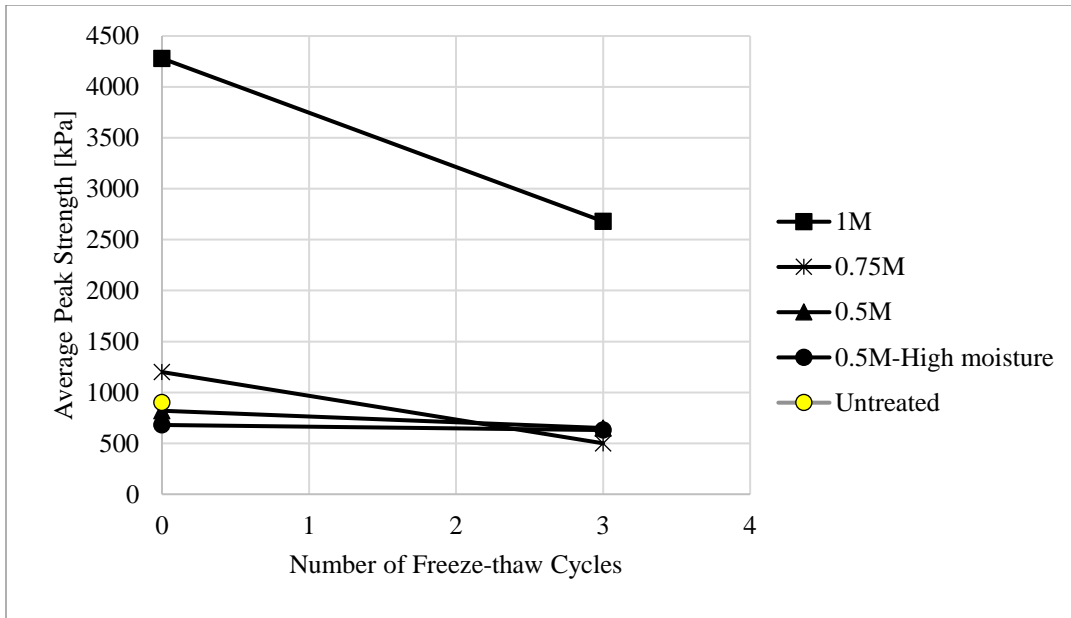


**Figure 4. 8.** Average Peak Strength of SW Specimens vs. Number of Freeze-Thaw Cycles

The penetration test results of all SW specimens are presented in Figure 4.9.

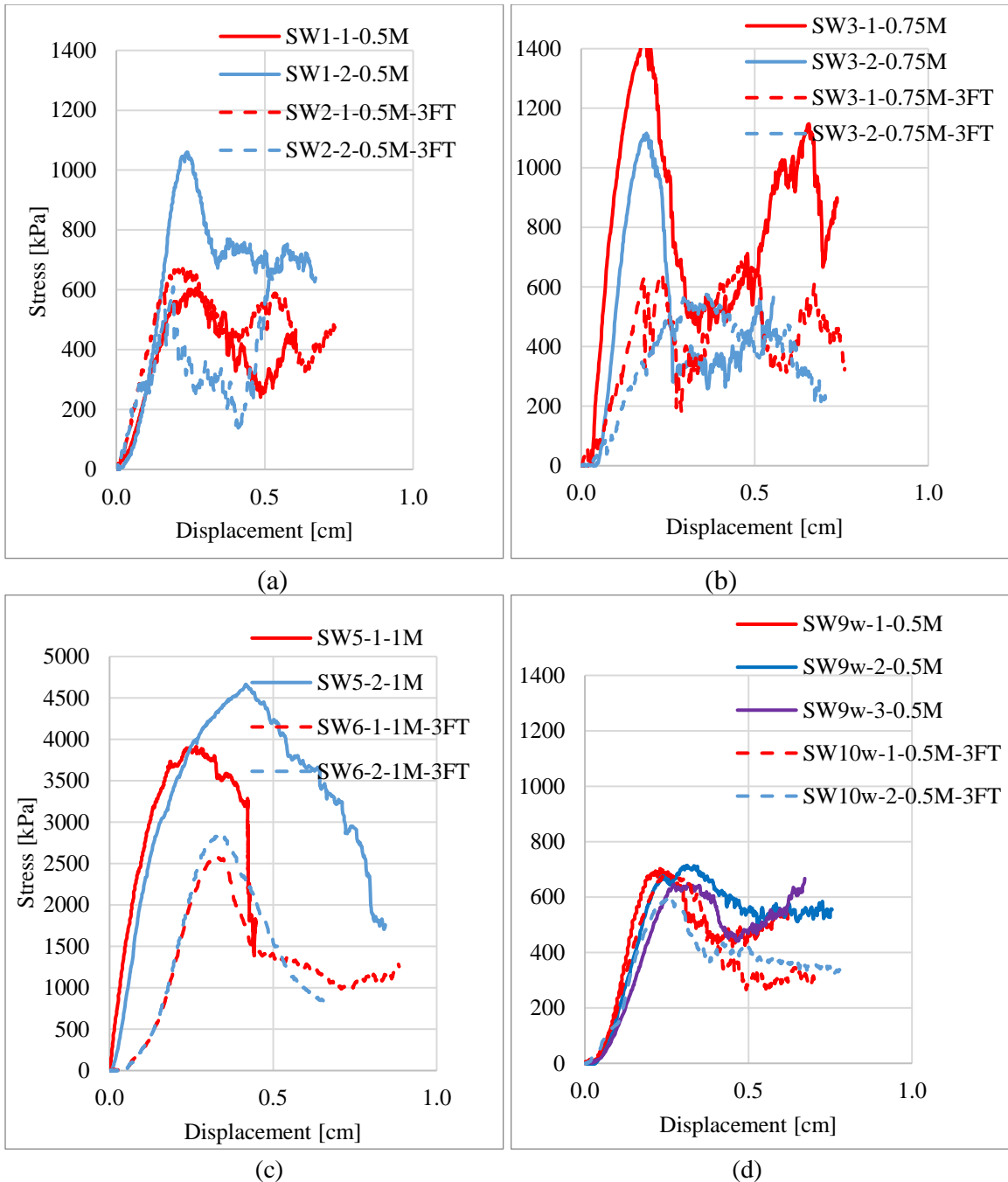


**Figure 4. 9.** Penetration Test Results of the Specimens from SW Soil Treated with Concentrations of 0.5M (a), 0.75M (b), 1M (c), and 0.5M with 30% Saturation (d); with No Freeze-Thaw (Solid Lines) and with Freeze-thaw (Dashed Lines) Cycles.

*SP-SM soil*

For the finer-grained fraction of SW soil, referred to herein as SP-SM, the 0.5M EICP-treated specimens showed a higher surface strength compared to the untreated specimens. A further increase was observed as the concentrations of urea and calcium chloride were raised to 1M and all the surface strength was retained after 10 cycles of freeze-thaw for this specimen, as can be seen in Figure 4.10. The penetration test results of all SP-SM specimens are presented in Figure 4.11.

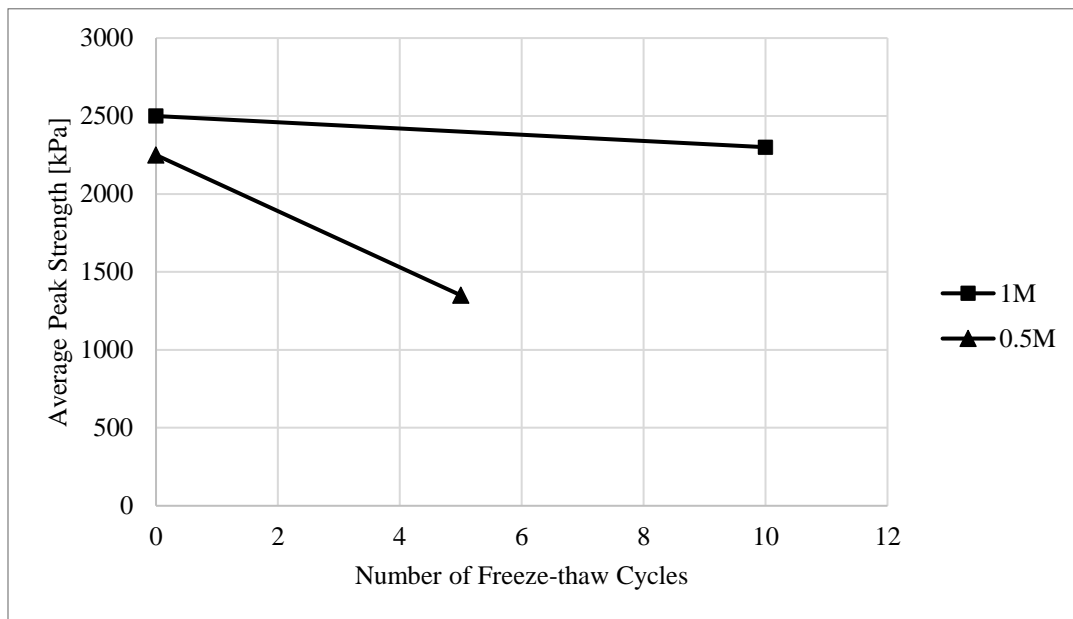


**Figure 4. 10.** Average Peak Strength of SP-SM Specimens vs. Number of Freeze-Thaw Cycles

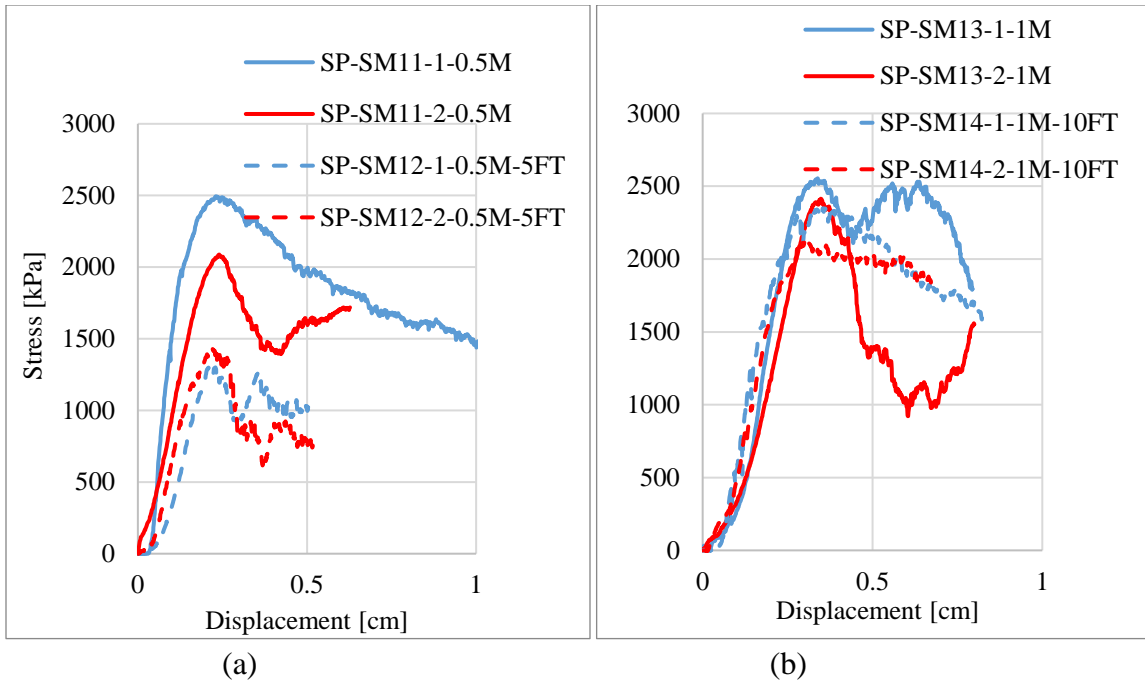


**Figure 4. 11.** Penetration Test Results of the Specimens from the Smaller Fraction (< 0.425 Mm) of SW Soil (Designated as SP-SM) Treated with Concentrations of 0.5M (a) And 1M (b); with No Freeze-Thaw (Solid Lines) and with Freeze-thaw (Dashed Lines) Cycles.

#### 4.3.2. PI-SWERL results

PI-SWERL testing was conducted on all the specimens in the laboratory setting. The total mass of soil eroded during the test (which are based on the particulate matter with a diameter of  $\leq 10\mu\text{m}$  referred to as PM10) per unit surface area ( $\text{mg}/\text{m}^2$ ) as a function of equivalent wind velocity ( $\text{cm}/\text{S}$ ) were compared for the specimens with different treatments with and without the freeze-thaw cycles.

The PM10 measurements show higher values in the treated specimens from SW soil compared to those from SP soil. This difference can be attributed to the higher fraction of fine particles in SW soil. The PM10 emissions from the treated specimens of SP soil are quite minimal. The total mass loss ( $\mu\text{g}$ ) of dust that has been suspended since

the beginning of the measurement until reaching the equivalent wind velocity of 85 cm/S for all specimens versus the number of freeze-thaw cycles are presented in Figures 4.12 to 4.14 to illustrate the effect of treatment and freeze-thaw cycles on fugitive dust emissions.

For the specimens from SP soil, the wind erosion resistance is directly correlated with the treatment concentration. All EICP-treated specimens show a higher resistance to wind erosion than the untreated specimen even after they undergo up to 7 freeze-thaw cycles.

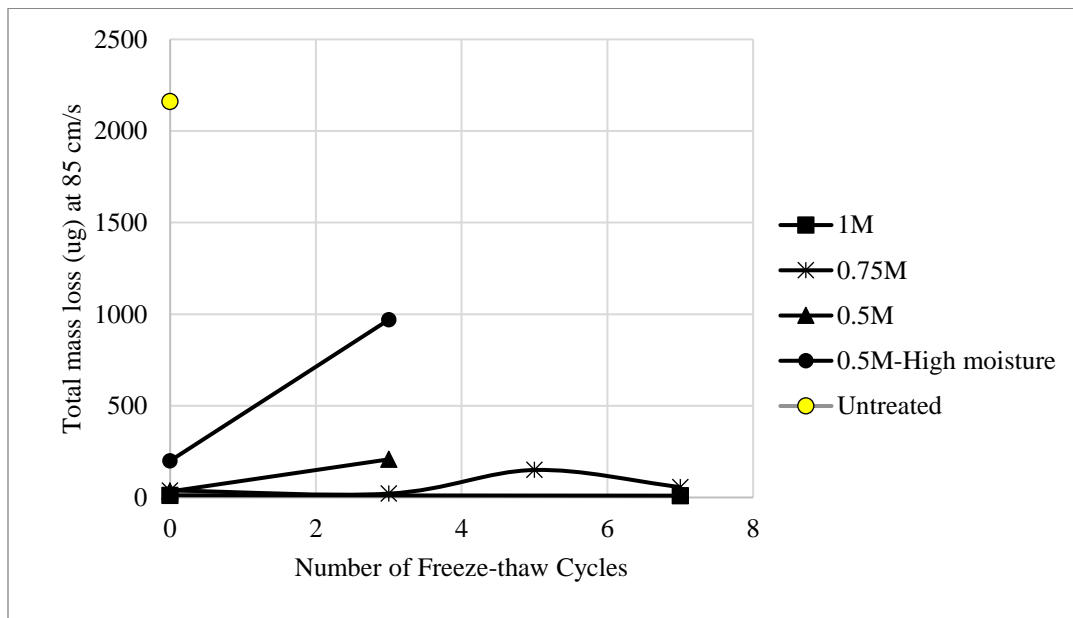


**Figure 4. 12.** Total Mass Emission (mg) at Velocity of 85 cm/s of SP Specimens vs. Number of Freeze-Thaw Cycles.

For the specimens from SW soil, the wind erosion resistance did not exhibit a direct correlation with the treatment concentration except at the highest concentration of 1M. Most specimens lost their resistance when subjected to the freeze-thaw cycles. However,

with the highest concentration of EICP treatment solution (1M), they showed an increased erosion resistance after treatment and after 3 freeze-thaw cycles.

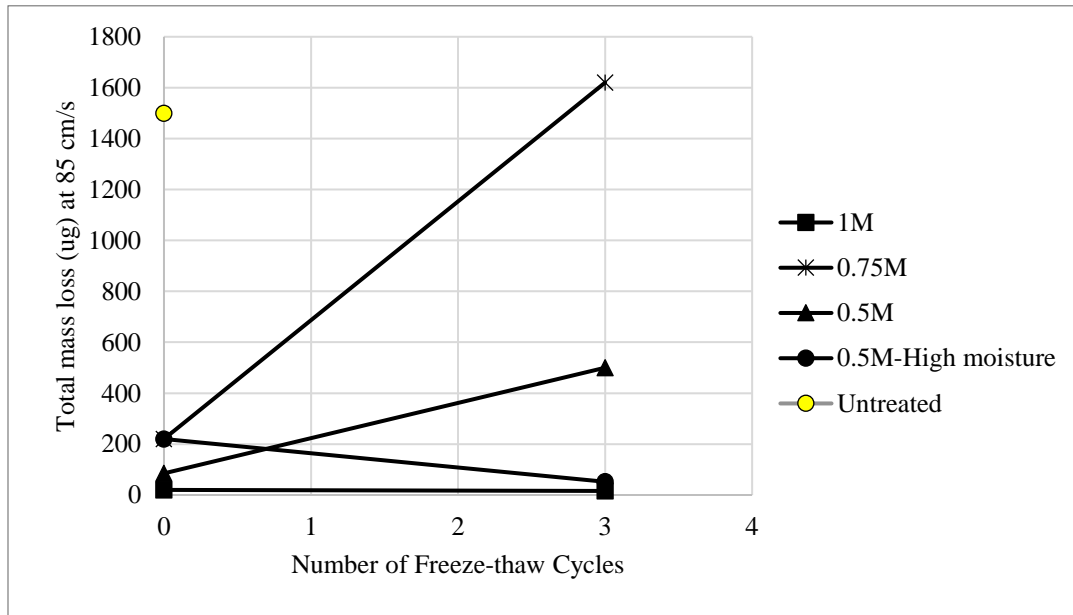


**Figure 4. 13.** Total Mass Emission (mg) at Velocity of 85 cm/s of SW Specimens vs. Number of Freeze-Thaw Cycles.

For the specimens of SP-SM soil, a subset of SW soil from which the coarse grains (> 0.425 mm) have been removed, the data from PI-SWERL testing correlated well with treatment concentration and the wind erosion resistance was durable when subjected to the freeze-thaw cycles. Moreover, the resistance of the specimen with the highest treatment concentration was still significantly higher after 10 freeze-thaw cycles compared to the specimen treated with a lower concentration and had 5 freeze-thaw cycles.

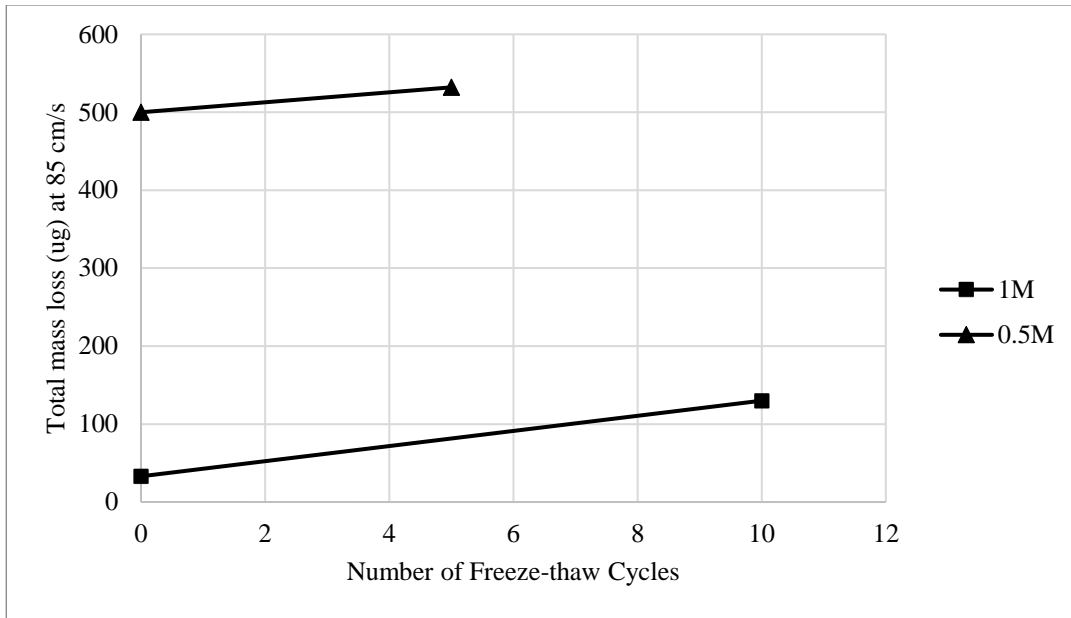


**Figure 4. 14.** Total Mass Emission (mg) at Velocity of 85 cm/s of SP-SM Specimens vs. Number of Freeze-Thaw Cycles.

The total mass of dust per unit area ( $\text{mg}/\text{m}^2$ ), that has been suspended since the beginning of the measurement versus the friction velocity for all samples are presented in Figures 4.15 to 4.17.

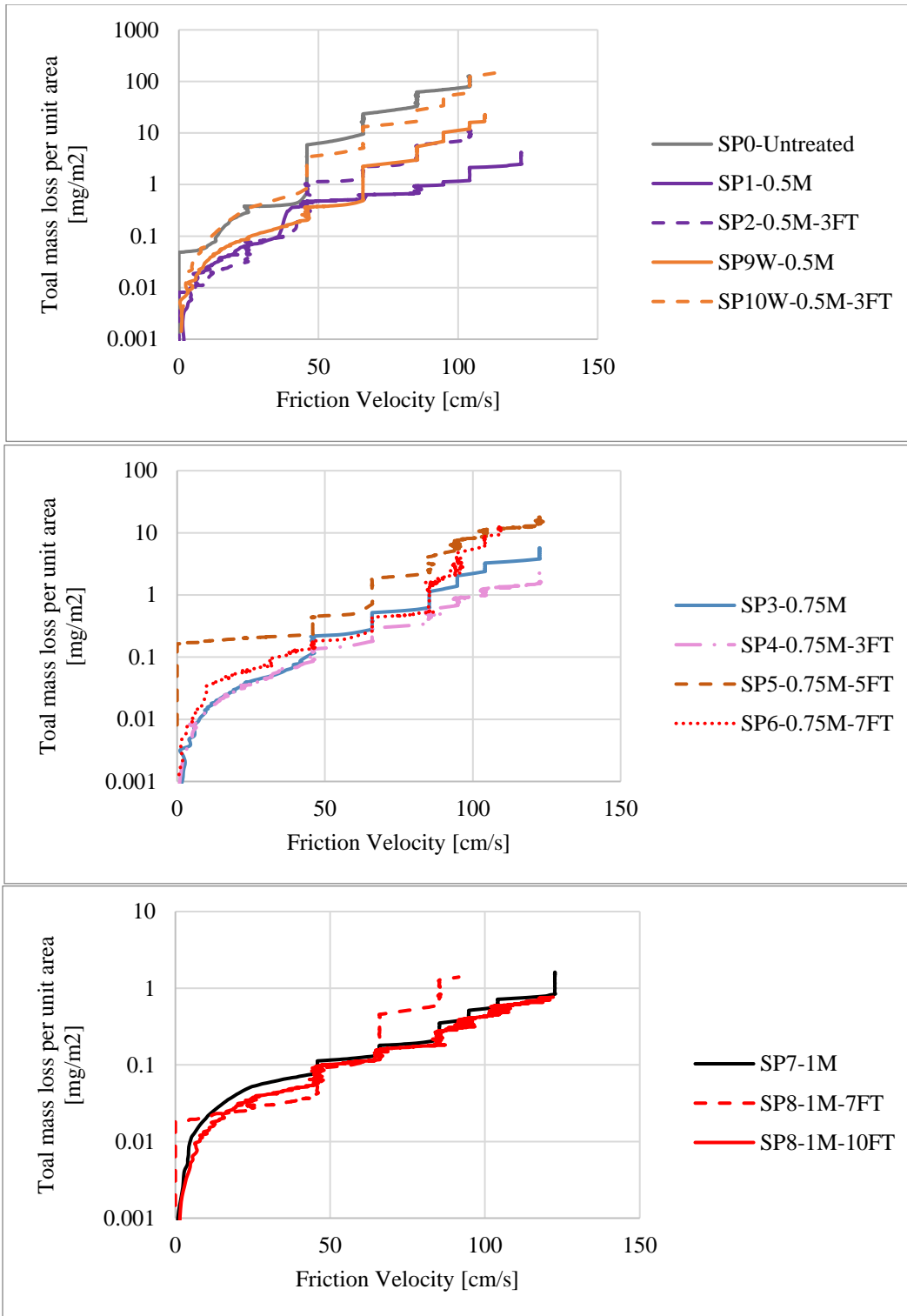


**Figure 4. 15.** The Total Mass Loss per Surface Area (mg/m<sup>2</sup>) vs. Friction Velocity for Specimens of SP Soil, without (Solid Lines) and with (Dash Lines) Freeze-Thaw Cycles.



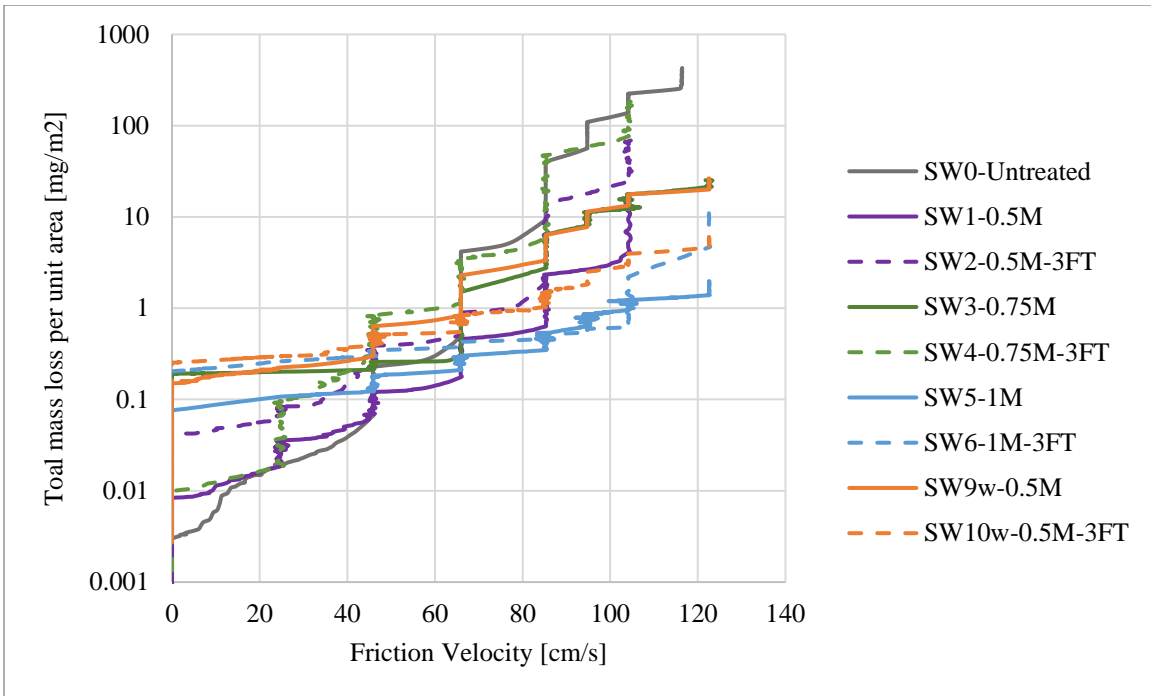


**Figure 4.16.** The Total Mass Loss per Surface Area ( $\text{mg}/\text{m}^2$ ) vs. Friction Velocity for Specimens of SW Soil, without (Solid Lines) and with (Dash Lines) Freeze-Thaw Cycles.

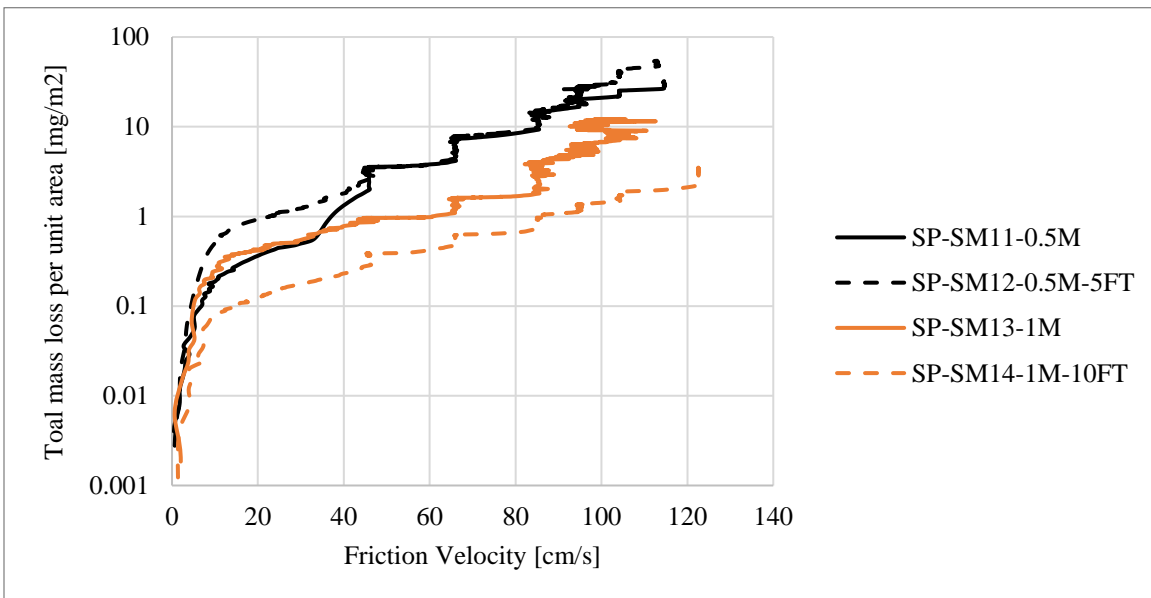


**Figure 4. 16.** The Total Mass Loss per Surface Area ( $\text{mg}/\text{m}^2$ ) vs. Friction Velocity for Specimens of SP-SM Soil, without (Solid Lines) and with (Dash Lines) Freeze-Thaw Cycles.

The OGS data did not show a good correlation with the specimens' crust stability based on data from other characterization methods and visual observation. A test was run on a clean surface to evaluate the OGS data when there was no sand emission and it showed false data of up to 1200 sand grain counts. This is probably because, over time, the OGD sensors are reported to become abraded and lose sensitivity, eventually providing no useful information (Salton Sea Emissions Monitoring Program, 2022).

#### 4.3.3. Calcium Carbonate Measurements Results

The calcium carbonate content of the crust of all samples was measured. The result showed the precipitation of carbonate on the surface of the specimens regardless of whether or not there was crust formation. Carbonate precipitation increased as the concentration of the urea and calcium chloride increased in the cementation solution. The average precipitated carbonate content of the specimens' crust is presented in Table 4.2 and 4.3.

#### 4.3.4. Discussion

In SP soil, the EICP-treated specimens consistently exhibit higher surface strength and wind erosion resistance compared to the untreated specimens. In SW soil, the effect of treatment on surface strength is uncertain. In specimens of SW soil, a dust-resistant crust either did not form with low cementation concentrations (0.5 and 0.75 molar) or formed but completely lost its dust resistance after undergoing freezing and thawing. Since SW soil contains a higher proportion of coarser sand grains and about 8% of gravel, a uniform cemented crust is not formed, while the treatment efficiently cements the soil particles in

SP soil. The presence of gravel fraction within the soil matrix poses challenges to achieving a cohesive crust when the soil is subjected to the cementation process, at least for the lower treatment levels of 0.5M and 0.75M. Consequently, a loose surface layer forms in the SW soil due to the inability of the gravel fraction to bond with other particles.

The slightly higher amount of silt fractions in SW soil and the well-graded particle size distribution of this soil, resulted in higher initial (untreated) surface strength. Another factor contributing to the higher initial surface strength is due, at least in part, to the higher ratio of the particle-probe diameter in SW soil compared to SP soil. SP soil is uniformly graded and appears to lack any inter-particle cohesion and therefore has lower initial strength.

For SP soil, when subjected to 3 freeze-thaw cycles, specimens treated with 0.5 and 0.75 M solutions experienced a decline in crust stability. However, subsequent freeze-thaw cycles did not significantly impact the surface strength and wind erosion resistance of the crust. The soil structure appears to have stabilized after 5 freeze-thaw cycles with subsequent cycles demonstrating negligible impact on it. With the application of a higher concentration of EICP treatment, the specimen's crust maintained its integrity even after undergoing 10 freeze-thaw cycles.

Regarding SW soil, since the untreated specimen showed a comparable surface strength with the treated specimens, the effect of freeze-thaw cycles is uncertain. There was a notable increase in crust strength when the concentration of the EICP was elevated to 1M. This specimen experienced a substantial reduction in surface strength after 3 freeze-thaw cycles, but the strength is still well above that of the untreated specimens.

Data from PI-SWERL showed a different trend for the same specimen, retaining the wind erosion resistance after 3 cycles of freeze-thaw.

Specimens from SP\_SM soil (containing grain sizes smaller than 0.425 mm from SW soil) showed a distinct and unbroken crust. This outcome indicates that the biocementation of the soil particles occurred through the removal of the coarser grains of this soil. The general behavior of these specimens was similar to that of SP soil by consistently showing higher resistance to wind erosion after treatment and retaining the strength of the crust after freeze-thaw cycles.

#### 4.4. Conclusion

The overall goal of this research was to evaluate the effectiveness of using the EICP technique for the reduction/prevention of dust in an iron mine tailings that are subject to freeze-thaw cycles. To achieve this goal, tailings specimens were treated using EICP and exposed to multiple freeze-thaw cycles in the laboratory. Two distinct soil types were tested. The dust emissions and crust strength of the treated tailings were evaluated through PI-SWERL tests, penetration tests, and calcium carbonate content measurements. The findings demonstrated somewhat different outcomes for each soil type.

For SP soil, a poorly graded sand containing only sand particles smaller than 0.425 mm, the biocemented crust exhibited resistance against wind erosion and improved surface strength. This soil experienced a partial decline in surface strength and erosion resistance when exposed to freeze-thaw cycles when treated at lower cementation levels,

i.e., 0.5M and 0.75M. However, at the highest cementation level of 1M the crust strength remained significantly intact even after 10 freeze-thaw cycles.

SW soil, a well graded sand with gravel particles, showed a high (but variable) penetration resistance without any treatment. Treatment with 0.5M and 0.75M EICP treatment solutions did not significantly increase penetration resistance or suppression of dust emissions. However, by increasing the concentration of cementation solution to 1M, an increase in erosion resistance after treatment was observed and the wind erosion resistance remained elevated after 3 freeze-thaw cycles. The removal of coarse particles from the well-graded soil facilitated effective binding of smaller soil particles by carbonate precipitation of EICP, forming a cohesive structure that was tolerant when exposed to 10 freeze-thaw cycles.

Treating the soil under conditions with high moisture content resulted in a limited crust formation. These aspects should be considered when implementing EICP in the practical field applications.

## CHAPTER 5

### 5. LABORATORY STUDIES ON ENZYME AND MICROBIALLY INDUCED CARBONATE PRECIPITATION FOR MITIGATION OF FUGITIVE DUST FROM SALINE SOIL

#### ABSTRACT

The potential for biocementation by Enzyme and Microbial Induced Carbonate Precipitation (EICP/MICP) via urea hydrolysis to reduce fugitive dust from saline sediments of Salton Sea by formation of a biocemented crust was evaluated in a laboratory study. The Salton Sea's sediments were created by shrinkage of the man-made lake as a result of a prolonged drought and reductions in agricultural runoff due to water conservation. This lake shrinkage resulted in increasing fugitive dust from impacted exposed playa soils which pose environmental and human health concerns. Bio-based EICP and MICP technologies offer a potentially sustainable and cost-effective mitigation method for fugitive dust by forming a dust-resistant biocemented crust on the soil through the precipitation of natural calcium carbonate ( $\text{CaCO}_3$ ) cement.

To evaluate the potential of biocementation for fugitive dust mitigation, a comprehensive laboratory testing program including elemental and mineralogical composition analyses was carried out on sediments from two locations on the lakeshore. Elemental and mineralogical composition analyses of the sediments showed variable soluble salt content (predominantly halite), from 4% (by mass) on the west side of the lake to 40% on the southeast side. After characterizing the sediments, the effectiveness of

both EICP and MICP was assessed experimentally using the Portable In Situ Wind Erosion Lab (PI-SWERL™) test and strain-controlled penetration tests on soil-filled pans treated by percolation of reactive solutions and by measuring the CaCO<sub>3</sub> content of treated samples.

The PI-SWERL and penetration tests showed that treatment formed a crust that increased the erosion resistance in all specimens. However, in the specimens with higher salt content the calcium carbonate content did not show any significant increase following treatment and the erosion resistance of the treated soil did not show a significant difference compared to soil treated with water only. In the specimens containing lower salt content, on the other hand, a carbonate crust was formed and the erosion resistance of the biocemented soil was higher than that of the untreated and of water-treated soil.

Further analysis confirmed that the hydrolysis of urea and consequent carbonate precipitation in the biocemented soil might be inhibited in soils with high salinity. The lack of carbonate precipitation of the specimens made of saline soil was attributed to the dissolution of salts into the treatment solution, which suppressed the urease activity. This study illustrates an important constraint that must be considered when treating saline soils using EICP or MICP.

## 5.1. Introduction

Climate change and human activity have led the water level of many lakes around the world to decrease, causing them to shrink significantly. The shrinking lakes can lead to

significant environmental and ecological impacts including increased salinity and pollution of soil and wildlife disturbances. Also, the exposed beds of shrinking water bodies, sometimes referred to as playas, are susceptible to dust storms that may have negative impacts on local communities (Zucca et al, 2021). Different measures have been implemented to address the dust problem associated with shrinking lakes. These methods include but are not limited to spraying water or other dust suppressants, planting vegetation, engineering solutions such as construction of barriers or windbreaks, physical covers such as geotextiles or geomembranes (Countess Environmental, 2006).

The Salton Sea, a highly saline lake in southern California, is the largest lake in the state in terms of surface area. The Salton Sea was initially created in the early 1900s by accidental diversion of the Colorado River into a late Pleistocene lakebed. The climate in the Salton Sea region is one of the great extremes. The local rainfall is about 2.5 inches per year while the temperatures can often reach above 110 degrees Fahrenheit (°F) in the summer and below freezing in the winter. The lake was sustained by irrigation wastewaters; however, recent drying has exposed a playa, leading to severe dust storms in the area. These dust storms have resulted in high levels of PM<sub>10</sub> (particulate matter with an aerodynamic diameter of  $\leq 10\mu\text{m}$ ), exceeding state and federal limits by about 10 times (Zucca et al. 2021; Johnston et al. 2019). The dust generated by the exposed playas is also impacted by the pesticides and herbicides associated with agricultural runoff, exacerbating human health and environmental impact concerns.

Studies predict that the exposed Salton Sea playas will increase to 38% by 2030, causing a substantial increase in PM<sub>10</sub> levels in adjacent areas (Parajuli and Zender 2018). King et al. (2011) investigated the potential for dust emissions around the Salton



Sea between 2005 and 2007. They studied the relationship between soil properties, including soil salt content, and in situ PM10 dust emissions using Portable In-Situ Wind Erosion Laboratory (PI-SWERL). They found that there was no statistically significant correlation between salt content and PM10 dust emissions and that these salt crusts can be a source of dust emissions. Regarding the formation of salt crusts, King et al. (2011) stated that salt minerals may precipitate either as loose, unconsolidated, individual, silt- to sand-sized crystals or as interlocking crystals. If crystals are in an interlocking form, then they can precipitate as a very hard, dust resistant crust (King et al. 2011).

In another study, Borda et al. (2020) modeled 13 years (2005–2017) of dust emission from Mar Chiquita (MC), the most extensive shrinking saline lake in South America. Based on a chemical characterization of dust, they found that a mean  $\sim 15\text{--}150\text{ mg m}^{-2}$  of soluble Na was deposited 300 km from the source during the season of strongest dust emissions. Based on their study, the salt content of MC has been deposited as loose individual crystals that can be a source of dust emissions. Therefore, the form of precipitated salt (interlocking crystals or loose individual crystals) will control the amount of dust particles that are available for suspension (Buck et al., in press), and these salt crust variables can vary on many different time scales. The salt minerals around the Salton Sea precipitated in variable forms that resulted in large variations in potential dust emissions (King et al., 2011). The locations in which the salt on the surface exists as loose crystals (rather than interlocking particles) have high dust susceptibility.

In recent years, there have been a number of efforts to address the dust problem at the Salton Sea. These efforts include planting vegetation to stabilize the lakebed, creating

dust control barriers, and developing new water management strategies (CNRA, DWR, and CDFW; 2020).

One of the innovative methods that has been extensively studied for dust mitigation in recent years is biocementation through enzyme induced carbonate precipitation (EICP) and microbially induced carbonate precipitation (MICP). Several researchers have shown the effectiveness of using EICP and MICP to create surface crusts and mitigate fugitive dust in different soil types (Bang et al. 2011; Gomez et al. 2015; Shanahan and Montoya 2016; Naeimi & Chu 2017; Wang et al. 2018; Woolley et al. 2023; Yu. 2023). Compared to alternative dust suppressants like water, hygroscopic salts, and biopolymers, the main advantage of a mineral crust would be enhanced durability when exposed to surface water washout and wetting-drying cycles (Ehsasi et al. 2022). However, the effectiveness of this method varies depending on the specific soil type being treated. Yuan et al. (2022) studied the effect of MICP in a highly saline environment. They used an indigenous high-yield urease-producing microorganism for a soil from a saline basin that improved the strength of highly saline silty soil. They also showed that under different salt concentration conditions, the native microbial strain from the tested soil was more stable than *Sporosarcina pasteurii* (*S. pasteurii*), the bacteria commonly used in laboratory studies of MICP, and had a higher urease production capability in a highly saline environment than bacteria *S. pasteurii*.

In this study, the potential for biocementation by Enzyme and Microbial Induced Carbonate Precipitation (EICP and MICP) to reduce fugitive dust from saline sediments of the Salton Sea playas is evaluated in the laboratory environment. Sediments from Salton Sea playas with varying salt contents were treated with varying EICP/MICP

treatment procedures and resulting crusts were tested for erosion resistance using PI-SWERL, for crust strength by penetration testing, and for calcium carbonate precipitation using the calcimeter. The results are compared with tests in the literature to assess the effect of soil salt content on EICP/MICP performance and are used to identify limitations of ureolytic biocementation and establish its potential utilization in biocementation applications on the Salton Sea playas.

## 5.2. Materials and Methods

### 5.2.1. Sediment Characterization

Salt minerals are common components in arid soils, and their high solubility can result in considerable variability in sediment characteristics over very short time frames and small distances (King et al. 2011). This phenomenon is clearly observed in the sediments of the Salton Sea, where the presence of salt minerals contributes to considerable variability in sediment characteristics around the lake. Understanding the characteristics of the sediment is crucial for the dust management around the Salton Sea. The following paragraphs present the characteristics of two types of sediment collected from around the lake that were investigated for dust mitigation in this study.

#### *Study Area and Location of Samples*

The sample from southeast side of the Salton Sea (designated as HS) was collected during a site visit. Subsequently, another sample (designated as LS) was provided by

Bureau of Reclamation from west side of the Salton Sea. The sample locations are marked in Figure 5.1.



**Figure 5. 1.** Sample Locations Around the Salton Sea

### *Grain Size Distribution*

The grain size distribution was determined for samples in general accordance with ASTM standard using both the wet and dry sieving. The results are presented in Table 5.1.

Gradations shown in this table are based upon the Unified Soil Classification System (USCS, ASTM D2487) with regards to percentages of gravel, sand, and fines (% passing the #200 sieve).

**Table 5. 1.** Grain Size Distribution of Samples

Sample	Size Fractions	Dry Sieving	Wet Sieving
HS	% Gravel	25.3	2.4
	% Sand	71.1	48.8
	% Fines (silt and clay)	3.7	48.8
LS	% Gravel	0.1	0.0
	% Sand	87.7	76.7
	% Fines (silt and clay)	12.2	23.3

There is a significant difference between the fines content of HS sample from wet sieving (48.8%) compared to dry sieving (3.7%). The difference can be attributed to disintegration of aggregates or particles that were cemented by evaporite (dried salt), as confirmed by the high soluble salt content in this soil, which is discussed later in this chapter. Dissolution of these salts during the wet sieving resulted in a large amount of particles passing sieve#200. Detailed grain size distribution plots are presented in Figure 5.2.

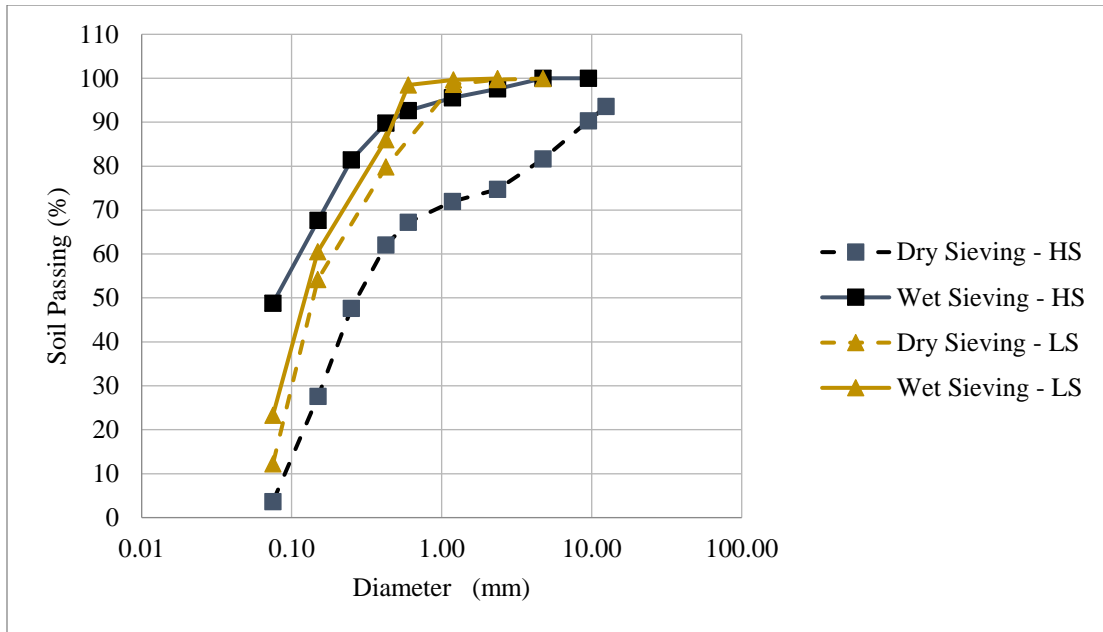


**Figure 5.2.** Grain Size Distribution of Two Salton Sea Samples in Wet and Dry Sieving

#### *Calcium Carbonate Content of Samples*

Calcium carbonate content (mass of  $\text{CaCO}_3$  per total dry mass of soil) was measured before and after treatment following ASTM D 4373-84, where the carbonate content is based on the volume of carbon dioxide gas generated by the reaction between the hydrochloric acid and the carbonates using a Calcimeter (Eijkelkamp). The carbonate content of HS sample prior to treatment was measured for both the bulk sample and the naturally crusted samples which could be distinguished by cemented soil clumps at the surface. LS sample had a more uniform appearance, and  $\text{CaCO}_3$  prior to treatment was only measured on the bulk sample. Table 5.2 presents the results of the carbonate content tests. The results on HS sample showed a lower carbonate content in the crust than in the bulk sample.

**Table 5. 2.** Carbonate Content of Samples

Sample		Carbonate content (%)
HS	Bulk sample	3.8 - 4
	Natural Crust	2.3 - 2.5
LS	Bulk sample	3.4 – 3.8

*Evaporation and SWRC*

The soil water retention characteristic (SWRC) curve is an important soil property that determines how an EICP or MICP treatment solution would be distributed throughout the sample if the sample is treated by percolation under unsaturated conditions (Cheng & Cord-Ruwisch, 2012, Cheng et al. 2013). The SWRC curve is also important to assess the role of evaporation and rainfall on treatment performance and crust durability. The SWRC curve of the two bulk samples were determined using the Hyprop device (Metergroup), which is based on the evaporation method described by Schindler et al. (2010). In this method, the sample is saturated prior to the test and the pore water is allowed to evaporate while both the suction in the sample and the weight loss due to evaporation are monitored continuously. Consequently, the volumetric water content is calculated and plotted against the average suction in the sample to obtain the SWRC curve. The tests were performed in the laboratory at room temperature and the resulting SWRC curves are presented in Figure 5.3.

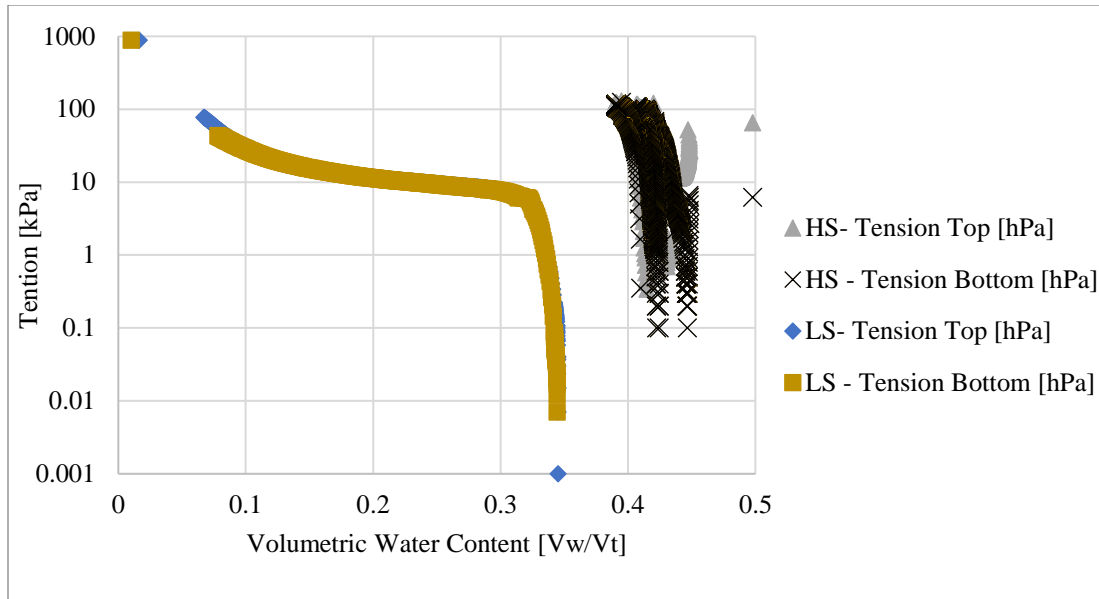


**Figure 5. 3.** SWRC Curve of Two Samples

As presented in Figure 5.4, the Hyprop test showed that HS sample had a very slow rate of evaporation ( $\approx 0.23$  g/day) compared to the evaporation rate in saturated clean sand (typically 20 g/day). At some stages of the test the water did not evaporate under the lab conditions. It was hypothesized that the low evaporation rate was either due to the formation of a very low permeability crust or due to osmotic suction or hygroscopic behavior associated with high soluble salt contents. It was interpreted that both the evaporation rate and measured suction in this soil are affected by the high salt content. For LS sample, the evaporation rate was much higher ( $\approx 13$  g/day), but still lower than that for a standard coarse sand, and the residual water content reached to about 2.5 g. after about six days.



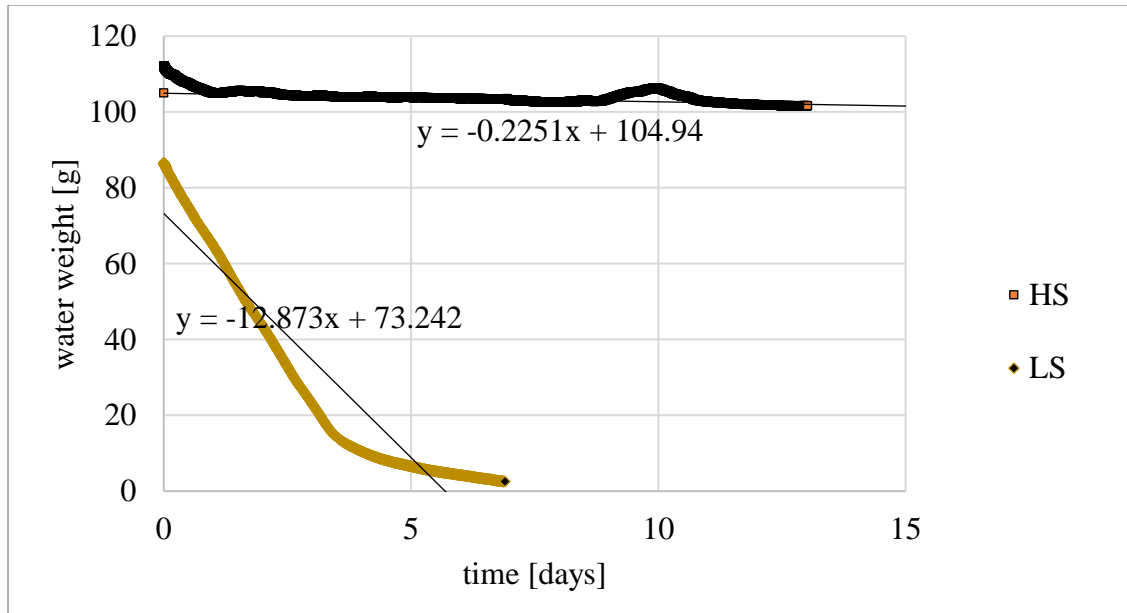


**Figure 5. 4.** Mass of Water Retained vs. Time in Two Samples with Best-Fit Linear Regression Lines.

#### *Soluble Salt Measurement*

To measure the salinity of the samples, 10 g of dried sample was added into 100 ml of deionized water. The samples were then capped and shaken for about an hour. The samples were stored for one week in a closed container to allow soluble salts in the soil to dissolve. The electric conductivity of the solutions was then measured to estimate the total soluble salt (TSS) of the soil. The linear relationship that exists between TSS and EC was used to estimate with a relatively good degree of accuracy the soluble salts in the soil (Sonon et al. 2015). The ratio of total soluble salt (TSS) to EC of various salt solutions ranges from 550 to 700 parts per million or milligrams per liter (ppm or mg/L) per dS/m and Sodium chloride has a TSS of 640 ppm per dS/m (Sonon et al. 2015). So, the EC of the solutions were measured and the TSS of the solution was estimated using the value for sodium chloride in Eq. 5.1. Note that the assumption that the salt was

predominant sodium chloride was confirmed by later X-ray diffraction (XRD) and Ion Chromatography (IC) testing:

$$\text{TSS (mg/L or ppm)} = \text{EC (dS/m)} \times 640 \quad (5.1)$$

The total soluble salt content of the samples (in %) was then estimated considering the amount of the samples mixed in the water. Table 5.3 presents the results of this analysis.

**Table 5. 3.** Soluble Salt Content of Samples Based on Electric Conductivity Measurements

Sample	Sample type	Sample name	Electrical conductivity (EC) (mS/cm)	TSS in solution (ppm)	TSS of soil (g)	Salt content of the soil samples (%)	Avg. Salt Content (%)
HS	Bulk soil	S1-Bulk	51	32640	3.26	32.6	31.3
		S2-Bulk	47	30080	3.00	30	
	Natural Crust	S1-Crust	75	48000	4.80	48	46.4
		S2-Crust	70	44800	4.48	44.8	
LS	Bulk soil	S1	6.35	4064	2.03	4.1	4
		S2	6.1	3904	1.95	3.9	

#### *Elemental Analysis of HS Sample*

#### *XRD Analysis*

Two specimens of HS, one from the crust and one from the bulk sample, were analyzed using X-ray diffraction (XRD). The following minerals were quantified to be present in each sample:

- Crust: halite (52%), starkeyite (25%), quartz (19%), calcite ( $\approx 2.3\%$ ), and thenardite ( $\approx 1.5\%$ ).

- Bulk: quartz (40%), starkeyite (28%), halite (22%), calcite ( $\approx 3.8\%$ ), gypsum ( $\approx 2.6\%$ ), thenardite ( $\approx 2.5\%$ ), and anhydrite ( $\approx 1.2\%$ ).

According to results from XRD analysis, the most common mineral in the natural crust of the sample was halite, which is the highly soluble kitchen salt sodium chloride. The bulk sample itself was mainly composed of quartz.

### *Ion Chromatography*

The solutions that were prepared for soil salinity measurements were diluted and analyzed using Ion chromatography (Dionex ICS 5000+, Sunnyvale, California). The results from these tests showed that sodium ( $\text{Na}^+$ ) and Chloride ( $\text{Cl}^-$ ) ions were the dominant ions in the solution, confirming the results from the XRD analysis. The results also showed the specimen contained small amount of other cations (magnesium ( $\text{Mg}^+$ ), potassium ( $\text{K}^+$ ), and calcium ( $\text{Ca}^+$ )) and anions (nitrate ( $\text{NO}_3^-$ ) and sulfate ( $\text{SO}_4^{2-}$ )). From the IC analysis, the bulk specimen is estimated to contain about 30% NaCl and the crust about 40% of NaCl, consistent with other types of measurements.

### 5.2.2. Bacteria Cultivation

The bacteria *Sporosarcina pasteurii* was used as the source of the enzyme urease for microbially induced carbonate precipitation (MICP) treatment in this study. The bacteria were cultivated in a medium containing 20 g L<sup>-1</sup> yeast extract, 10 g L<sup>-1</sup> NH<sub>4</sub>Cl, and 24 mg L<sup>-1</sup> NiCl<sub>2</sub>. The pH of the medium was adjusted to 9 by slowly adding 4 mol/L NaOH. For the cultivation, about 10 mL of an already active bacterial culture from earlier

cultivation studies was used as an inoculum and added to 500 mL of prepared medium. Bacteria were cultivated under aerobic conditions for 24-30 hours at 25°C in MAX Q 4000 Benchtop Orbital Shaker. after cultivation bacteria were transferred to the refrigerator and stored at 4°C in their growth medium before they were used. The urease activity was measured prior to every treatment using the electrical conductivity (EC) method (Whiffin et al. 2007). The concentration of the bacteria in suspension was measured indirectly with a spectrophotometer (OD 600). The urease activity of the suspension with bacteria was in a range of 6–8 mM urea/min with an OD600 range of 1.6–2.0 for every treatment.

### 5.2.3. Enzyme Preparation

Urease enzyme extracted from jack beans (*Canavalia ensiformis*) was used for enzyme induced carbonate precipitation (EICP) treatment in this study. The preparation of the urease enzyme solution was based on the crude extraction process described by Khodadadi Tirkolaei et al. (2020). First, 50 g of jack beans were soaked in 200 mL of tap water overnight. The mixture of jack beans and water was then homogenized in a kitchen blender. The resulting suspension was filtered twice, passing through a cheesecloth to filter out coarse solids and through glass wool to filter finer solids and fat globules. The twice-filtered solution was collected and stored in the refrigerator for further use in this project. The activity of the crude extract that is extracted in this way is in the range of 100 to 300 U/ml (Yu, 2023). Twenty-five (25) mL/L of enzyme solution was used in each batch of EICP treatment solution.

#### 5.2.4. Specimen Preparation and Treatment

Soil specimens were prepared inside pie pans with a volume of 1.48 L, a top surface diameter of 22 cm, a bottom diameter of 18 cm, and a depth of 3.5 cm. Both MICP and EICP treatment solutions were prepared as two separate solutions: 1) a suspension containing the ureolytic bacteria for MICP or urease enzyme for EICP and 2) a cementation solution containing calcium chloride ( $\text{CaCl}_2$ ) and urea ( $\text{CO}(\text{NH}_2)_2$ ). For EICP solution, 4 g/L of dry milk powder was also added into the suspension containing urease enzyme at the time of application. Specimens were treated by spraying the treatment solution onto their surface immediately after mixing the two solutions. For all the specimens, the bacteria suspension/urease enzyme and cementation solutions were applied at a 1:1 volume ratio with a total volume of  $3 \text{ L/m}^2$ , which corresponds to 120 mL per pan. The molar ratio of urea to calcium chloride was kept at 1.5:1.

For HS sample (from the southeast side), two concentrations of the urea and calcium chloride solution were applied to investigate the effect of reagent concentration: low (0.5 Molar of urea and 0.33 Molar of calcium chloride) and high (1.5 Molar of urea and 1 Molar of calcium chloride) concentrations. Two control specimens were treated with water and salt (containing 0.5M urea and 0.33M  $\text{CaCl}_2$ ) with the same concentration of and an equivalent volume as the samples treated with biocementation solutions ( $3 \text{ L/m}^2$ ). In addition, one specimen (# 4) was treated with three applications of MICP (0.5M urea and 0.33M  $\text{CaCl}_2$ ) via surface spraying at 24 hours intervals for a total volume of  $9 \text{ L/m}^2$  to investigate the effect of the treatment solution volume. Samples were allowed to dry in the room condition for 24 hours and in the oven at a temperature of  $55^\circ \text{C}$  for another 24 hours before any testing.

For LS sample (from the west side), due to the scarcity of the soil, EICP treatment was applied in two concentrations: intermediate (1 Molar of urea and 0.67 Molar of calcium chloride) and high (1.5 Molar of urea and 1 Molar of calcium chloride), with the water-treated sample as the control sample. Also, one MICP-treated specimen of LS sample was prepared inside plastic container with a volume of 100 cm<sup>3</sup>, a diameter of 8.2 cm, and a depth of 3.8 cm. Samples were allowed to dry in the room condition for 24 hours and in the oven at a temperature of 55° c for another 24 hours before any testing.

#### 5.2.6. PI-SWERL Test

The portable in-situ wind erosion lab (PI-SWERL), developed by Desert Research Institute (DRI) (Etyemezian, et al., 2007), is an efficient method of measuring the potential of wind erosion in most landforms and the laboratory setting. This device has a spinning blade in cylindrical chamber that creates a known wind shear, entraining soil, sand, and dust particles into the chamber. The wind shear is quantified in terms of the friction velocity of the wind on the soil surface. Dust particulate sensors measure the concentration of particulate matter with an aerodynamic diameter of  $\leq 10\mu\text{m}$  (PM10) entrained in the chamber during a load cycle of constant friction velocity, typically for about 10 minutes. The test employs a series of cycles of increasing wind shear up to the limit of the device. Although the wind shear is applied in a circular fashion versus linear (as found in nature), PI-SWERL results compare favorably to data from larger wind tunnel tests (Sweeney et al, 2008). This device was used in a laboratory setting, to measure the potential for wind erosion (fugitive dust emission) from the surface of the

soil in each pan specimen. The figures of the device and the set up to use it on the pan samples are shown in Figure 5.5.

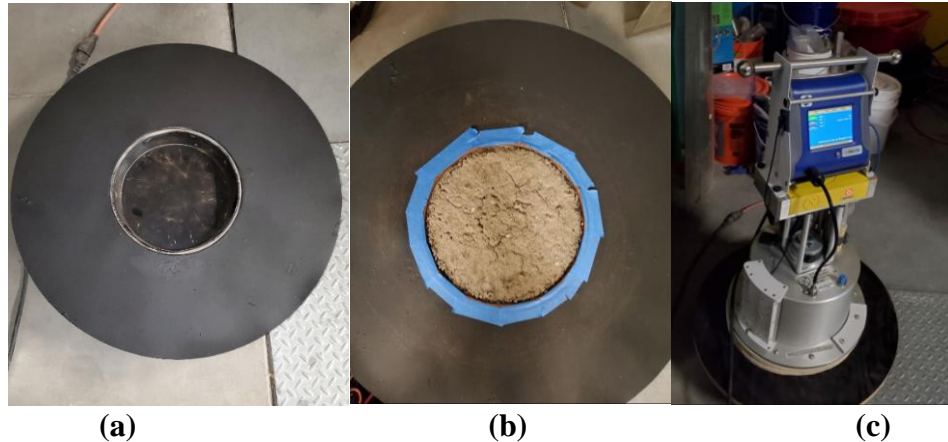


**Figure 5. 5.** (a) Specimen Holder. (b) a Pan Specimen Placed and Taped in the Holder before Running PI-SWERL Test, (c) PI-SWERL Device on the Specimen Holder

#### 5.2.7. Penetration Test

The detachment of soil particles from the surface causes wind erosion, thus the amount of fugitive dust depends on the surface shear strength of the soil (Chen et al. 2014). Chen et al. (2014) recommended the penetration test with a simple flat-ended cylindrical penetrometer for the crust evaluation as they found a strong correlation between the weight loss from the wind tunnel test and penetration test results using this type of probe. Therefore, penetration tests were used on the treated pan specimens in this study to evaluate the strength of the cemented crust. The penetration test is conducted by pushing a cylindrical flat-ended steel probe, 6 mm in diameter, into the samples. The probe was affixed to a load cell and pushed into the samples at a constant rate of 1 mm/min while the normal force and the vertical deformation were recorded.

#### 5.2.8. Carbonate Content Measurement

Carbonate content was measured following ASTM D 4373-84, where the carbonate content is based on the volume of carbon dioxide gas generated by the reaction between the hydrochloric acid and the carbonates using a Calcimeter (Eijkelkamp, Wilmington NC, USA). The calcium carbonate content of the biocemented crust of each specimen was measured after treatment to provide insight into changes in the calcite content upon treatment. To measure the calcium carbonate content, discrete samples were collected from the top 3 mm of each pan and mixed thoroughly to obtain a representative sample. the carbonate content of each sample was measured using the Calcimeter.

#### 5.2.9. Salt Effect on Enzyme Activity

Experiments were conducted to isolate the impact of salt on the activity of the urease enzyme. For this purpose, 500 g of HS sample was added to 2 L of deionized water. The samples were then capped and shaken for about an hour. The samples were then stored for one week in a closed container under lab conditions to allow the salt to dissolve. The resulting solution was decanted, and the remaining soil was oven dried at 55° C. Samples were prepared in falcon tubes by mixing and compacting of 50 grams of the dried soil with 1 pore volume of either EICP or MICP solutions. Concentrations of 1.5 Molar of urea and 1 Molar of calcium chloride were applied with the bacteria and enzyme solution to treat the samples.



### 5.3. Results and Discussion

#### 5.3.1. PI-SWERL Test Results

The DustTrack nephelometer measures concentrations of PM<sub>10</sub> (mg/m<sup>3</sup>) over four orders of magnitude as the rotational speed of the blade progressively increased. Concentrations measured by the DustTrack are converted to total mass of dust (in micrograms) that has been suspended since the beginning of the measurement in subsequent analyses by the software that accompanies the PI-SWERL device. In this study, the PM<sub>10</sub> concentrations (mg/m<sup>3</sup>) and the dust mass per unit surface area (mg/m<sup>2</sup>) is reported. This value is determined by dividing the total dust mass by the effective surface area of the PI-SWERL (0.035 m<sup>2</sup>) from which PM<sub>10</sub> is generated. Mass loss per unit surface area (mg/m<sup>2</sup>) from the PI-SWERL testing on untreated, water treated, EICP treated, MICP treated, and salt treated samples of HS sample are presented in Figures 5.5 and 5.6.

The results from PI-SWERL testing on the treated specimens from HS sample showed that the water treated sample had a higher dust emission potential compared to the salt treated, EICP treated, and MICP treated specimens. The salt treated, EICP treated, and MICP treated specimens showed similar behavior with respect to dust emissivity based upon dust concentration (PM<sub>10</sub> (mg/m<sup>3</sup>)) and total mass of dust (in micrograms) eroded from these samples. The total dust that was emitted from the water treated sample was significantly lower than that of the untreated sample (i.e., the wind erosion resistance was significantly higher). This increased dust resistance was attributed to the salt crust that formed after spraying water onto the sample followed by evaporation of the water during oven drying.

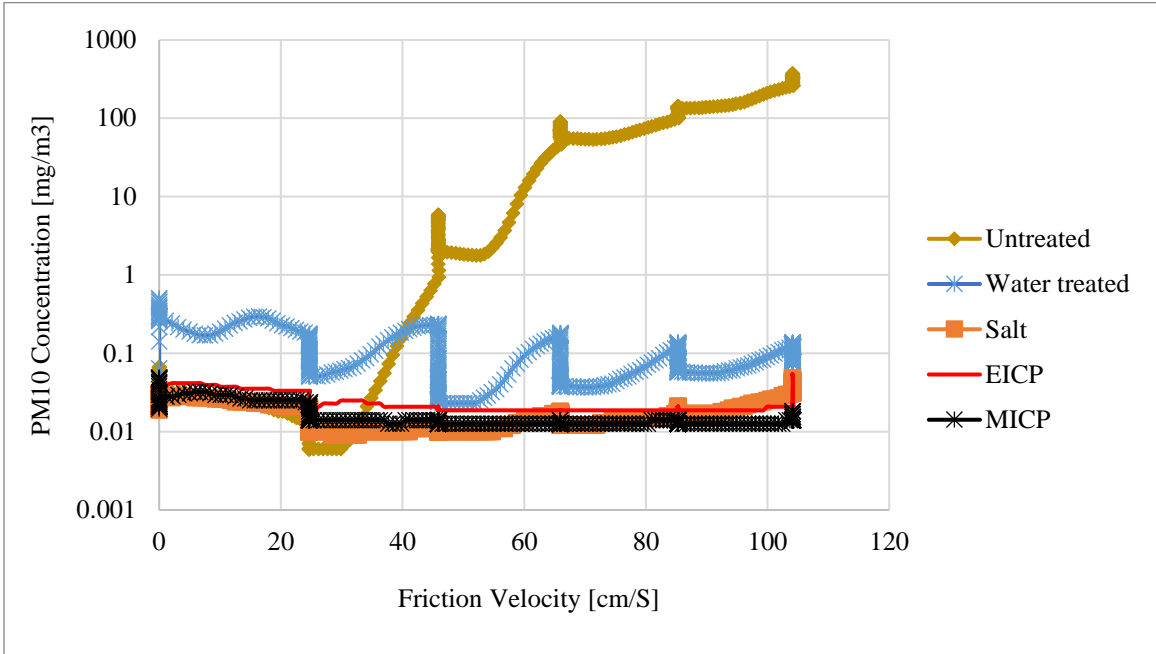


**Figure 5. 6.** PM10 Emission from HS Samples: EICP, MICP, Salt, Water-treated, and Untreated Samples vs. Friction Velocity of the PI-SWERL.

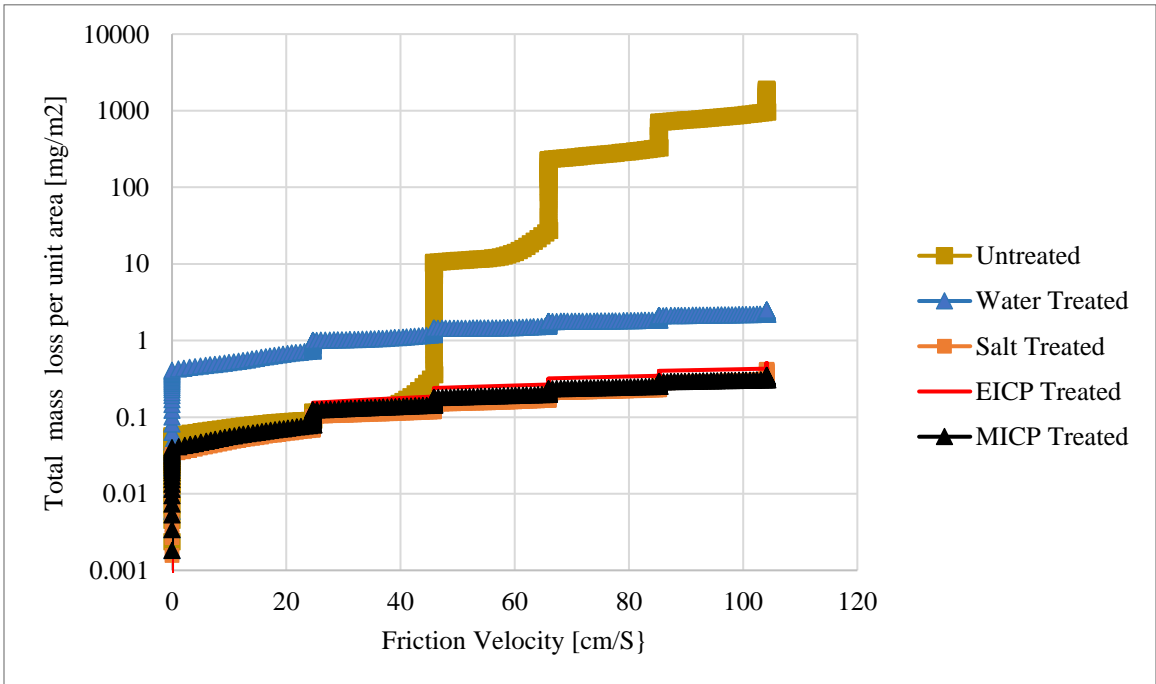


**Figure 5. 7.** Total Mass Loss per Unit Area from HS Samples: EICP, MICP, Salt, Water-treated, and Untreated Samples vs. Friction Velocity of the PI-SWERL.

Figures 5.8 and 5.9 show the PM10 concentration ( $\text{mg}/\text{m}^3$ ) and the total mass of dust emission from treated and untreated samples for LS sample (west side). For the LS samples, the EICP treated samples showed a lower dust emissivity compared to the water treated sample. Water treating did not create a distinct crust in these samples and had a higher mass loss compared to the water treated samples of the sediments with high salt content (HS samples).

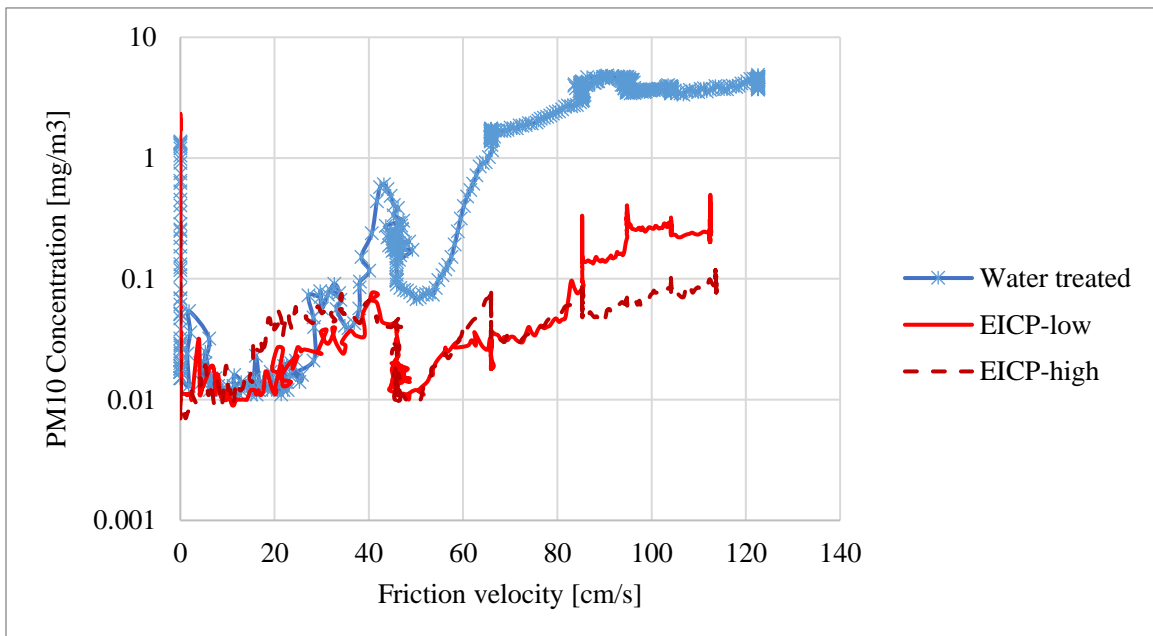


**Figure 5. 8.** PM10 Emission from LS Samples: Low and High Concentrations of EICP and Water-treated Samples.

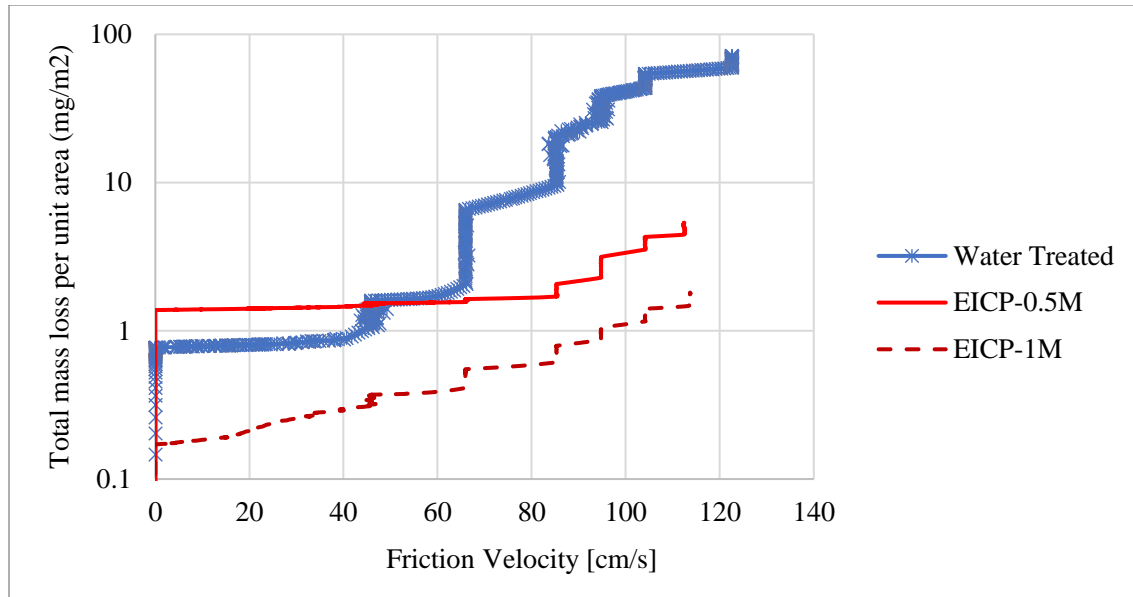


**Figure 5. 9.** Total Dust Mass from LS Samples: Low and High Concentrations of EICP and Water-treated Samples.

### 5.3.2. Penetration Test Results

The results from the penetration test (summarized in Table 5.4) are consistent with the results from the PI-SWERL tests. For HS sample, all treated specimens including the water treated sample have a higher penetration resistance than the sample that is not treated. The water-treated sample shows a lower surface strength compared to the salt and EICP/MICP treated samples. The penetration resistance of the sample treated with salt is slightly less than that for the sample treated with EICP (for a similar amount of salt), while it is higher than that for the sample treated with MICP. Moreover, a higher concentration of MICP (sample#3B) and a higher number of treatments (sample#4) did not improve the surface strength compared to the sample that was only treated once with a lower concentration (sample#3A). For LS sample, all specimens showed lower peak strength than for HS sample, but the EICP and MICP treatment increased the surface

strength of the specimens compared to the control with water and a higher concentration of the treatment solution resulted in higher surface strength. The figures below show the penetration test results of all specimens.

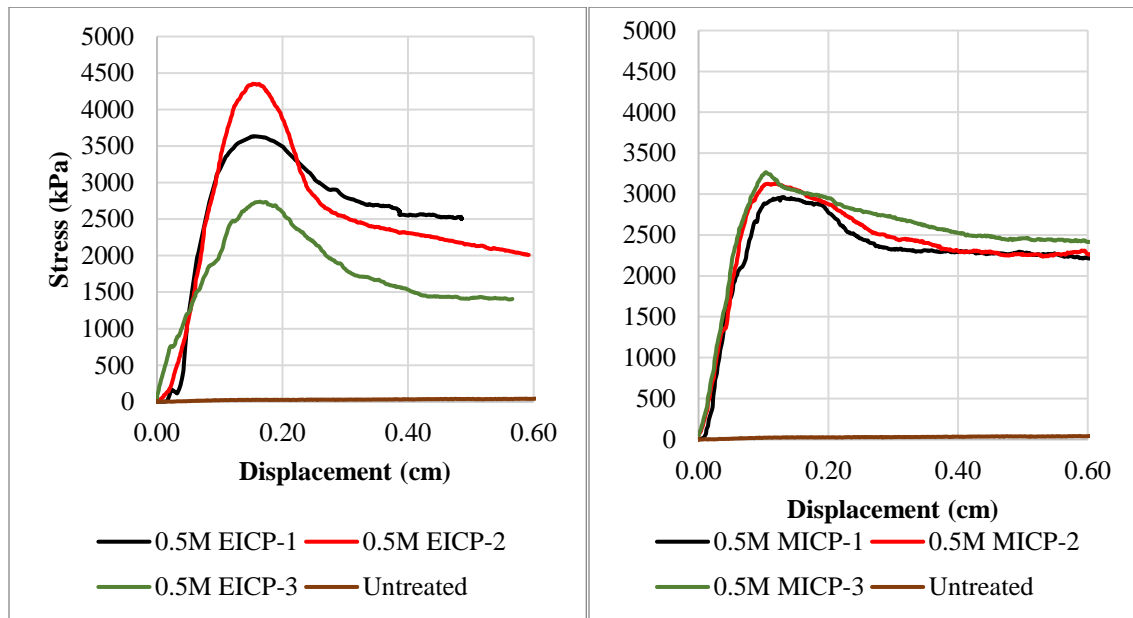


**Figure 5. 10.** Penetration Test Results of HS Samples: Treated with 0.5M EICP (left) and 0.5M MICP (right)

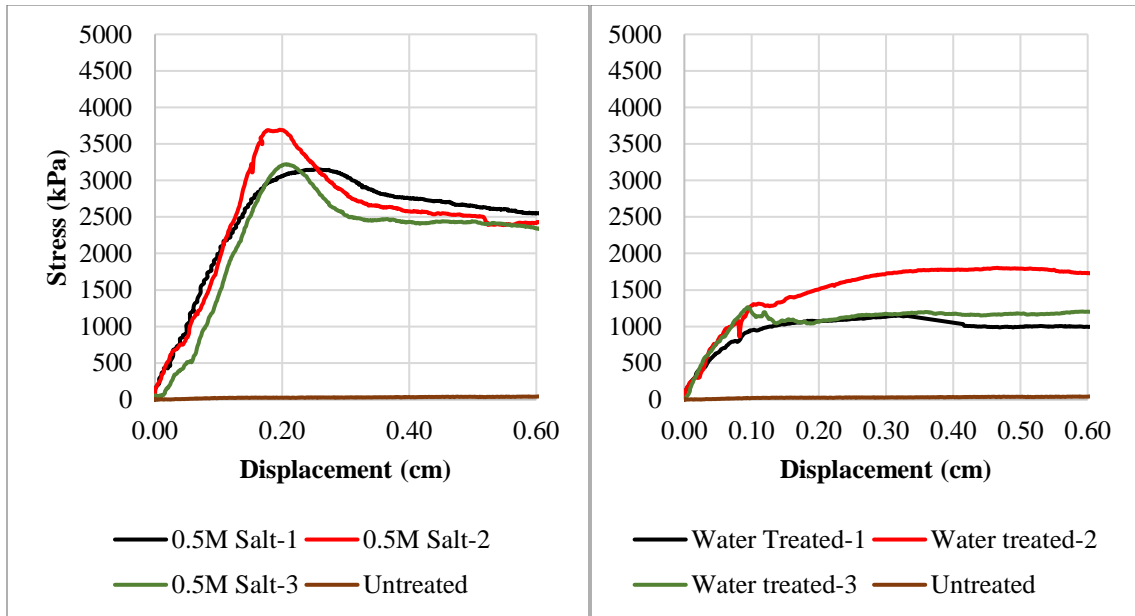


**Figure 5.11.** Penetration Test Results of HS Samples: Treated with Salt (left) and Water (right)

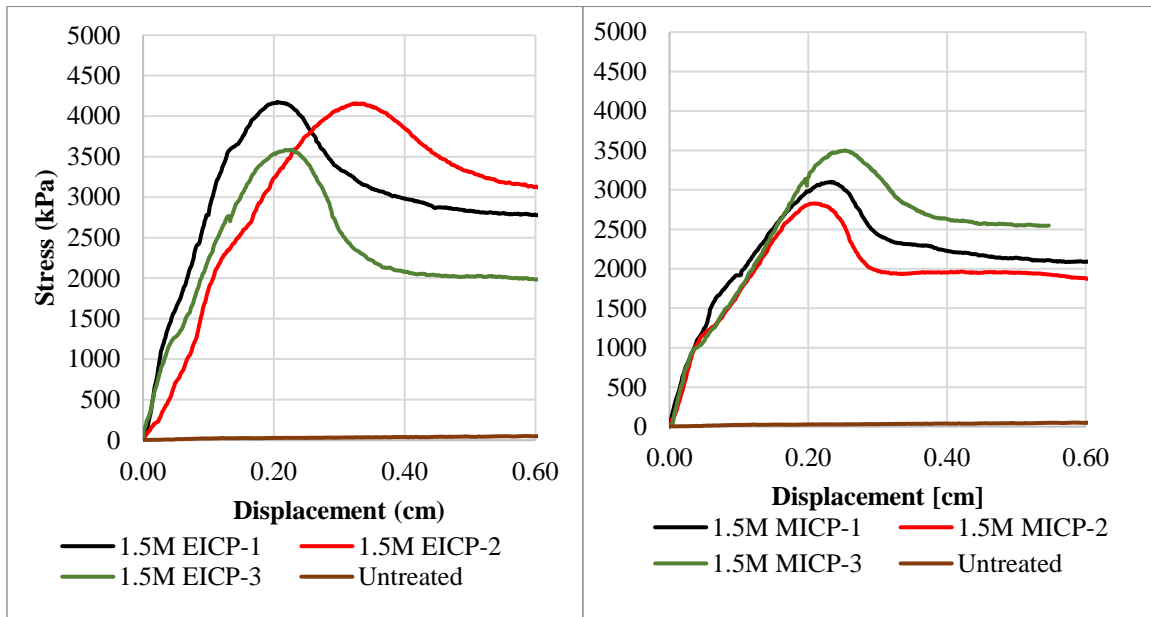


**Figure 5.12.** Penetration Test Results of HS Samples: Treated with 1.5M EICP (left) and 1.5M MICP (right)

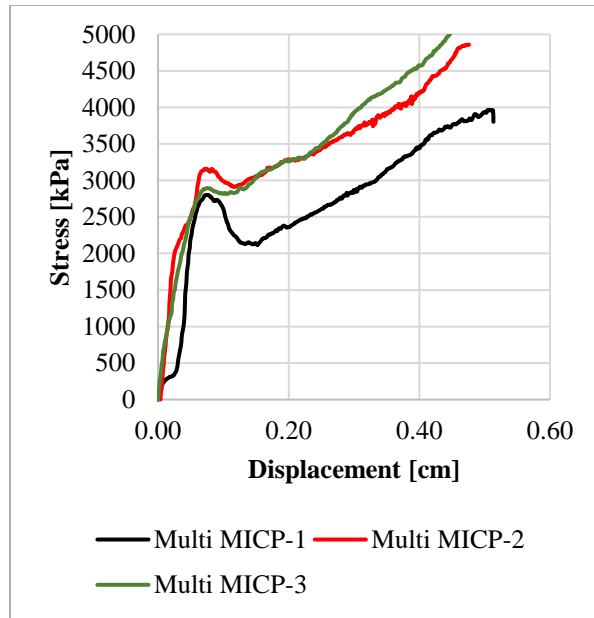


**Figure 5.13.** Penetration Test Results of HS Sample: Treated with MICP Three Times.

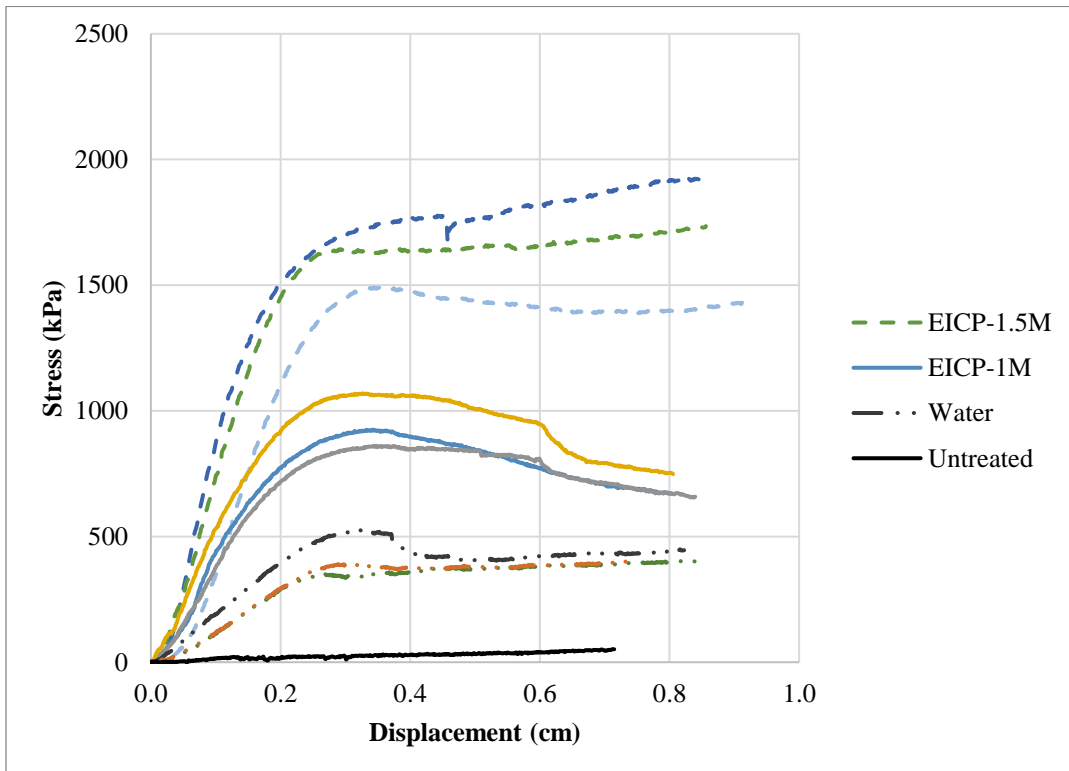


**Figure 5.14.** Penetration Test Results of LS Samples: EICP-treated Samples (Low and High Concentrations) vs. Water-treated Sample

**Table 5. 4. Summary of Samples with Different Treatments**

Sample#	Specimen#	Treatment solution	Concentration	Peak strength (kPa)	Displacement at peak strength (cm)
High salinity soil (HS)	0	Untreated	-	No Peak	-
	1A	Water (control)	-	1100	0.11
	1B	Salt of Urea+CaCl <sub>2</sub> (control)	0.5M urea+0.33M CaCl <sub>2</sub>	3350	0.20
		2A	EICP (low)	0.5M urea+0.33M CaCl <sub>2</sub>	3560
	2B	EICP (high)	1.5M urea+1M CaCl <sub>2</sub>	3960	0.25
	3A	MICP (low)	0.5M urea+0.33M CaCl <sub>2</sub>	3100	0.12
		3B	MICP (high)	1.5M urea+1M CaCl <sub>2</sub>	3100
	4	MICP (multiple treatments)	3*(0.5M urea+0.33M CaCl <sub>2</sub> )	3000	0.08
	Low salinity soil (LS)	0	Untreated	-	No Peak
1		Water (control)	-	400	0.3
2A		EICP (low)	1M urea+0.67M CaCl <sub>2</sub>	950	0.3
		2B	EICP (high)	1.5M urea+1M CaCl <sub>2</sub>	1600
3*		MICP (high)	1.5M urea+1M CaCl <sub>2</sub>	1050	0.3

\* Based on only one penetration in a smaller size of the specimen due to the sample scarcity

### 5.3.3. Result of Calcium Carbonate Content Measurement

The calcium carbonate content of samples from the crust were measured for each treated specimen to provide insight into the carbonate content induced by the treatment. For HS soil, the calcium carbonate content of the crust of EICP/MICP treated samples were in the same range as the calcium carbonate content measured for the bulk soil sample (3.8 – 4%) before treatment. The unchanged carbonate content of the samples suggests that the



EICP/MICP treatment did not result in additional precipitation of carbonate for this soil. On the other hand, for LS soil specimens, the calcium carbonate content of the surficial soil (i.e., the crust) of the treated specimens (high concentration EICP and MICP specimens) was  $1 \pm 0.2\%$  higher than the carbonate content measured for the bulk sample of this soil, which suggests that for specimens of LS soil, crusts were formed due to the calcite precipitation through biocementation.

#### 5.3.4. Discussion on salt effect

Yuan et al. (2022) conducted a study on Microbially Induced Calcium Carbonate Precipitation (MICP) within the high salinity environment of the Qaidam Basin. Their investigation focused on assessing the salt tolerance of microorganisms and their fundamental MICP capabilities. In their preliminary research, they observed that *Bacillus subtilis* exhibited a notably reduced growth rate when exposed to a 5% salt concentration environment compared to a salt-free environment during a 48-hour timeframe. Additionally, their study indicated that artificially cultivated *Sporosarcina pasteurii* was not resilient to the high salinity conditions present in the Qaidam Basin. The soil samples analyzed in their study exhibited soluble salt levels ranging between 8% and 12%, with chloride being the predominant anion, followed by sulfate ions. Among cations, sodium was the most prevalent, followed by calcium and magnesium ions. Given the considerably elevated salinity levels in HS soil from Salton Sea, the findings of our study that the enzyme from jack beans and *Sporosarcina pasteurii* were found to be intolerant to the highly saline environment, align with the findings reported in the referenced study.

Yuan et al. (2022) reveal in their study that a new type of high-yield urease-producing microorganism discovered in the high-salinity environment in the cold and arid area of the Qinghai-Tibetan Plateau, can precipitate vaterite and mineralized crystals in a highly saline silty soil column. This precipitation of minerals have a strengthening effect on saline silty soil particles, demonstrating the effectiveness and feasibility of MICP through a new strain of native salt-tolerant and high-yield urease-producing microorganism in a highly saline environment.

Almajed et al (2018) suggested that the precipitation ratio, which indicates what percentage of the substrates actually precipitate, decreases considerably in solutions with an  $EC_{initial}$  higher than a threshold value called the critical electrical conductivity ( $EC_{critical}$ ) (Figure 5.15). Khodadadi Tirkolaei (2016) showed a similar relation for MICP in which the cell concentration replaces enzyme concentration (Figure 5.16).

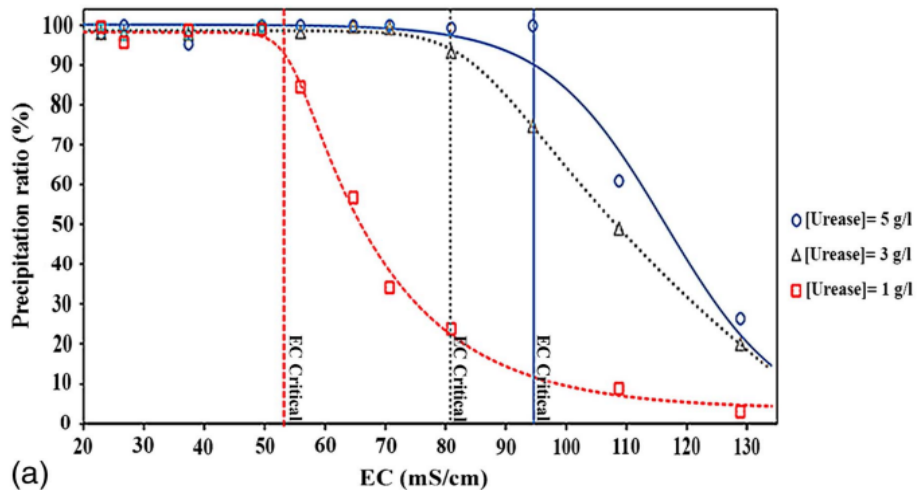


**Figure 5. 15.** Precipitation Ratio Versus Electrical Conductivity of the Treatment Solution at Different Enzyme Concentration (Almajed et al, 2018)

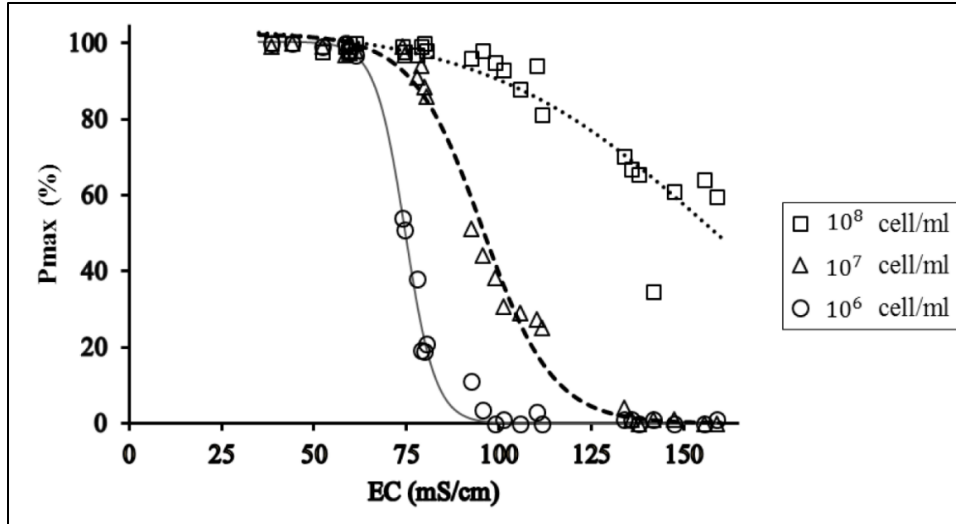


**Figure 5. 16.** Precipitation Ratio versus Electrical Conductivity of the Treatment Solution at Different Cell Concentration. (Khodadadi Tirkolaei, 2016)

Considering the high salinity of the HS soil in this study, it seems likely that the EC (in response to the salinity) of the treatment solution increases soon after it is sprayed over the soil through the dissolution of the soluble sodium chloride to a value greater than  $EC_{critical}$ , adversely impacting the efficiency of the biocementation treatment process and inhibiting the precipitation of carbonate on the soil surface in both ECIP and MICP.

To investigate whether the carbonate precipitation in the EICP and MICP treated specimens was inhibited by the high salinity of this particular soil, the salt effect was investigated by treating the same HS sample after the salt was removed. The resulting carbonate content measurements for the unsalted samples of HS sample with no treatment and with EICP and MICP treatment (Concentrations of 1.5 Molar of urea and 1 Molar of calcium chloride) are presented in table below.

**Table 5. 5.** Results of Carbonate Content Measurement of Unsalted Soil

Treatment method	Carbonate content (%)	Average carbonate content (%)
Untreated#1	6.8	6.7*
Untreated#2	6.6	
EICP#1	11.5	11.4
EICP#2	11.2	
MICP#1	10.5	11.5
MICP#2	12.5	

\* The carbonate content is higher than that in original HS soil after removing the soluble salts first

Carbonate content of the specimens after treatment is higher than that of untreated specimens, showing that carbonate is precipitated in the specimens of soil 1 after washing the salt content of the soil. The results from these experiments provide evidence that the inhibitory effect observed in the initial soil samples was due to the presence of salt.

#### 5.4. Conclusion

In this study, the potential of using MICP and EICP by urea hydrolysis for dust suppression on the Salton Sea playa was evaluated for selected sediment samples. Characterization of the material showed that HS sample contains 30 – 40% salt (mainly as sodium chloride) and LS sample contains about 4-5% salt. An experimental study was performed to assess the treatment performance and strength of the crusts formed from treatment of these two samples using the PI-SWER test, penetration testing, and calcium carbonate content analysis.

Based on both measured values of the PM10 concentration of dust generated in PI-SWERL testing and the surface strength from penetration testing, the erosion resistance of the water treated sample increased compared to the untreated sample,

indicating a crust was created by water application followed by evaporation.

Biocementation treatment resulted in higher erosion resistance compared to the water treated samples for both samples. However, for the HS soil (the high salt content soil), the erosion resistance of the MICP and EICP treated specimens was comparable with that of the salt and water treated specimens. For the LS samples, the EICP treated samples showed a lower dust emissivity compared to the water treated sample.

Based on the calcium carbonate measurements, neither MICP nor EICP treatment showed any sign of calcium carbonate precipitation for HS sample, indicating that the created crusts on the specimens and the increased erosion resistance was attributed to the salt crust formed by evaporation rather than by calcite precipitation through biocementation. For LS soil (the low salt content soil), the measured carbonate precipitation of about 1% in the crust of the treated specimens appears to have contributed to the surface strength and wind erosion resistance of the treated specimens.

For HS soil, it is hypothesized that dissolution of the soluble salt in the soil into the EICP and MICP treatment solutions increased the treatment solution salinity to greater than the critical value for carbonate precipitation and suppressed the urease activity.

The findings of this study align with Yuan et al.'s (2022) discovery that artificially cultivated *Sporosarcina pasteurii* also exhibited intolerance in the high saline environment of Qaidam Basin. The enzyme from jack beans and *Sporosarcina pasteurii* were found to be intolerant to the highly saline environment.

The results have shown that precipitation of evaporative salts can result in a strong crust with strong erosion resistance. Wetting the sample or adding salt to the water

can increase erosion resistance. However, if the salt precipitates as loose unconsolidated crystals, the binding effect may be limited. Secondly the results have shown that MICP or EICP do not result in calcium carbonate crust for saline soils.

## CHAPTER 6

### 6. EVALUATION OF THE APPLICATION AND DURABILITY OF MICROBIALLY INDUCED CARBONATE PRECIPITATION FOR FUGITIVE DUST CONTROL OF SILTY SAND

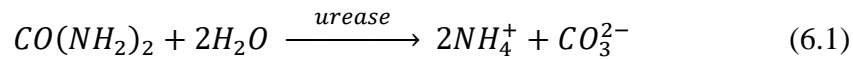
#### ABSTRACT

To scale up the application of biocementation as a dust mitigation technique, a field trial was conducted on a landfill in Mesa, Arizona. Applications of enzyme-induced carbonate precipitation (EICP), xanthan gum enhanced EICP (XEICP), and microbially induced carbonate precipitation (MICP) were demonstrated alongside control plots of magnesium chloride ( $MgCl_2$ ) and no treatment. These technologies were demonstrated in parallel plots of 6×30 meters each, spaced 6 meters apart. The application of MICP, challenges related to this technique, and the results for the MICP plot are presented herein. These MICP results are compared to the results from the other test plots in the field trial. The wind erosion resistance was measured using the Portable In-Situ Wind EROsion Lab (PI-SWERL™) device and the crust strength was characterized by pocket penetrometer and Torvane testing in the field. Fugitive dust concentrations generated by intentional disturbance of the field plots were also collected. The carbonate content of crust samples was measured pre- and post-treatments in the laboratory. Isotope ratio mass spectrometry (IRMS) analysis was also conducted on the crust samples to better distinguish precipitated carbonate from background carbonate in the MICP plot. The findings from the field and laboratory testing indicated only limited precipitation of carbonate in the

soil crust through MICP treatment that resulted in slightly lower durability compared to the EICP-treated plot.

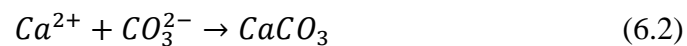
### 6.1. Introduction

Microbially induced carbonate precipitation (MICP) is a biocementation technique in which the ureolytic activity of bacteria is used to hydrolyze urea. Equation 6.1 shows the outcome of the urea hydrolysis reaction:



The source of the urease is ureolytic microbes in MICP and free urease enzyme in EICP (enzyme induced carbonate precipitation). For calcium carbonate precipitation, a source of calcium ions is required. Calcium chloride ( $CaCl_2$ ), which can easily be dissolved in water, is commonly used as the source of the calcium ions.

Under the right geochemical conditions (e.g., pH, alkalinity), an aqueous solution of carbonate ions formed by urea hydrolysis and calcium ions in solution results in the precipitation of solid calcium carbonate crystals as shown by Equation 6.2:



The precipitated calcium carbonate has been shown in the laboratory to form a crust by binding the soil particles together when the solution is sprayed or poured on the soil surface (Ehsasi et al., 2022).

Biocementation through MICP for dust mitigation in various soil types has been investigated by several researchers on the laboratory scale (e.g., Chae et al., 2021; Ehsasi et al., 2022). However, the application of MICP in field conditions has not been



extensively explored. Most field studies have concentrated on clean sandy soils when investigating MICP as a dust mitigation technique (Gomez et al., 2015; Meng et al. 2021). There is a need to investigate the potential of using MICP for dust mitigation in other soil types within field settings.

In this study, a field trial of dust mitigation through MICP treatment was conducted on a silty sand with gravel interim cover soil on an inactive section of the Salt River Landfill in Mesa, AZ (the SRL site). Dust mitigation treatment using MICP was a component of a larger project conducted by the Center for Bio-mediated and Bio-inspired Geotechnics (CBBG) at Arizona State University (ASU) and documented by Woolley (2023) (work in progress) and Yu (2023). In the larger project, five parallel dust mitigation test plots were investigated, including the plots treated with EICP, XEICP (EICP with xanthan gum), and MICP and magnesium chloride ( $MgCl_2$ ) and untreated control plots. Figure 6.1 shows the configuration of the test plots at the SRL test site.

The MICP test plot at the SRL site is the focus of this study. The primary objectives of this testing program were to:

- Study the effectiveness of MICP as a dust mitigation technique in silty sand with gravel.
- Investigate the feasibility of MICP treatment as a dust mitigation method on the field-scale.
- Evaluate the effectiveness and durability of MICP as a dust mitigation technique in the arid climate of Arizona.
- Compare the effectiveness of MICP with the other techniques that were applied in this project.

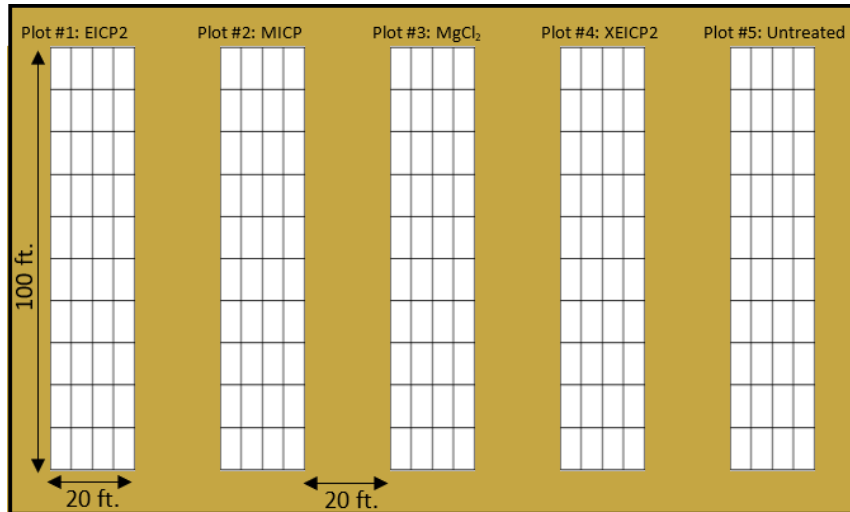


**Figure 6. 1.** Configuration of Test Plots Layout for Field Trial at SRL Test Site (Not to Scale) (Woolley, 2023).

Field testing conducted on the test sections included Portable In-Situ Wind Erosion Laboratory (PI-SWERL) testing to measure the erosion resistance of the crust and pocket penetrometer and Torvane testing to measure surface strength of the crust. Additionally, calcium carbonate (CaCO<sub>3</sub>) content was measured on specimens recovered from the field test sections using a calcimeter, wherein the volume of carbon dioxide gas produced during the reaction between hydrochloric acid and the carbonates is used to assess carbonate content. Isotope ratio mass spectrometry (IRMS) analysis was also conducted in the laboratory to better distinguish precipitated carbonate from background carbonate.

## 6.2. Materials and Methods

### 6.2.1. Soil Characterization

Soil characterization was conducted by Yu (2023) in the geotechnical laboratory at Arizona State University and the results are presented in Table 6.1. The results of the

particle size distribution analysis, performed in accordance with ASTM D422-63 standards, are presented in Figure 6.2.

**Table 6. 1. SRL Soil Properties (Yu, 2023).**

Parameter	SRL Soil
D <sub>60</sub>	0.75
D <sub>30</sub>	0.14
D <sub>10</sub>	0.03
% < #200 sieve	14-25
Cu	25
Cc	0.871
D <sub>d</sub>	2.303
LL	15.3%
PI	NP
USCS Classification	SM

The soil's fine fractions were tested for liquid limit and plastic limit based on ASTM D4318-05. These tests showed the fraction of soil passing the number 40 sieve had a liquid limit of 15% and was non-plastic. In accordance with ASTM D2487, the Unified Soil Classification System (USCS), the soil is categorized as silty sand with gravel (SM).

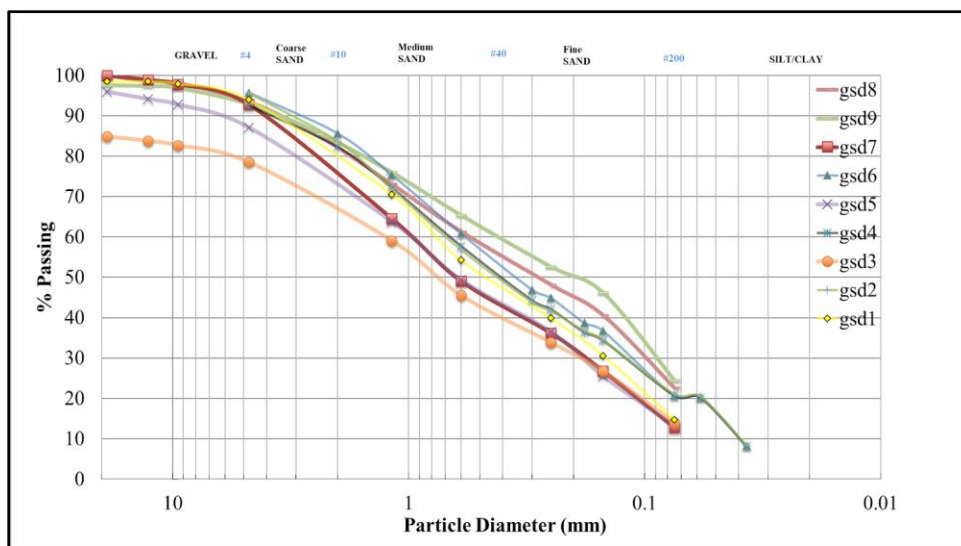


**Figure 6. 2.** Grain Size Distribution for SRL Soil Samples (Yu, 2023).

### 6.2.2. Bacteria Cultivation

The bacteria *Sporosarcina pasteurii* was used as the source of the enzyme urease. The bacteria were cultivated aerobically in a plastic drum under non-sterile conditions in the laboratory with an ambient temperature of approximately 25°C using 150 L of nutrient broth. For the bacteria cultivation, 2L of a previously cultured solution that was stored in the refrigerator was used as the inoculum. The growth medium in the drum contained 20 g/L yeast extract, 10 g/L NH<sub>4</sub>Cl, 6 g/L urea, and 24 mg/L NiCl<sub>2</sub>. The pH of the medium was adjusted to 9 by adding NaOH and subsequently maintained at this level throughout the growth process by continuous addition of NaOH. The oxygen was supplied using a KoiAir 1 aeration kit with an air flow of 0.8 CFM. The nutrient broth was stirred continuously with a drill and paint mixer attachment that was securely affixed on top of the drum. To prevent depletion of nutrients, additional substrates equal to one-third of the initial substrates were added into the cultivation solution after 30 hours of growth. Figure 6.3 shows the drum and the process of addition of material into the growth medium.



**Figure 6. 3.** Bacteria Cultivation in a Plastic Drum in the Laboratory

The activity of the ureolytic bacteria was measured to be 200 mM urea/hour using the electrical conductivity method (Whiffin, 2004) with an OD of 1.77 at 600nm after 40 hours of growth. The bacteria were diluted with water to reach a final volume of 226 L before application in the field, which reduced the urease activity of the treatment solution to about 133 mM urea/h.

### 6.2.3. MICP Treatment in the Field

EICP, XEICP (EICP with xanthan gum), MICP, and  $MgCl_2$  treatment solutions were applied on parallel plots of 6×30 meters each, spaced 6 meters apart. The MICP treatment was applied as a two component mixture: 1) 226 L of the bacteria *Sporosarcina pasteurii* (the source of the enzyme urease); and 2) 226 L of a cementation solution containing 1.2M Urea and 1.1 M of calcium chloride. The concentration of urea and calcium

chloride was determined through laboratory experiments conducted for EICP treatment. These same concentrations were employed in the MICP treatment for the sake of comparison. Commercial grade calcium chloride and agricultural grade urea (46% Nitrogen) were used to prepare the cementation solution.

Table 6.2 summarizes the treatments, concentrations, and application rates for each plot at the SRL site. The treatment procedure using EICP, XEICP, and MgCl<sub>2</sub> is described in detail by Woolley, 2023.

**Table 6. 2.** Concentrations and Application Rates for Treatment Plots in SRL Site (Woolley, 2023)

Plot	Treatment Volume (L/m <sup>2</sup> )	Treatment Concentration
#1: EICP	2.4	1.1M CaCl <sub>2</sub> , 1.2M Urea, 25 mL/L enzyme (~200 U/mL), 4.0 g/L dry milk
#2: MICP	3.6	Cementation solution: 1.1M CaCl <sub>2</sub> , 1.2M Urea + Bacterial (urease activity = 133 mM urea/hr)
#3: MgCl <sub>2</sub>	1.2	3.2M MgCl <sub>2</sub> (30% m/V)
#4: XEICP	2.4	1.1M CaCl <sub>2</sub> , 1.2M Urea, 25 mL/L enzyme (~200 U/mL), 4.0 g/L dry milk, 1.0 g/L xanthan gum, 5 mL/L glycerin
#5: Control	Untreated	

The MICP treatment was applied during the peak of daytime heat in the month of April, in the arid climate of Arizona. The temperature during deployment was about 90 F and the relative humidity was about 15-20%. To apply the surficial treatment solutions, a two-step percolation method was used where two people applied the treatment solutions sequentially and synchronously. The solutions were applied with two separate hand-held

sprayers from a tank on a pickup truck that followed closely behind. Application of the cementation solution followed the application of the Bacteria by about 1 minute. The total treatment duration was about 30 minutes.

Due to the high temperature, the applied MICP solution exhibited rapid evaporation following deployment that could be visually observed (the soil color became darker when wetted and lighter when it dried out). Due to concern that the rapid evaporation inhibited the complete hydrolysis of urea and the reaction with the cementation solution, the team decided to apply a second treatment. The second treatment was applied the next day in the morning (about 18 hours after the first application) and included only cementation solution with the same volume (226 L) and concentrations of urea and calcium chloride as in the first treatment.

The total solution that was applied onto the MICP plot was on average  $1.2 \text{ L/m}^2$  of bacteria and  $2.4 \text{ L/m}^2$  of cementation solution. Figures 6.4 and 6.5 show the MICP application process, the treatment in progress and the plot immediately after.



**Figure 6. 4.** Preparing the Cementation Solution and the MICP Treatment in Progress in SRL Field.



**Figure 6. 5.** Aerial View of the Field Trial Area Immediately after Treatment of MICP Plot.

#### 6.2.4. PI-SWERL Test

The Portable In-Situ Wind ERosion Laboratory (PI-SWERL) was used to measure the potential for wind erosion and dust emission from the surface of the soil in the field



before and after treatment. An overview of the PI-SWERL device is given in the preceding chapter of this thesis (Chapter 5). The PI-SWERL test was conducted at multiple spots across the MICP plot to provide representative coverage.

#### 6.2.5. Surface Strength Test

Wind erosion, and consequently the amount of wind-blown dust, depends on the soil's surface shear strength (Chen et al. 2014). In this study, pocket penetrometer and Torvane testing were used to measure surface shear strength across the plot. A Humboldt pocket Torvane (H-4212MH) and a Humboldt soil pocket penetrometer (H-4195) with a diameter of about 6 mm were used for this purpose.

#### 6.2.6. Carbonate Content Measurement

The average carbonate content of the plot before and after treatment was measured to provide insight into changes in the calcite content resulting from treatment. Carbonate content was measured with a Calcimeter (Eijkelkamp, Wilmington NC, USA) as described by ASTM D 4373-84. The Calcimeter quantifies the carbonate content based on the volume of carbon dioxide gas produced during the reaction between hydrochloric acid and the carbonates in the soil. Samples from MICP plot were collected from 30 points both before and after treatment, to measure carbonate content. Samples were collected from the surface down to a depth of 1 centimeter. Each sample was homogenized and 2 to 3 grams of them were used for carbonate content measurement.

### 6.2.7. Isotope Ratio Mass Spectrometry

Isotope ratio mass spectrometry (IRMS) was conducted to distinguish between naturally occurring carbonates and carbonates created by MICP treatment. Carbonate samples were analyzed using gasbench-IRMS, a specific type of isotope ratio mass spectrometry (IRMS) designed for measuring isotopic compositions of gases, specifically CO<sub>2</sub> released during carbonate digestion (Woolley, 2023). First, the gasbench-IRMS analysis was employed to determine the isotopic signature of MICP-carbonate precipitated using the treatment solution in the absence of soil. Then, this test was conducted on ten MICP-treated soil samples collected from the test plot. Data obtained by Woolley (2023) for the isotope signature of the carbonates in the untreated soil from the test plot area were used to distinguish precipitated carbonate from background carbonate in the MICP plot.

### 6.2.8. Induced Disturbance Testing

Field measurements on the test plots included assessing the effect of induced disturbances generated by driving a four-wheel drive truck (with and without dragging a portion of chain link fence behind the truck) over the total length of each plot and half of their width. One half of the plot remained undisturbed for repeated surface characterization at later time intervals. The truck was operated over a duration of ten to fifteen minutes at two different speeds, and by dragging the chain link fence at two distinct speeds. Peak PM<sub>10</sub> concentrations were measured using TSI Dust Trak<sup>TM</sup> that was located downwind at the end of a plot and along the centerline of the plot area during the induced dust event. The specific testing procedure involved the following steps (Woolley, 2023):

1. Baseline monitoring for up to one hour prior to starting disturbances,
2. Three passes of a four-wheel drive vehicle at 5 mph,
3. Three passes of the four-wheel drive vehicle at 10 mph,
4. One pass of the four-wheel drive vehicle dragging chain fencing at 5 mph,
5. One pass of the four-wheel drive vehicle dragging chain fencing at 10 mph.

Figure 6.6 shows the four-wheel drive vehicle dragging the chain link fence over the MICP plot in step 5 (10 mph).



**Figure 6. 6.** Induced Dust Event Along the MICP Plot with the Truck Dragging a Chain Link Fence at Speed of 10 mph.

### 6.3. Results and Discussion

#### 6.3.1. PI-SWERL Test Results

The PI-SWERL was deployed in the field at locations within each test plot. For the MICP plot, the PI-SWERL was run at 5 locations before, 10 locations within two weeks after,

and an additional 5 locations three months after the treatment. The total emission flux (Ef) from PI-SWERL data is calculated as in Eq. 6.3:

$$Total\ Emission\ Flux = E_f = \sum \frac{Instant\ Flux\ (\frac{\mu g}{s})}{A_{eff}\ (m^2)} \quad (6.3)$$

where  $A_{eff}$  ( $m^2$ ) is the effective surface area from which the instant flux of PM10 ( $\mu g/s$ ) is generated. The PI-SWERL has an effective surface area of  $0.035m^2$  (Dust Quant LLC. 2018; Etyemezian et al. 2014). The threshold friction velocity (TFV) is defined as the velocity at which the emission flux of PM10 particles reaches a cumulative rate of  $200\ \mu g/m^2s$  (Munkhtsetseg et al, .2016). A comprehensive comparison of the results obtained from all treated plots as well as from the untreated plot is displayed in Figure 6.7. This figure presents the TFV for each plot at three distinct times: pre-treatment, one to two weeks after treatment, and three months following treatment.

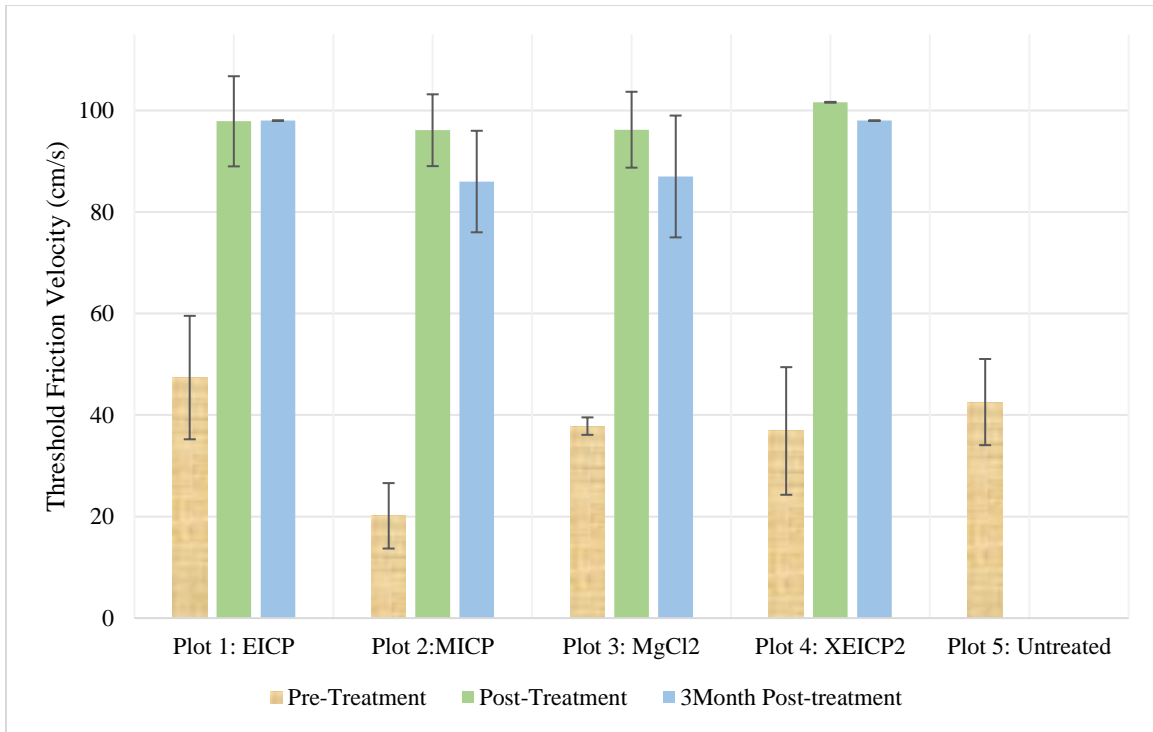


**Figure 6. 7.** PI-SWERL Measured TFV Values for Untreated and Treated Soil Surfaces (Results Averaged from 5 or More Test Runs at Locations Throughout the Treatment Plot Areas) (Woolley, 2023; Yu, 2023).

The PI-SWERL results showed heterogeneity across the test plots. The MICP plot had the lowest and the EICP plot had the highest pre-treatment TFV. Based on the PI-SWERL data within 2 weeks after treatment, all treatments resulted in improvement of TFV in the same order of magnitude. Based on the tests results from three months after treatment, the EICP plot was superior with respect to retained TFV, i.e., had the highest durability. After three months, both the MICP and MgCl<sub>2</sub>-treated plots exhibited a reduction of approximately 10% from their post treatment TFV.

More detailed results of PI-SWERL testing, presented in terms of the average PM<sub>10</sub> concentration (the concentration of particulate matter with an effective particle diameter of 10 micrometers or less in the chamber of PI-SWERL in mg/m<sup>3</sup>) versus

friction velocity for each test plot are presented in Figure 6.8. These results are for the measurements taken three months after the treatment. All the plots that received treatment demonstrated a significantly higher erosion resistance compared to the untreated plot. The EICP plot consistently showed the highest wind erosion resistance (i.e., lower PM 10 concentrations) throughout the range of friction velocities.

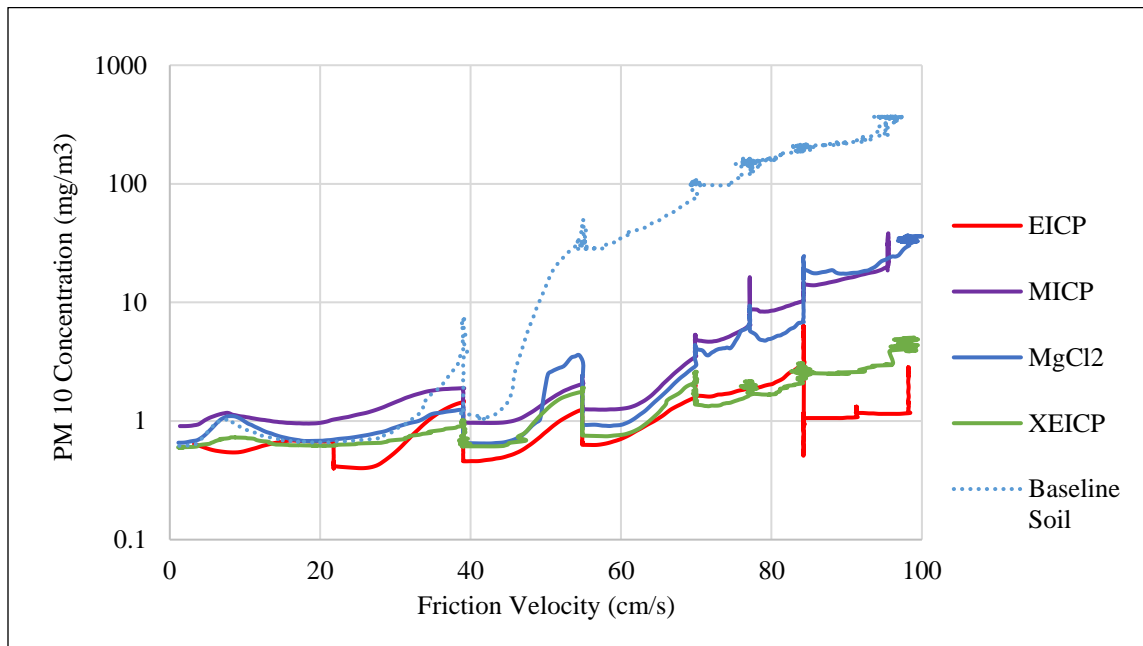


**Figure 6. 8.** PI-SWERL Results from all Plots: Average PM10 Concentration from Each Plot vs. Threshold Friction Velocity. (Yu, 2023).

### 6.3.2. Surface Resistance Testing

The strength of the soil crust before and after treatment was evaluated using pocket penetrometer and Torvane measurements. The average penetration resistance and Torvane shear resistance of the MICP plot along with the results from the other plots from Woolley (2023) are presented in Tables 6.3 and 6.4, respectively. All the post-treatment measurements were done within two weeks of treatment.

**Table 6. 3. Average Pocket Penetration Resistance (kPa) of the Soil Crust**

Plot	Pre-Treatment			Post-Treatment			Increase in penetration resistance (%)
	Average	Std. Dev	No. of Tests	Average	Std. Dev	No. of Tests	
EICP	1.6	1.0	68	4.0	0.7	82	150
MICP	1.8	1	35	3.5	0.8	90	94
MgCl <sub>2</sub>	1.5	1.2	109	2.6	0.6	112	73
XEICP	1.2	0.6	42	3.0	0.4	190	150
Untreated	1.4	1.0	125	-	-	-	-

**Table 6. 4. Average Torvane Shear Resistance (kPa) of the Soil Crust**

Plot	Pre-Treatment			Post-Treatment			Increase in shear resistance (%)
	Average	Std. Dev	No. of Tests	Average	Std. Dev	No. of Tests	
EICP	2.9	1.4	91	7.8	3.2	158	170
MICP	2.8	0.9	30	7.0	2.5	30	150
MgCl <sub>2</sub>	2.7	2.0	115	5.2	0.7	111	92
XEICP	2.8	1.1	73	6.5	1.8	187	132
Untreated	2.8	1.0	98	-	-	-	-

The surface resistance of all plots was improved by treatment. The plots showed a varying degree of improvement in resistance, with the highest improvement in the EICP-treated plot, followed by the XEICP plot and then the MICP plot. The lowest increase in the degree of improvement was recorded for the plot treated with MgCl<sub>2</sub>.

### 6.3.3. Calcium Carbonate Content Measurement

The study area exhibited a high background carbonate content with significant variability in carbonate distribution across the plot. This variability made assessing the precipitated carbonate content challenging, as the amount of carbonate precipitated was of the same order of magnitude as the variability. Nevertheless, discrete samples were collected from

across the plot before and after treatment and were tested for carbonate content. The results revealed a slightly higher carbonate content, on average, in the MICP treated samples (average carbonate content of 2.48% by mass) compared to the untreated samples (average carbonate content of 2.37% by mass). Table 6.5 presents the carbonate content measurements of all plots prior to treatment (background carbonate content of the soil), within two weeks of the treatment, and three months after treatment.

**Table 6. 5.** Average Total CaCO<sub>3</sub> Content (% by mass) in the Crust of Field Specimens (Wooley, 2023; Yu, 2023)

Plot	pre-treatment			2-weeks-post-treatment			3-month- post-treatment	
	Average	SD	No. of specimens	Average	SD	No. of specimens	Average	No. of specimens
EICP	1.88	0.48	71	2.05	0.69	71	2.1	9
MICP	2.37	0.6	28	2.48	0.8	30	2.35	9
MgCl <sub>2</sub>	1.82	0.19	11	1.73	0.29	17	1.6	9
XEICP	1.60	0.43	33	1.99	0.49	45	1.85	9

Comparing the results from pre-treatment to the results obtained within two weeks after treatment, the XEICP-treated plot showed the highest carbonate precipitation (0.39% additional carbonate by mass) and the EICP-treated plot showed slightly higher precipitation (0.17% additional carbonate by mass) than the MICP-treated plot (0.11% additional carbonate by mass).



#### 6.3.4. Isotope Ratio Mass Spectrometry

The  $\delta^{13}\text{C}$  values from the Gasbench-IRMS analysis are summarized in Table 6.6. IRMS testing of the MICP test tube precipitate resulted in a  $\delta^{13}\text{C}$  signature of about -41, comparable with that from EICP, i.e. -45 to -50 ‰VPDB. These values show that precipitated carbonates from MICP, and those from EICP, are isotopically lighter (more negative ‰VPDB) than the carbonates from many other carbonate forming processes (Wagner et al. 2018, Woolley, 2023). The IRMS values from the untreated soil are in the range of -4.8 to -8.5, consistent with the values from natural carbonate forming process. IRMS values on crust samples collected from the treated test plots yielded a range of  $\delta^{13}\text{C}$  values of -5.4 to -13.1. The  $\delta^{13}\text{C}$  for MICP treated soil is lower than that for the untreated soil, indicating some of the carbonate in the crust of the treated soil is from MICP. Also, the range of  $\delta^{13}\text{C}$  of the EICP-treated soil is slightly lower than that of the MICP-treated soil, consistent with the lower  $\delta^{13}\text{C}$  of the precipitated EICP (without soil) in the laboratory compared to that of MICP (without soil).

**Table 6. 6.** Isotopic Signature Ranges of  $\delta^{13}\text{C}$  for Carbon in Carbonates from SRL Soil Test Specimens and Lab Made EICP and MICP Precipitations.

Specimen	$\delta^{13}\text{C}$ ‰VPDB	% $\text{CaCO}_3$ (avg)	# of specimens (n)
EICP Treatment (no soil)	-45.9 to -50.4	$97.2 \pm 2.8\%$	4
Untreated SRL soil	-4.8 to -8.5	$1.2 \pm 0.4\%$	5
EICP Treated SRL soil	-6.6 to -15.1	$2.1 \pm 0.7\%$	7
MICP Treatment (no soil)	-41.4 to -41.5	$94\% \pm 1\%$	2
MICP Treated SRL soil	-5.4 to -13.1	$3 \pm 1.2\%$	10

### 6.3.5. Induced Disturbance Measurements

The peak PM10 concentrations measured during induced disturbance testing results by TSI Dust Trak™ are presented in Figure 6.9, illustrating PM10 measurements for the surface conditions before and after treatment.

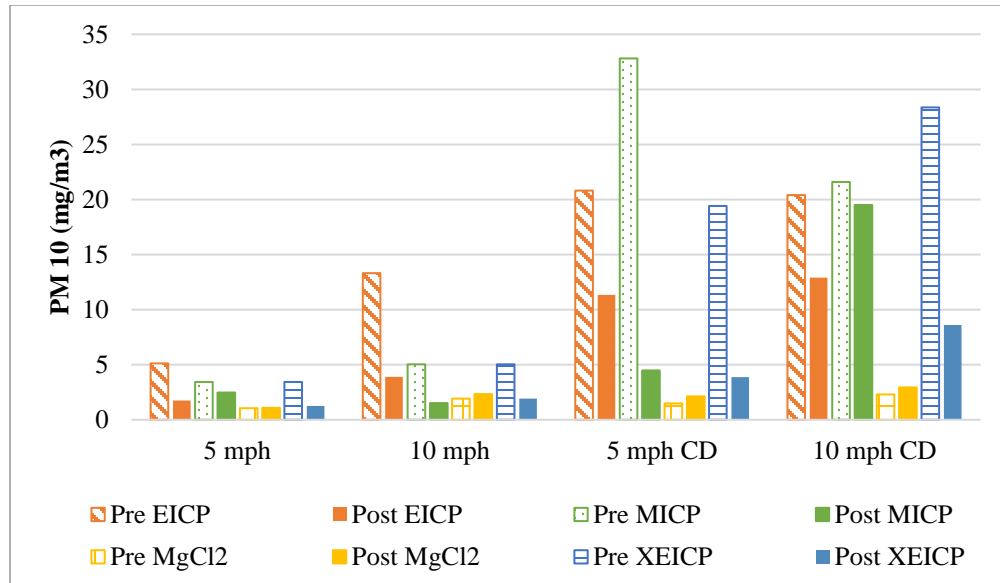


**Figure 6.9.** Comparison of Dust Pollution from the induced Disturbance Testing for both Pre- and Post-treated Surface Conditions. Note “CD” Stands for the Addition of the Chain Drag. (Woolley, 2023)

Both EICP- and XEICP-treated plots yielded a significant reduction in dust emissions across all speeds, whether the chain was being dragged or not. The MICP-treated plot showed a significant improvement in disturbance resistance in all cases except when the speed was set at 10 mph with the chain attached. The MgCl<sub>2</sub> plot showed a higher resistance to induced disturbance before and after treatment and in all conditions.

### 6.3.6. Discussion

The conditions during growth and storage of the bacteria affect the specific urease activity significantly (van Paassen, 2009). Due to the cultivation in a non-sterile condition and probably insufficient oxygen supply during the cultivation, the activity of the bacteria cultivated in this study was measured to be 200 mM urea/hour with an OD of 1.77 at 600nm after 40 hours of growth. This is lower than the activity of bacteria cultivated in a smaller bioreactor (600 mM urea/hour) in the laboratory with same concentration of nutrients from our previous experiments (Ehsasi et al. 2022).

Rapid evaporation may have inhibited the complete hydrolysis of urea and limited the precipitation of  $\text{CaCO}_3$  in the first treatment that was applied during the peak of daytime heat. Consequently, an additional application was necessary, leading to the second treatment. Application scheduled during the cooler part of the day, could help to avoid this issue and result in nutrient conservation.

Based on the results from PI-SWERL testing, the MICP plot showed an improvement in erosion resistance about two weeks after treatment. Based on the PI-SWERL tests results from three months post- treatment, the EICP plot had the highest durability. Over this three month period, both the MICP- and  $\text{MgCl}_2$ -treated plots experienced a reduction of approximately 10% in their erosion resistance compared to their initial post-treatment levels. These findings suggest that the initial increase in erosion resistance of the MICP-treated plot may be partially attributed to salt precipitation.

The results obtained from carbonate content measurements and isotope ratio mass spectroscopy indicated a slightly higher carbonate content in the MICP-treated samples compared to the untreated samples.

The theoretical precipitated carbonate content based on the applied volume of cementation solution on this soil would be about 7% by mass, assuming the soil was saturated during precipitation with a typical porosity of 40%. In case soil was 50% saturated during precipitation 3.5% increase in carbonate content of soil would be expected. Having only an average increase in  $\text{CaCO}_3$  content of about 0.1% indicates the process was not very efficient.

This finding suggests a minimal conversion of urea and calcium chloride into calcium carbonate. The incomplete conversion of urea and calcium chloride to calcium carbonate in MICP-treated plot might be partially attributed to the high silt content ( $\approx 20\%$ ) of the soil that causes filtration of bacteria at the surface. This observation aligns with Mitchell & Santamarina 2005 study, which highlighted that bacteria-based ground improvement methods are effective within specific grain size ranges. This The efficiency of the method could perhaps also be determined by measuring residual ammonia, calcium or urea in a dry sample suspended in known amount of water.

The results of pocket penetrometer and Torvane tests showed that the plot treated with  $\text{MgCl}_2$  exhibited the lowest surface resistance. This observation indicates that the formation of a salt crust has less impact in improving the surface resistance compared to the carbonate bonding resulting from MICP and EICP processes.

When subjected to induced disturbance, all the treated plots showed an improvement (reduction) in dust generation. EICP, XEICP, and MICP Plots showed

increasing dust susceptibility with increasing driving speed and when subjected to dragging the chain behind the truck. However, data obtained from the  $\text{MgCl}_2$  treated plot appears to be unreliable, which could be attributed to several factors. These may include the possibility of incorrect placement of dust monitor, wind direction during testing (potentially blowing dust away from the monitoring system), potential defects in the dust monitoring equipment during the test, or the original (pre-treatment) compactness of the  $\text{MgCl}_2$ -treated plot surface, which might have made it more resistant to disturbance when driven over.

#### 6.4. Conclusion

The efficacy of biocementation for fugitive dust mitigation in the field scale was evaluated. Four different treatments were applied to parallel test plots: enzyme-induced carbonate precipitation (EICP), xanthan gum enhanced EICP (XEICP), microbially induced carbonate precipitation (MICP), and magnesium chloride ( $\text{MgCl}_2$ ). Each plot measured 6x30 meters and they were spaced 6 meters apart. The focus of this study is the MICP test plot. Challenges associated with the application of the MICP technique and results of post-treatment testing are included.

Wind erosion resistance was assessed using the Portable In-Situ Wind Erosion Lab (PI-SWERL™) device and crust strength was characterized via Torvane and pocket penetrometer tests. To confirm carbonate precipitation via biocementation, carbonate content was measured before and after treatment using the Calcimeter. Additionally,

isotope ratio mass spectrometry (IRMS) was used to differentiate precipitated carbonate from background carbonate.

The comprehensive results from both field and laboratory testing revealed limited carbonate precipitation within the soil crust due to the MICP treatment. The erosion resistance of the MICP-treated plot exhibited a significant increase following treatment. The MICP crust subsequently experienced a 10% reduction in strength over the three months following treatment. The EICP-treated plot maintained its erosion resistance at the same level over the same three months period.

The induced disturbance test revealed that all EICP, XEICP, and MICP-treated plots exhibited increased resistance to disturbance following treatment. The XEICP plot demonstrated the highest efficiency after treatment.

When considering all the data collected from field and laboratory assessments, in general MICP-treated plot showed lower efficacy in comparison to the EICP- and XEICP-treated plot. While the  $MgCl_2$  showed the best performance when subjected to the chain drag, this data may not be reliable and environmental constraints hinder the application of  $MgCl_2$  in many jurisdictions. In these cases, both MICP and EICP may provide effective alternatives.

## CHAPTER 7

### 7. SUMMARY, CONCLUSIONS, AND RECOMMENDATIONS FOR FURTHER STUDY

#### 7.1. Summary

The application of Enzyme and Microbial Induced Carbonate Precipitation (EICP/MICP) as dust mitigation techniques have been studied for several soil types and under diverse environmental conditions in this dissertation. A summary and the findings from each chapter containing original research are presented as follows:

**In Chapter 3**, MICP was used to stabilize two types of mine tailings, silty sand (SM) and low plasticity silt (ML), in the laboratory. The treatment solution was applied in different ways and varying concentrations to determine the effect of the application method. The effect of treatment was evaluated by performing strain-controlled penetration tests and measuring the  $\text{CaCO}_3$  content after treatment and after several washing and drying cycles.

The results indicated that an increased carbonate content associated with increasing the solution concentration and number of treatment applications enhanced penetration resistance. When subjected to a single cycle of MICP with 1M urea and 0.67 M calcium chloride, specimens lost surface strength and showed no clear penetration resistance peak after two wash-dry cycles, indicating crust weakening. However, three MICP treatments with a 1 M urea and 0.67 M calcium chloride solution resulted in significantly higher peak surface strength than other method and the specimens treated

multiple times maintained their strength and  $\text{CaCO}_3$  content even after three washing and drying cycles.

**In chapter 4**, two types of iron ore mine tailings, a poorly graded fine sand (SP) and a well-graded sand (SW), were tested to evaluate the effect of freeze-thaw cycles on the fugitive dust resistance of EICP-treated specimens. Specimens were treated with two applications of equimolar urea and calcium chloride treatment solutions with different concentrations, i.e., 0.5, 0.75, and 1 M. The dust emission was evaluated through Portable In Situ Wind Erosion Lab (PI-SWERL™) tests, the crust strength was evaluated with penetration tests, and calcium carbonate content was evaluated with Calcimeter tests. The findings demonstrated somewhat different outcomes for each soil type.

For the SP fine sand, dry specimens exhibited increased resistance against wind erosion and penetration after treatment for all treatment solution concentrations. When exposed to freeze-thaw cycles, specimens experienced a partial decline in surface strength and erosion resistance at lower cementation levels, i.e., 0.5M and 0.75M. However, at the highest cementation level of 1M the crust strength and erosion resistance remained significantly intact even after 10 freeze-thaw cycles.

For the SW sand, treatment of dry specimens with 0.5M or 0.75M treatment solutions did not significantly increase penetration resistance or suppression of dust emissions. However, by increasing the concentration of cementation solution to 1 M, an increase in erosion resistance after treatment was observed and the erosion resistance remained elevated after 3 freeze-thaw cycles. The removal of coarse particles from the SW sand facilitated effective binding of smaller soil particles by carbonate precipitation



of EICP at lower cementation level of 0.5M, forming a cohesive structure that was tolerant when exposed to 10 freeze-thaw cycles.

For both soils (SP and SW), treating the soil under conditions with high moisture content resulted in a limited crust formation. These aspects should be considered when implementing EICP in the practical field applications.

**In chapter 5**, the potential of using MICP and EICP for dust suppression on the Salton Sea playa was evaluated for selected soil samples, including a high salinity soil containing 30 – 40% salt (designated as HS) and low salinity soil containing 4-5% salt (designated as LS). The treatment performance and strength of the crust for these two soil types were assessed using the PI-SWERL test, penetration testing, and calcium carbonate content analysis.

For the HS soil, the erosion resistance of the MICP and EICP treated specimens was comparable with that of soils treated with Urea and  $\text{CaCl}_2$  solution containing 0.5M urea and 0.33M  $\text{CaCl}_2$ , an equivalent concentration of cementation solution as in the MICP and EICP solutions. Neither MICP nor EICP treatment showed any sign of calcium carbonate precipitation for the HS soil, indicating that the crusts and the increased erosion resistance on these specimens was attributed to the salt crust formed by evaporation rather than by calcite precipitation through biocementation. For the LS soil, a measured carbonate precipitation of about 1% in the crust after treatment with EICP and MICP solutions containing 1.5M urea and 1M  $\text{CaCl}_2$  appears to have contributed to the surface strength and wind erosion resistance of the treated specimens.

For the HS soil, it is hypothesized that dissolution of the soluble salt in the soil into the EICP and MICP treatment solutions increased the solution salinity to greater than

the critical value for carbonate precipitation due to suppression of the urease activity. In summary, neither MICP nor EICP treatment resulted in calcium carbonate precipitation or crust formation for the highly saline soil.

**In chapter 6**, the application of MICP conducted on interim cover soil at a landfill in Mesa, Arizona was studied. Dust mitigation treatment using MICP was a component of a larger project at this site conducted by the Center for Bio-mediated and Bio-inspired Geotechnics (CBBG) at Arizona State University (ASU). In the larger project, five parallel dust mitigation test plots were investigated, including plots treated with EICP, XEICP (EICP with xanthan gum), and MICP and magnesium chloride ( $MgCl_2$ ) and an untreated control plot. Challenges associated with the application of the MICP technique and results of post-treatment testing are included in this dissertation.

Carbonate content testing of the MICP test plot showed a very low efficiency of carbonate precipitation, having only an average increase of about 0.1% compared to the expected theoretical precipitation of 3.5% (assuming 50% of saturation during the treatment) after initial treatment with 1.2 L/m<sup>2</sup> of bacteria and 1.2 L/m<sup>2</sup> of cementation solution containing 1.1M  $CaCl_2$  and 1.2M Urea and persisted even after the second application of cementation solution in the following day. Rapid evaporation may have inhibited the complete hydrolysis of urea and the subsequent reactions during the first application of treatment solution, as treatment was applied during the peak of daytime heat. Consequently, an additional application was employed.

The results from both field and laboratory testing of the soil at this site revealed limited carbonate precipitation within the soil crust due to the MICP treatment. However, the erosion resistance of the MICP-treated plot did exhibit a significant increase

following treatment based upon PI-SWERL testing and dust monitoring of the test plots after excited by vehicle traffic and a piece of chain link fence pulled by a pick-up truck. The MICP crust subsequently experienced a 10% reduction in strength over the three months following treatment. As addressed by Woolley (2023), the EICP-treated plot maintained its erosion resistance at the same level over the same three months period. When considering all the data collected from field and laboratory assessments at this site, in general MICP-treated plot showed lower efficacy in comparison to the EICP-treated plot.

## 7.2. Conclusion

### 7.2.1. Effect of soil type

The efficacy of biocementation treatments (MICP and EICP) varies when applied to soils with different grain sizes and distributions and salinity. This is illustrated by:

- The study in Chapter 4, where testing on two differently graded tailings materials from the same source demonstrated that treating by application of EICP solutions at lower concentrations (i.e., containing equimolar concentrations of urea and calcium chloride of 0.5M and 0.75M) yielded effective results for SP (fine sand) soil but the same solutions were ineffective for the SW soil that contained large gravel-sized particles. A higher concentration cementation solution (1M urea and calcium chloride) was required to achieve a cemented crust in the soil that contained larger particle sizes.

- The incomplete conversion of urea and calcium chloride to calcium carbonate in the MICP-treated plot in the field described in Chapter 6. This incomplete conversion may be partially attributed to the high silt content ( $\approx 20\%$ ) of the soil that causes filtration of bacteria at the surface. The relatively smaller size of urease enzyme extracted from jack beans, compared to ureolytic bacteria, makes them a more suitable option for application in finer-grained granular soils. This characteristic of EICP results in creating a more effective crust in finer-grained soil condition; and
- The application of MICP and EICP on the Salton Sea soils exhibited enhanced performance in soils with lower salt content. These results illustrate how salinity of the soil might be a factor in the efficacy of biocementation as dust mitigation method.

#### 7.2.2. Effect of environmental conditions

The influence of environmental conditions on the efficacy of biocementation is illustrated by:

- The low efficiency of both MICP and EICP in the field application described in Chapter 6, where the high temperature during deployment appears to have resulted in rapid evaporation that inhibited the complete hydrolysis of urea and the precipitation of carbonate.
- The laboratory testing in Chapter 4, wherein EICP-treated tailings with a higher initial moisture condition showed lower surface strength and wind erosion

resistance compared to the EICP-treated tailings with a lower initial moisture content.

- The laboratory testing on the influence of wetting-drying cycles on tailings stabilized for fugitive dust mitigation using MICP, presented in Chapters 3, which showed that when a dust-resistance crust formed through MICP remained mostly intact even after undergoing multiple cycles of wetting-drying.
- The laboratory testing on the influence of freeze-thaw cycles on tailings stabilized for fugitive dust mitigation using EICP, presented in Chapter 4, which showed that the ability of a dust-resistance crust formed through EICP to resist multiple cycles of freeze-thaw depended on treatment solution concentration and soil grain size.

### 7.3. Recommendations

- There is a need to develop innovative approaches for applying MICP and EICP to granular soils with a high percentage of silt and clay. Expanding the scope of MICP research to address the unique challenges posed by these diverse soil types would be a valuable contribution to developing effective strategies for wind erosion control.
- Additional studies need to be conducted for various grain sizes of soils so that optimum concentrations and associated application volumes specifically applicable to individual grain size distributions of soils can be identified.

- In soils with a significant presence of background carbonates, assessing precipitated carbonate levels can be challenging. Therefore, alternative approaches, such as measuring the ammonium levels and residual urea in the soil, should be considered for a more accurate evaluation of the amount of precipitation induced by either EICP or MICP in such soils.
- To determine the viability of MICP and EICP in soils containing soluble salts, the existence of a threshold soluble salt content should be investigated. This threshold could serve as a decisive parameter governing the precipitation of carbonate. Investigating this threshold involves conducting experiments on a range of soils with varying salt content.
- Research and interpretation of the data measured by the optical gate sensors (OGS) of the PI-SWERL instrument is recommended. Analysis of these data can provide valuable insights into the measurement of saltating particle counts for soil with dominant sand size particles. Note that these sensors become abraded and lose sensitivity over time and may need to be replaced frequently to provide useful data.

## REFERENCES

- Almajed, A., Khodadadi Tirkolaei, H. and Kavazanjian Jr, E., 2018. Baseline investigation on enzyme-induced calcium carbonate precipitation. *Journal of Geotechnical and Geoenvironmental Engineering*, 144(11), p.04018081.
- ASTM D2487-17 (2020). Standard Practice for Classification of Soils for Engineering Purposes (Unified Soil Classification System)
- ASTM D5084-16 (2016). Standard Test Methods for Measurement of Hydraulic Conductivity of Saturated Porous Materials Using a Flexible Wall Permeameter.
- ASTM D5312-92. (1997). Standard Test Method for Evaluation of Durability of Rock for Erosion Control Under Freezing and Thawing Conditions, ASTM International. West Conshohocken, PA. <https://doi.org/10.1520/D5312-92R97>.
- Bang, S., Min, S.H., and Bang, S.S. (2011) Application of Microbiologically Induced Soil Stabilization Technique for Dust Suppression. *International Journal of Geo-Engineering*, Vol. 3, No. 2, pp. 27-37.
- Borda, L. G., Cosentino, N. J., Iturri, L. A., García, M. G., & Gaiero, D. M. (2022). Is dust derived from shrinking saline lakes a risk to soil sodification in southern South America? *Journal of Geophysical Research: Earth Surface*, 127(4), e2021JF006585. doi:10.1029/2021JF006585
- Buck, B.J., King, J., Etyemezian, V., in press, Effects of salt mineralogy on dust emissions: Salton Sea California, USA, *Soil Science Society of America Journal*.
- Campbell, D. J., and O'Sullivan, M. F. (1990). The cone penetrometer in relation to trafficability, compaction, and tillage. *Soil analysis: Physical methods*, K. Smith and C. E. Mullins, eds., Marcel Dekker, New York, 399–429.
- Chae, S. H., Chung, H., & Nam, K. (2021). Evaluation of microbially Induced calcite precipitation (MICP) methods on different soil types for wind erosion control. *Environmental Engineering Research*, 26(1).
- Chen, R., Lee, I., & Zhang, L. (2014). Biopolymer stabilization of mine tailings for dust control. *Journal of Geotechnical and Geoenvironmental Engineering*, 141(2). [https://doi.org/10.1061/\(ASCE\)GT.1943-5606.0001240](https://doi.org/10.1061/(ASCE)GT.1943-5606.0001240)

- Cheng, L., & Cord-Ruwisch, R. (2012). In situ soil cementation with ureolytic bacteria by surface percolation. *Ecological Engineering*, 42, 64-72.
- Cheng, L., Cord-Ruwisch, R., & Shahin, M. A. (2013). Cementation of sand soil by microbially induced calcite precipitation at various degrees of saturation. *Canadian Geotechnical Journal*, 50(1), 81-90.
- CNRA, DWR, and CDFW (California Natural Resources Agency, California Department of Water Resources, and California Department of Fish and Wildlife). (2020). Salton Sea Management Program Dust Suppression Action Plan. <https://saltonseaca.gov/wp-content/uploads/2020/10/DSAP-7-31-2020.pdf>
- Countess Environmental. (2006). WRAP (Western Regional Air Partnership) Fugitive Dust Handbook Chapter. Denver, CO, USA.
- Daniel, C. R., Howie, J. A., Campanella, R. G., and Sy, A. (2004). Characterization of SPT grain size effects in gravels. Proc., 2nd Int. Conf. on Site Characterization (ISC'2), Millpress, Rotterdam, Netherlands.
- DeJong, J.T., Fritzges, M.B. and Nusslein, K. (2006). Microbial induced cementation to control sand response to undrained shear. *ASCE J. Geotech. Geoenviron. Eng.* 132, 1381–1392.
- DeJong, J.T., Ghafghazi M., Sturm A.P., Wilson D.W., den Dulk J., Armstrong R.J., Perez A., and Davis C.A. (2017). Instrumented Becker Penetration Test 1. Equipment, Operation, and Performance. *ASCE J. Geotech. and GeoEnv. Eng.*, [https://doi.org/10.1061/\(ASCE\)GT.1943-5606.0001717](https://doi.org/10.1061/(ASCE)GT.1943-5606.0001717).
- Dust Quant LLC. (2018). "User's Guide for the Miniature PI-SWERL." *Model MPS-2b*, Dust-Quant LLC., 5-7.
- Ehsasi, F., Van Paassen, L., & Wang, L. (2022). Stabilization of Mine Tailings Using Microbiological Induced Carbonate Precipitation for Dust Mitigation: Treatment Optimization and Durability Assessment. In *Geo-Congress 2022* (pp. 326-334).
- Etyemezian, V, Nikolich, G., Ahonen, S., Pitchford, M., Sweeney, M., Purcell, R., Gillies, J., Kuhns, H. (2007). The Portable In Situ Wind Erosion Laboratory (PI-SWERL): A new method to measure PM10 windblown dust properties and potential for emissions, *Atmospheric Environment*, Volume 41, Issue 18, Pages 3789-3796, ISSN 1352-2310, <https://doi.org/10.1016/j.atmosenv.2007.01.018>.



- Etyemezian, V., Gillies, J. A., Shinoda, M., Nikolich, G., King, J., and Bardis, A.R. (2014). "Accounting for surface roughness on measurements conducted with PI-SWERL: Evaluation of a subjective visual approach and a photogrammetric technique." *Aeolian Research*, 13, 35-50.
- Etyemezian, V., Nikolich, G., Ahonen, S., Pitchford, M., Sweeney, M., Purcell, R., & Kuhns, H. (2007). The Portable In Situ Wind Erosion Laboratory (PI-SWERL): A new method to measure PM10 windblown dust properties and potential for emissions. *Atmospheric Environment*, 41(18), 3789-3796.
- Gomez, M.G., Dworatzek, S.M., Martinez, B.C., deVlaming, L.A., DeJong, J.T., Hunt, C.E., Major, D.W. (2015). Field-scale bio-cementation tests to improve sands. *Proc ICE Ground Improv* 168(3):206–216. doi: 10.1680/grim.13.00052.
- Gowthaman, S., Nakashima, K., & Kawasaki, S. (2020). Freeze-thaw durability and shear responses of cemented slope soil treated by microbial induced carbonate precipitation. *Soils and Foundations*, 60(4), 840-855.
- Harkes, M.P., Booster, J.L., van Paassen, L.A., van Loosdrecht, M.C.M. (2008). Microbial induced carbonate precipitation as ground improvement method - bacterial fixation and empirical correlation CaCO<sub>3</sub> vs strength. 1st International Conference on Bio-Geo-Civil Engineering, Netherlands, June 23-25: 37-41.
- Khodadadi T.H., (2016). Primary Study on Ureolysis-Based Microbially-Induced Calcium Carbonate Precipitation Technique for Geotechnical Applications. Dissertation of the Doctor of Philosophy Degree, Eastern Mediterranean University (EMU).
- Khodadadi, T.H., Javadi, N., Krishnan, V., Hamdan, N., Kavazanjian, E.J. (2020). Crude urease extract for biocementation. *J. Mater. Civil Eng.*  
[https://doi.org/10.1061/\(ASCE\)MT.1943-5533.0003466](https://doi.org/10.1061/(ASCE)MT.1943-5533.0003466)
- King, J., Etyemezian, V., Sweeney, M., Buck, B.J., Nikolich, G. (2011). Dust emission variability at the Salton Sea, California, USA. *Aeolian Research* 3:67–79, 10.1016/j.aeolia.2011.03.005.
- Lakshminarayanan, L., (2022) Fundamental Studies on Enzyme Induced Carbonate Precipitation. Dissertation of the Doctor of Philosophy Degree, Arizona State University.

- Maleki, M., Ebrahimi, S., Asadzadeh, F., Emami Tabrizi, M. (2016) Performance of microbial-induced carbonate precipitation on wind erosion control of sandy soil. *Int J Environ Sci Technol* 13:937–944. <https://doi.org/10.1007/s13762-015-0921-z>
- Mendez, M.O. and Maier, R.M. (2008) Phytostabilization of Mine Tailings in Arid and Semiarid Environments—An Emerging Remediation Technology. *Environmental Health Perspectives*, 116, 278-283. <http://dx.doi.org/10.1289/ehp.10608>
- Meng, H., Gao, Y., He, J., Qi, Y., & Hang, L. (2021). Microbially induced carbonate precipitation for wind erosion control of desert soil: Field-scale tests. *Geoderma*, 383, 114723.
- Meyer, F.D., Bang, S., Min, S., Stetler, L.D., Bang, S.S., (2011). Microbiologically induced soil stabilization: application of *Sporosarcinapasteurii* for fugitive dust control. *Geo-Frontiers* 41165:4002–4011.
- Mitchell, J. K., and Santamarina, J. C. (2005). "Biological Considerations in Geotechnical Engineering." *Journal of Geotechnical and Geoenvironmental Engineering*, 131(10), 1222-1233.
- Montoya, B. M., DeJong, J. T., Boulanger, R. W., Wilson, D. W., Gerhard, R., Ganchenko, A., & Chou, J.C. (2012). Liquefaction Mitigation Using Microbial Induced Calcite Precipitation. <https://doi.org/10.1061/9780784412121.197>
- Munkhtsetseg, E., Shinoda, M., Gillies, J. A., Kimura, R., King, J., and Nikolich, G. (2016). "Relationships between soil moisture and dust emissions in a bare sandy soil of Mongolia." *Particuology*, 28, 131-137.
- Naeimi, M., Chu, J. (2017). Comparison of conventional and biotreated methods as dust suppressants. *Environ Sci Pollut Res* 24:23341–23350. <https://doi.org/10.1007/s11356-017-9889-1>
- Rice, M. A., Mullins, C. E., and McEwan, I. K. (1997). An analysis of soil crust strength in relation to potential abrasion by saltating particles. *Earth Surf. Processes Landforms*, 22(9), 869–883.
- Rice, M. A., Willetts, B. B., and McEwan, I. K. (1996). Wind erosion of crusted soil sediments. *Earth Surf. Processes Landforms*, 21(3), 279– 293.

- Shanahan, C., & Montoya, B. M. (2016). Erosion Reduction of Coastal Sands Using Microbial Induced Calcite Precipitation. In Geo-Chicago 2016 (pp. 42-51).
- Sharma, M., Satyam, N., & Reddy, K. R. (2021). Effect of freeze-thaw cycles on engineering properties of biocemented sand under different treatment conditions. *Engineering Geology*, 284, 106022.
- Sonon, L., Saha, U, Kissel, D., (2015) Soil Salinity: Testing, Data Interpretation and Recommendations. Agricultural and Environmental Services Laboratories, University of Georgia. <https://extension.uga.edu/publications/detail.html?number=C1019&title=soil-salinity-testing-data-interpretation-and-recommendations>
- Sweeney, M., Etyemezian V., Macpherson, T., Nickling, W., Gillies, J., Nikolich, G., McDonald, E. (2008) "Comparison of PI-SWERL with dust emission measurements from a straight-line field wind tunnel," *Journal of Geophysical Research: Earth Surface* 13, F1. <https://doi.org/10.1029/2007JF000830>.
- Van Paassen, L.A., Ghose, R., van der Linden, T.J.M., Van der Star, W.R.L., van Loosdrecht, M.C.M. (2010). Quantifying biomediated ground improvement by ureolysis: large-scale biogROUT experiment. *J Geotech Geoenviron Eng* 136(12):1721–1728.
- Van Paassen, L.A., Harkes, M.P., Van Zwieten, G.A., Van der Zon, W.H., Van der Star, W.R.L. & Van Loosdrecht, M.C.M. (2009). Scale up of BioGrout: a biological ground reinforcement method. 17th International Conference on Soil Mechanics & Geotechnical Engineering, 5-9 October, Alexandria, Egypt, in press.
- Wang, Z., Zhang, N., Ding, J. et al. (2018). Experimental study on wind erosion resistance and strength of sands treated with microbial-induced calcium carbonate precipitation. *Adv Mater Sci Eng*. <https://doi.org/10.1155/2018/3463298>
- Watson, J.G., Chow, J.C. (2000). Reconciling Urban Fugitive Dust Emissions Inventory and Ambient Source Contribution Estimates: Summary of Current Knowledge and Needed Research. Desert Research Institute (DRI) Document No. 6110.4F.
- Whiffin, V.S., van Paassen, L.A., and Harkes, M.P. (2007). Microbial Carbonate Precipitation as a Soil Improvement Technique. *Geomicrobiology Journal*, 25 (5): 417-423.

- Wijewickreme, D., Sanin, M. V., and Greenaway, G. R. (2005). Cyclic shear response of fine-grained mine tailings. *Can. Geotech. J.*, 42(5), 1408–1421.
- Woolley, M. A., (2023) Laboratory and Field Evaluation of Enzyme Induced Carbonate Precipitation (EICP) for Fugitive Dust Mitigation. Dissertation of the Doctor of Philosophy Degree, Arizona State University.
- Woolley, M. A., Van Paassen, L., & Kavazanjian, E. (2020). Impact on Surface Hydraulic Conductivity of EICP Treatment for Fugitive Dust Mitigation. Geotechnical Special Publication. <https://doi.org/10.1061/9780784482834.015>
- Woolley, M., Hamdan, N., and Kavazanjian, E. (2022) “The Durability of EICP Crusts Subjected to Ultraviolet (UV) Radiation,” Proceedings, 20th International Conference on Soil Mechanics and Geotechnical Engineering (ICSMGE), Sydney, 1-5 May.
- Yu, X. (2023). Laboratory and Field Testing in Support of Field Studies of Enzyme Induced Carbonate Precipitation (EICP) for Fugitive Dust Control. Master Thesis, Arizona State University.
- Yuan, Y., Yuan, Z., Xi, Y. (2022) Effect of Microbially Induced Carbonate Precipitation (MICP) in the Highly Saline Silty Soil of the Cold Plateau Area of the Qinghai-Tibetan Plateau. *KSCE J Civ Eng* 26, 4407–4418. <https://doi.org/10.1007/s12205-022-1695-8>
- Zhang L, Ren F, Li H, Cheng D, Sun B. (2021). The Influence Mechanism of Freeze-Thaw on Soil Erosion: A Review. *Water* 13, no. 8: 1010. <https://doi.org/10.3390/w13081010>
- Zucca, C., Middleton N., Kang, U., Liniger, H. (2021). Shrinking water bodies as hotspots of sand and dust storms: The role of land degradation and sustainable soil and water management. <https://doi.org/10.1016/j.catena.2021.105669>